Ph.D. DISSERTATION

Partially Information Coupled Polar Codes with Coupling Depth J

결합 길이가 J인 부분 정보 결합 극 부호

BY

HYOUNGBAE AHN

FEBRUARY 2020

DEPARTMENT OF ELECTRICAL AND
COMPUTER ENGINEERING
COLLEGE OF ENGINEERING
SEOUL NATIONAL UNIVERSITY

Ph.D. DISSERTATION

Partially Information Coupled Polar Codes with Coupling Depth J

결합 길이가 J인 부분 정보 결합 극 부호

BY

HYOUNGBAE AHN

FEBRUARY 2020

DEPARTMENT OF ELECTRICAL AND
COMPUTER ENGINEERING
COLLEGE OF ENGINEERING
SEOUL NATIONAL UNIVERSITY

Partially Information Coupled Polar Codes with Coupling Depth J

결합 길이가 J인 부분 정보 결합 극 부호

지도교수 노 종 선
이 논문을 공학박사 학위논문으로 제출함

2020년 2월

서울대학교 대학원

전기 · 정보 공학부

안 형 배

안형배의 공학박사 학위 논문을 인준함

2020년 2월

위 원 장: _____
부위원장: _____
위 원: _____
위 원: _____
위 원: _____

Abstract

In this dissertation, there are three main contributions:

i) Propose a new parameter, called *coupling depth* which generalizes the coupling scheme of partially information coupled (PIC) polar codes [36] and a construction method of PIC polar codes with coupling depth J.

ii) Propose a polar code block (CB) decoding algorithm for the proposed PIC polar codes and propose various inter-CB decoding algorithms and modify the *look-back* and *go-back* decoding algorithm introduced in [36].

iii) Propose an error rate evaluation of the modified parallel inter-CB decoder and optimize a pair of parameters, the chain length and coupling depth of the proposed PIC polar codes.

In the conventional PIC polar codes [36], there are systematic polar CBs arranged in a line, and each CB shares some part of systematic information bits only with adjacent immediate CBs. In the proposed PIC polar codes, each CB shares systematic information bits with adjacent J CBs both in the head and tail directions. The coupling depth denoted by J is the number of CBs that one CB shares information bits in the head (or tail) direction. The proposed PIC polar codes are referred to as PIC polar codes with coupling depth J.

In order to encode PIC polar codes, three stages are performed sequentially: i) message segmentation and dummy bit insertion, ii) systematic polar CB encoding, iii) CB concatenation. To introduce the concept of the coupling depth, a generalized scheme of message segmentation and dummy bit insertion is proposed. Under this scheme, the effective code length and rate are derived.

There are two main decoding stages of the PIC polar codes: i) polar CB decoding, ii) inter-CB decoding. In this dissertation, the polar CB decoding stage is modified to

apply the new parameter, coupling depth. Also, several inter-CB decoding schemes are proposed: i) two modified inter-CB decoding algorithms, ii) modified look-back and go-back inter-CB decoding algorithm with coupling depth $J = 2$, iii) sequential and probabilistic re-decoding inter-CB decoding algorithm.

In terms of computational complexity, the polar CB decoding stage consumes most time of the entire decoding process of PIC polar codes. For this reason, a new error rate evaluation of the modified parallel inter-CB decoder in the ensemble sense is proposed, which can be calculated by skipping the polar CB decoding stage. Using this evaluation, a pair of parameters, chain length L and coupling depth J, of PIC polar codes can be optimized for given fixed code and message lengths of CBs, channel state information, and target transport block error rate. As a part of complexity analysis, the upper bound of complexity under parallel inter-CB decoding algorithm is proposed and proved. Numerical results confirm the effectiveness of the proposed coupling scheme defined by the coupling depth and the proposed error rate evaluation for PIC polar codes.

keywords: Error correcting codes, polar codes, spatial coupling, partially information coupled (PIC) codes, successive cancellation list (SCL) decoding, coupling depth.
student number: 2014-21672

Contents

List of Tables

List of Figures

Chapter 1

Introduction

1.1 Background

A channel is defined as a medium over which a signal, carrying information that composes a message, is sent. Most channels in real life are noisy and this noise hinders reliable transmission through the channel. In 1948, C. E. Shannon proved that a reliable transmission via a fixed noisy channel can be achieved by using the randomly generated codes, the random codes, encoded from the message. He also proved that there exists the maximum rate for a reliable message transmission and named this rate channel capacity.

However, these random codes are not practical because of their exponentially complicated encoding and decoding schemes. Therefore, there are a lot of studies to find practically feasible channel codes and corresponding decoding algorithms to achieve channel capacity [2]–[7]. Ever since 1948, many practical codes are discovered and most of them can mainly be classified by block codes and convolutional codes.

Block codes are based on abstract algebra and each of them can be defined by a mapping from a block of information bits to a block of coded bits. Examples of block codes are Hamming codes [8], Golay codes [9], Reed-Muller codes [10], [11], Bose–Chaudhuri–Hocquenghem (BCH) codes [13], [12], Reed-Solomon (RS) codes

[14], low-density parity-check (LDPC) codes [15], [16], [17], and polar codes [18].

The ideal decoding algorithm of block codes is the maximum likelihood (ML) decoding algorithm if all codewords are equally likely to be sent. However, since the complexity of this algorithm is proportional to two to the power of message length, the ML decoding algorithm is not easy to be implemented. Therefore, decoding algorithms of channel codes are designed to have low-complexity while providing good performance.

In contrast to the concept of block codes, tree codes are defined by a mapping from not only the current information block but also the previous information blocks to the code block. Examples of tree codes are convolutional codes [19] and turbo codes[20]. In 1967, A. Viterbi showed that convolutional codes could be ML decoded using trellis diagram. This decoding algorithm is called Viterbi decoding algorithm.

Polar codes and their theoretical background were established by E. Arikan in 2008. The biggest significance of polar codes is that these codes are the firstly proven capacity-achieving codes for any given binary discrete memoryless channels (B-DMCs). According to the channel polarization theorem, any independent copies of B-DMCs can be transformed into a certain set of channels, called bit-channels, by the channel polarization operation. Then, the symmetric capacities of bit-channels converge to either 0 or 1 in probability [18]. Note that the symmetric capacity is one of the measures of B-DMCs and the detailed definition will be introduced later. If this measure is 0, the B-DMC is perfectly noisy and if this is 1, the B-DMC is noiseless. In other words, the bit-channels are polarized either perfectly noisy or noiseless.

The two phases, called the channel combining phase and the channel splitting phase, and their recursive structures in the channel polarization operation motivate the construction and the standard decoding scheme of polar codes. The main idea of the polar code construction is to transmit information only to such good polarized bit-channels. Various methods have been studied to find and determine those good bit-channels in polar codes [21], [22], [23]. And various methods of constructing effective

polar codes have been researched [24], [25], [26]. Also, various generalized encoding schemes have been studied [27], [28], [29].

The main idea of the standard decoding scheme of polar codes is to use the previously decoded information bits while each bit is decoded successively. This fundamental decoding algorithm is called the successive cancellation (SC) decoding algorithm [18]. Although these encoding and decoding schemes of polar codes have theoretical backgrounds, there is a problem in practice. The SC decoding algorithm of polar codes has poor performance compared to other fundamental decoding algorithms of competitive codes, such as belief propagation (BP) decoding algorithm of LDPC codes or iterative maximum a posteriori (MAP) decoding algorithm of turbo codes. There are two main reasons of this performance degradation. First, the SC decoding algorithm has no way to prevent error propagation. Second, the minimum distance, one of the measurements of the linear block codes which is closely related to the ML decoding performance, of the conventional polar codes is not good.

In 2015, I. Tal and A. Vardy proposed a modification of the SC decoding algorithm [30]. They applied a list decoding technique to the SC decoding algorithm to prevent error propagation and named this algorithm successive cancellation list (SCL) decoding algorithm. They observed that the performance of SCL decoding algorithm nearly approaches to the maximum-likelihood (ML) decoding algorithm over the additive white Gaussian noise (AWGN) channel at high signal-to-noise ratio (SNR). In this paper [30], they also announced that concatenating some cyclic-redundancy-check (CRC) code increases the decoding performance by ensuring a good minimum distance. The corresponding SCL decoding algorithm of this CRC-concatenated polar codes is called CRC-aided SCL (CASCL) decoding algorithm. In addition to this CA-SCL decoding algorithm, various algorithms for efficient decoding have been developed in terms of performance improvement [31], [32] or complexity reduction [33], [34].

The complexity of the SC or SCL decoding algorithm is known to be proportional

to $N\log N$, where N is the code length of polar codes. Therefore, there are a lot of studies to overcome the encoding and decoding complexity of long polar codes efficiently and one of the results of these studies is spatially coupling scheme. In this scheme, a long codeword is segmented into several code blocks (CBs) in line, which are coupled with the neighbored CBs, respectively. Information coupling scheme is a special realization of spatial coupling of error-correcting codes. In this scheme, L. Yang *et al.* proposed that a long codeword is segmented into systematically encoded CBs and each of them shares some information bits with adjacent CBs [35]. In 2018, they published the paper, "Partially information coupled polar codes" [36], where a class of partially information coupled (PIC) polar codes and corresponding decoding algorithm was proposed. They also developed an analytical framework for these codes and optimized the coupling schemes based on this framework. Finally, they evaluated the error performance and decoding complexity of PIC polar codes.

The advantage of this coupling structure is that decoding of PIC polar codes is effective not only in complexity by segmenting a long codeword into several CBs, but also in performance by updating extrinsic information from the coupling structure. In order to increase the advantages of coupling structure, modified coupling schemes and corresponding encoding and decoding schemes are proposed in this dissertation.

1.2 Overview of Dissertation

This dissertation is organized as follows. In Chapter 2, polar codes and PIC polar codes are reviewed. In Section 2.1, the preliminaries and notations for polar codes are presented. The encoding and decoding algorithms of polar codes are also described. In Section 2.2, the code structure and encoding and decoding schemes of PIC polar codes are reviewed. The performance analysis for these codes is also discussed.

In Chapter 3, the coupling scheme of PIC polar codes is generalized by the parameter, coupling depth. In Section 3.1, a new coupling scheme is proposed and a new

parameter called coupling depth is defined. In Section 3.2, a message segmentation and coupling stage of the proposed PIC polar codes is proposed, which is far different from that stage of the conventional PIC polar codes. In Section 3.3, the encoding structure of the proposed PIC polar codes with coupling depth J is proposed.

In Chapter 4, decoding schemes of the modified PIC polar codes are proposed and generalized. The decoding of PIC polar codes consists of two main stages, polar CB decoding and inter-CB decoding. In Section 4.1, polar CB decoding for the proposed PIC polar codes with coupling depth J is introduced. In Section 4.2, two parallel inter-CB decoding schemes for the proposed PIC polar codes are proposed and a modified parallel inter-CB decoding scheme is also proposed. In Section 4.3, two sequential inter-CB decoding schemes for the proposed PIC polar codes are proposed and a modified sequential inter-CB decoding scheme is also proposed. In Section 4.4, the look-back and go-back inter-CB decoding algorithm in [36] is modified for the coupling depth $J = 2$. In Section 4.5, a new inter-CB decoding scheme, called sequential and probabilistic re-decoding inter-CB decoding scheme is proposed.

In Chapter 5, a new error rate evaluation in the ensemble sense is proposed for the modified parallel inter-CB decoding scheme of the proposed PIC polar codes and an optimization technique of a pair of parameters is proposed based on the proposed error rate evaluation, which are described in Section 5.1. Furthermore, as a complexity analysis, the upper bound of the conventional parallel inter-CB decoder and that of the modified parallel inter-CB decoder are derived in Section 5.2.

In Chapter 6, various numerical results are shown to justify the works in this dissertation. Various parameters of the proposed PIC polar codes, such as the CB length N, uncoupled message length K_{u}, coupled message length K_{c}, coupling depth J, chain length L, list size $\mathcal{L}$, and effective code rates, are used as comparison groups in Section 6.1–6.7. In Section 6.8, the evaluated transport block error rates (TBERs) are compared to the simulated TBERs by Monte-Carlo simulation. In Section 6.9, the complexities of the proposed inter-CB decoders are compared.

In Chapter 7, the results in this dissertation are summarized. Also, the future research works are discussed at the end of this chapter.

Chapter 2

Overview of Partially Information Coupled Polar Codes

In this chapter, some preliminaries of PIC polar codes are introduced. In the first section, the channel polarization theorem is reviewed and encoding and decoding schemes of polar codes are described. In the second section, the concept of PIC polar codes is introduced. This section consists of four subsections, each of which covers the encoding structure, the polar CB decoding scheme, the inter-CB decoding scheme, and the performance analysis of PIC polar codes, respectively.

2.1 Polar Codes

Before introducing the channel polarization theorem, some notations and preliminaries of the information theory are reviewed first. Use the notations x_1^N and x_i^j as shorthands for denoting a row vector $(x_1, \cdots, x_N)$ and its subvector $(x_i, \cdots, x_j)$, where $1 \leq i \leq j \leq N$. Given a vector x_1^N and an index set $\mathcal{A} \subset \{1, \cdots, N\}$, $x_{\mathcal{A}}$ denotes the subvector $(x_i \colon i \in \mathcal{A})$. Given an $N \times N$ matrix $\mathbf{G}_N$ and sets $\mathcal{A}, \mathcal{B} \subset \{1, \cdots, N\}$, $\mathbf{G}_{\mathcal{AB}}$ denotes the submatrix of $\mathbf{G}_N$ with elements $\{g_{i,j}\}_{i \in \mathcal{A}, j \in \mathcal{B}}$.

Consider a B-DMC $W \colon \mathcal{X} \to \mathcal{Y}$ with input alphabet $\mathcal{X} = \{0, 1\}$ and output alphabet $\mathcal{Y}$. Denote $W(y|x)$ as the channel transition probability that $y \in \mathcal{Y}$ is observed when $x \in \mathcal{X}$ is transmitted. Let $W^N \colon \mathcal{X}^N \to \mathcal{Y}^N$ be N parallel copies of B-DMC W

with transition probability $W^N(y_1^N|x_1^N) = W(y_1|x_1)\cdots W(y_N|x_N)$. This notation is used to represent the *combined channel* explained later. Let $W_N^{(i)}\colon \mathcal{X} \to \mathcal{Y}^N \times \mathcal{X}^{i-1}$ be the i-th *bit-channel* obtained by splitting W^N for i, $1 \leq i \leq N$.

There are two significant measures of B-DMCs, called the symmetric capacity and the Bhattacharyya parameter. The symmetric capacity refers the highest rate at which reliable communication is possible across W, which is defined as [18]

$$I(W) \triangleq \sum_{y\in\mathcal{Y}} \sum_{x\in\mathcal{X}} \frac{1}{2} W(y|x) \log \frac{W(y|x)}{\frac{1}{2}W(y|0) + \frac{1}{2}W(y|1)}. \tag{2.1}$$

The Bhattacharyya parameter refers an upper bound on the error probability of maximum-likelihood (ML) decision, which is defined as [18]

$$Z(W) \triangleq \sum_{y\in\mathcal{Y}} \sqrt{W(y|0)W(y|1)}. \tag{2.2}$$

Those two measures are used to prove the channel polarization theorem. As explained in the previous chapter, for a B-DMC W, $I(W) \to 0$ means that the channel W becomes perfectly noisy and $I(W) \to 1$ means that the channel W becomes noiseless. On the contrary, $Z(W) \to 0$ means that the channel W becomes noiseless and $Z(W) \to 1$ means the channel W becomes perfectly noisy. For example, consider a binary erasure channel (BEC) W_{e} with erasure probability ϵ. The symmetric capacity of W_{e} is $I(W_{\mathrm{e}}) = 1 - \epsilon$ and the Bhattacharyya parameter of W_{e} is $Z(W_{\mathrm{e}}) = \epsilon$ [18].

As introduced in Chapter 1, polar codes are recently discovered channel codes and these codes achieve the symmetric capacity $I(W)$ of any given B-DMC W. There are three subsections in this section. First, the channel polarization theorem, a theoretical basis of polar codes, is introduced. This theorem consists of two phases and each phase motivates the code construction and the fundamental decoding scheme of polar codes, respectively. In the second subsection, the standard non-systematic encoding and systematic encoding of polar codes are introduced. In the last subsection, several decoding schemes of polar codes are introduced.

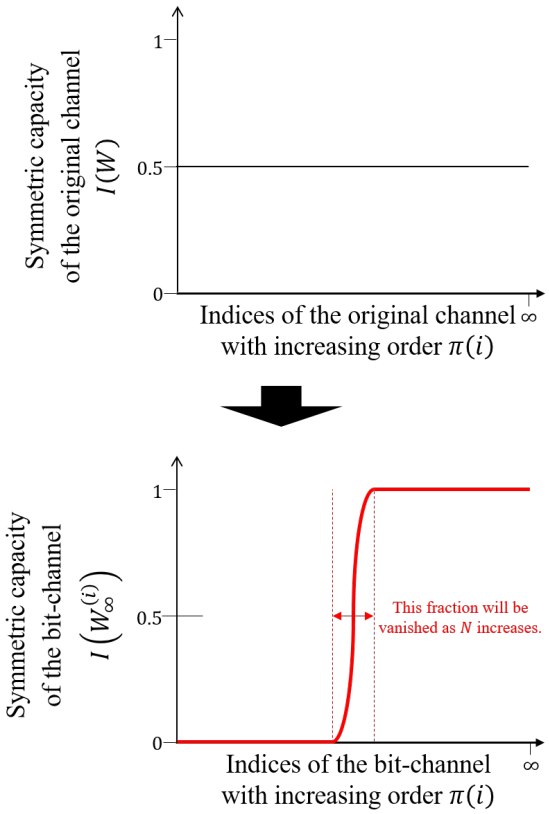

Figure 2.1: Channel polarization effect.

2.1.1 Channel Polarization

The channel polarization effect illustrated in Figure 2.1 is caused by two-phase operation, which consists of channel combining phase and channel splitting phase. This operation turns N independent copies of B-DMC W into a set of N bit-channels $\{W_N^{(i)}: 1 \leq i \leq N\}$. Under well-designed channel combining and splitting phases, the symmetric capacity of the i-th bit-channel $I(W_N^{(i)})$ converges to either 0 or 1 in probability as N increases, which refers that each bit-channel becomes perfectly noisy or noiseless. Since each bit-channel, made by the two-phase operation, becomes polarized either perfectly noisy or noiseless regardless of the type of B-DMC, E. Arikan named it *channel polarization operation*.

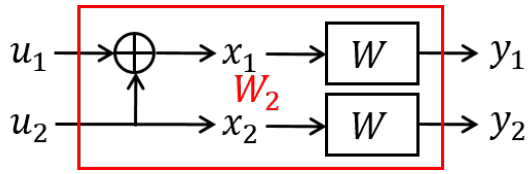

Figure 2.2: Channel combining at the first level.

a) Channel combining

In the channel combining stage, copies of a given B-DMC W are combined in a recursive manner to produce a vector channel $W_N : \mathcal{X}^N \to \mathcal{Y}^N$, where N can be any power of 2, $N = 2^n$ for an integer $n \geq 0$. Initially, only a single copy of W is considered and set $W_1 \triangleq W$.

At the first level, two$(= 2^1)$ independent copies of W_1 are combined into the channel $W_2 : \mathcal{X}^2 \to \mathcal{Y}^2$ illustrated in Figure 2.2 with the transition probabilities

$$W_2(y_1, y_2|x_1, x_2) = W_1(y_1|u_1 \oplus u_2)W_1(y_2|u_2). \tag{2.3}$$

The relationship between x_1^2 and u_1^2 can be represented as

$$x_1^2 = u_1^2\mathbf{G}_2, \tag{2.4}$$

where $\mathbf{G}_2$ is defined as

$$\mathbf{G}_2 = \begin{bmatrix} 1 & 0 \\ 1 & 1 \end{bmatrix}. \tag{2.5}$$

The matrix $\mathbf{G}_2$ is the key matrix to express the generator matrix of polar codes with code length $N = 2^n$ and called the Arikan's kernel matrix, also denoted by $\mathbf{F}$.

Let y_1^2 be the output vector of the combined channel W_2. To understand the reason why (2.3) is defined that way, it is necessary to understand the relationship between the decoding u_1^2 from y_1^2, and two bit-channels $W_2^{(1)}$ and $W_2^{(2)}$. The bit-channels $W_2^{(1)}$: $\mathcal{X} \to \mathcal{Y}^2$ and $W_2^{(2)}$: $\mathcal{X} \to \mathcal{Y}^2 \times \mathcal{X}$ have transition probabilities $W_2^{(1)}(y_1, y_2|u_1)$ and $W_2^{(1)}(y_1, y_2, u_1|u_2)$, respectively. The bit-channel $W_2^{(1)}$ corresponds to the channel from u_1 to y_1 and y_2 and $W_2^{(2)}$ corresponds to the channel from u_2 to y_1, y_2, and the past channel input u_1, provided that u_1 is known perfectly.

Consider the case $W = W_{\mathrm{e}}$ as an example, where W_{e} is a BEC with erasure probability ϵ. From (2.3), decoding u_1 from the channel outputs y_1 and y_2 is possible if and only if both y_1 and y_2 are not erasures. That means, $W_2^{(1)}$ can be expressed as BEC with erasure probability $1-(1-\epsilon)^2$ in this example. Likewise, decoding u_2 from the channel outputs y_1 and y_2 and the previous channel input u_1 is possible if and only if at least one of y_1 and y_2 is not an erasure. Then, $W_2^{(2)}$ can be expressed as BEC with erasure probability ϵ^2 in this example. Note that $0 \leq \epsilon^2 \leq \epsilon \leq 1-(1-\epsilon)^2 \leq 1$, for any $0 \leq \epsilon \leq 1$. From this example, it is verified that the bit-channels $W_2^{(1)}$ and $W_2^{(2)}$ are more and less noisy than the original channel W, respectively.

To generalize the above example, the bit-channels $W_2^{(1)}$ and $W_2^{(2)}$ can be measured by the symmetric capacity of W as

$$I(W_2^{(1)}) + I(W_2^{(2)}) = 2I(W) \tag{2.6}$$

and

$$I(W_2^{(1)}) \leq 2I(W) \leq I(W_2^{(2)}) \tag{2.7}$$

with equality in (2.7) if and only if $I(W)$ equals 0 or 1. And they can also be measured by the Bhattacharyya parameter of W as

$$Z(W_2^{(1)}) \leq 2Z(W) - Z(W)^2 \tag{2.8}$$

and

$$Z(W_2^{(2)}) = Z(W)^2 \tag{2.9}$$

with equality in (2.8) if and only if W is a BEC. (2.6)–(2.9) are proved in [18].

The channel combining at the second level is similar to that at the first one, but with some fixed permutation step between the levels. This permutation is called the reverse shuffle permutation and expressed as $R_4 = \pi(1,3,2,4)$ in Figure 2.3. The transition probability of the combined channel $W_4 : \mathcal{X}^4 \to \mathcal{Y}^4$ can be expressed by the product of two W_2's as

$$W_4(y_1^4|x_1^4) = W_2(y_1^2|u_1 \oplus u_2, u_3 \oplus u_4) W_2(y_3^4|u_2, u_4), \tag{2.10}$$

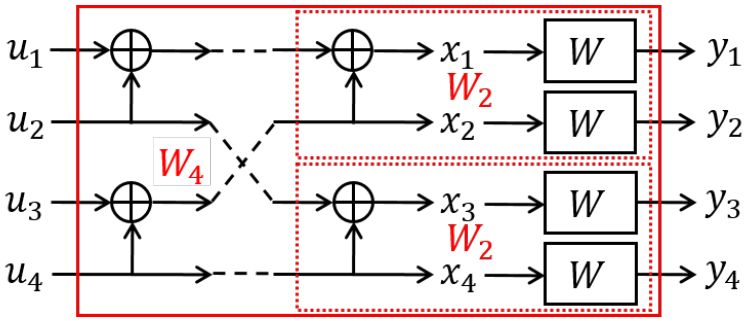

Figure 2.3: Channel combining at the second level.

which can be expressed by the product of four W's as

$$W_4(y_1^4|x_1^4) = W(y_1|u_1 \oplus u_2 \oplus u_3 \oplus u_4)W(y_2|u_3 \oplus u_4)W(y_3|u_2 \oplus u_4)W(y_4|u_4). \tag{2.11}$$

The relationship between x_1^4 and u_1^4 can be represented as

$$x_1^4 = u_1^4 \mathbf{G}_4, \tag{2.12}$$

where $\mathbf{G}_4$ is defined as

$$\mathbf{G}_4 = \begin{bmatrix} 1 & 0 & 0 & 0 \\ 1 & 0 & 1 & 0 \\ 1 & 1 & 0 & 0 \\ 1 & 1 & 1 & 1 \end{bmatrix}. \tag{2.13}$$

Using the identity $(\mathbf{AC}) \otimes (\mathbf{BD}) = (\mathbf{A} \otimes \mathbf{B})(\mathbf{C} \otimes \mathbf{D})$, the generator matrix $\mathbf{G}_4$ can be derived as

$$\begin{aligned} \mathbf{G}_4 &= (\mathbf{I}_2 \otimes \mathbf{G}_2)\mathbf{R}_4(\mathbf{I}_2 \otimes \mathbf{G}_2) \\ &= \mathbf{R}_4(\mathbf{G}_2 \otimes \mathbf{I}_2)(\mathbf{I}_2 \otimes \mathbf{G}_2) \\ &= \mathbf{R}_4\mathbf{G}_2 \otimes \mathbf{G}_2, \end{aligned} \tag{2.14}$$

where $\mathbf{I}_2$ is a 2×2 identity matrix and $\mathbf{R}_4$ is the matrix expression of the reverse shuffle permutation R_4.

Similarly, for $N = 2^n$, W_N can be expressed as the product of two $W_{N/2}$'s in the n-th level, and the generator matrix $\mathbf{G}_N$ can be derived by $\mathbf{G}_2$. Before describing the

details, two permutations, the reverse shuffle permutation and the bit-reversal permutation, are reviewed first. For $N = 2^n$, the reverse shuffle permutation R_N is defined as

$$R_N \triangleq \pi(1, 3, \cdots, N-1, 2, 4, \cdots, N) \tag{2.15}$$

and the matrix expression of the bit-reversal permutation $\mathbf{B}_N$ is defined as

$$\mathbf{B}_N \triangleq (\mathbf{I}_1 \otimes \mathbf{R}_N)(\mathbf{I}_2 \otimes \mathbf{R}_{N/2}) \cdots (\mathbf{I}_{N/2} \otimes \mathbf{R}_2), \tag{2.16}$$

where $\mathbf{I}_N$ is the $N \times N$ identity matrix and $\mathbf{R}_N$ is the matrix expression of the reverse shuffle permutation R_N. Using mathematical induction, $\mathbf{B}_N$ can be expressed as

$$\mathbf{B}_N = \mathbf{R}_N(\mathbf{I}_2 \otimes \mathbf{B}_{N/2}). \tag{2.17}$$

The reason why the bit-reversal permutation is called by that name is because the binary expression of each permuted element can be obtained by reversing that of each original element. For example, $B_8 = \pi(1, 5, 3, 7, 2, 6, 4, 8)$ because

$$\begin{array}{ccccc} 1 & 0 & 000 & 000 & 0 & 1 \\ 2 & 1 & 001 & 100 & 4 & 5 \\ 3 & 2 & 010 & 010 & 2 & 3 \\ 4 & 3 & 011 & 110 & 6 & 7 \\ 5 & 4 & 100 & 001 & 1 & 2 \\ 6 & 5 & 101 & 101 & 5 & 6 \\ 7 & 6 & 110 & 011 & 3 & 4 \\ 8 & 7 & 111 & 111 & 7 & 8. \end{array}$$

$$\begin{array}{ccccc} \longrightarrow & \longrightarrow & & \xrightarrow[\text{operation}]{\text{Bit}-\text{reverse}} & \longrightarrow & \longrightarrow \end{array}$$

At the n-th level, the transition probabilities of two channels W_N and W^N are defined as

$$W_N(y_1^N|x_1^N) = W^N(y_1^N|u_1^N\mathbf{G}_N) \tag{2.18}$$

for all $u_1^N \in \mathcal{X}^N$, $x_1^N \in \mathcal{X}^N$, and $y_1^N \in \mathcal{Y}^N$, where $\mathbf{G}_N$ is an $N \times N$ matrix. The relationship between the combined channel W_N and $W_{N/2}$ is illustrated in Figure 2.4.

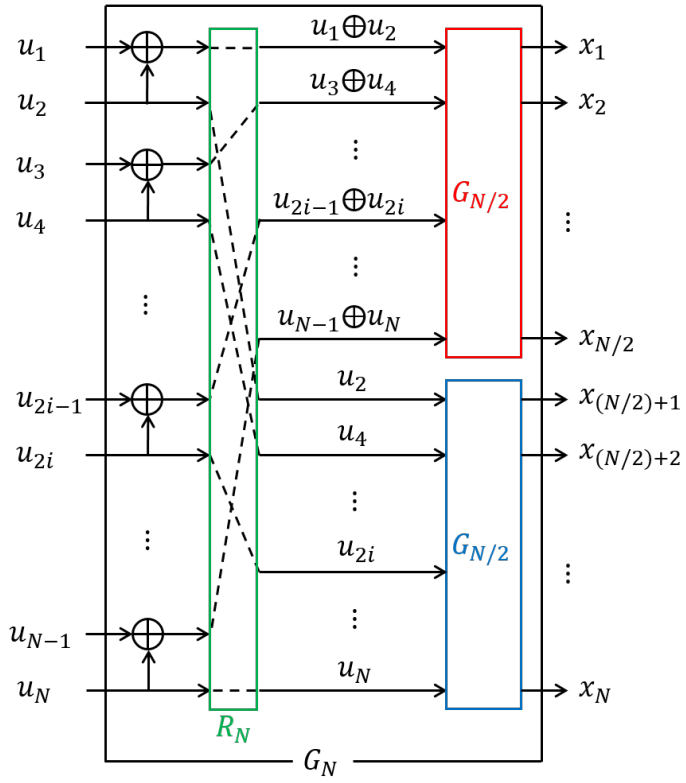

Figure 2.4: Channel combining at the n-th level.

As in this figure, the generator matrix $\mathbf{G}_N$ can be expressed by $\mathbf{R}_N$, $\mathbf{G}_2$, and $\mathbf{G}_{N/2}$ as

$$\begin{aligned} \mathbf{G}_N &= (\mathbf{I}_{N/2} \otimes \mathbf{G}_2)\mathbf{R}_N(\mathbf{I}_2 \otimes \mathbf{G}_{N/2}) \\ &= \mathbf{R}_N(\mathbf{G}_2 \otimes \mathbf{I}_{N/2})(\mathbf{I}_2 \otimes \mathbf{G}_{N/2}) \\ &= \mathbf{R}_N\mathbf{G}_2 \otimes \mathbf{G}_{N/2}, \end{aligned} \tag{2.19}$$

where $\mathbf{I}_N$ is the $N \times N$ identity matrix and $\mathbf{R}_N$ is the matrix expression of the reverse shuffle permutation R_N. Using mathematical induction and (2.17), the generator matrix $\mathbf{G}_N$ can be derived as

$$\mathbf{G}_N = \mathbf{B}_N\mathbf{F}^{\otimes n}, \tag{2.20}$$

where $\mathbf{F} = \mathbf{G}_2 = \left[\begin{smallmatrix} 1 & 0 \\ 1 & 1 \end{smallmatrix}\right]$ and $\mathbf{B}_N$ is the matrix expression of the bit-reversal permutation B_N.

b) Channel splitting

In the channel splitting stage, the combined channel W_N is split into N binary input bit-channels $W_N^{(i)}\colon \mathcal{X} \to \mathcal{Y}^N \times \mathcal{X}^{i-1}, 1 \le i \le N$ by the chain-rule. Suppose that the input message u_1^N is uniformly distributed. Each of these bit-channels can be represented by the transition probabilities as

$$\begin{aligned} W_N^{(i)}(y_1^N, u_1^{i-1}|u_i) &\triangleq \sum_{u_{i+1}^N \in \mathcal{X}^{N-i}} \Pr\{y_1^N, u_1^{i-1}, u_{i+1}^N|u_i\} \\ &= \sum_{u_{i+1}^N \in \mathcal{X}^{N-i}} \frac{1}{2^{N-1}} \cdot \frac{\Pr\{y_1^N, u_1^{i-1}, u_{i+1}^N|u_i\} \cdot \Pr\{u_i\}}{\Pr\{u_1^N\}} \\ &= \sum_{u_{i+1}^N \in \mathcal{X}^{N-i}} \frac{1}{2^{N-1}} \cdot \frac{\Pr\{y_1^N, u_1^N\}}{\Pr\{u_1^N\}} \\ &= \sum_{u_{i+1}^N \in \mathcal{X}^{N-i}} \frac{1}{2^{N-1}} W_N(y_1^N|u_1^N), \end{aligned} \tag{2.21}$$

where (y_1^N, u_1^{i-1}) and u_i denote the output vector and input of $W_N^{(i)}$, respectively.

As mentioned in [18], to gain an intuitive understanding of the channels $\{W_N^{(i)}\}$, consider a *genie-aided successive cancellation* decoder, whose i-th decision element is estimated after decoding the past elements $\hat{u}_1^{i-1}$ perfectly. If the distribution of the input element is uniform, then the i-th bit-channel $W_N^{(i)}$ is the effective channel seen by the i-th decision element in this scenario.

The channel splitting stage can also be represented recursively. At the first level, the bit-channels $W_2^{(1)}$ and $W_2^{(2)}$ can be expressed by W as

$$\begin{aligned} W_2^{(1)}(y_1^2|u_1) &= \sum_{u_2} \frac{1}{2} W(y_1|v_1) \cdot W_{N/2}^{(i)}(y_2|w_1) \\ W_2^{(1)}(y_1^2, u_1|u_2) &= \frac{1}{2} W(y_1|v_1) \cdot W_{N/2}^{(i)}(y_2|w_1), \end{aligned} \tag{2.22}$$

where $v_1 = u_1 \oplus u_2$ and $w_1 = u_2$.

Similarly, at the n-th level, the bit-channels with odd index $W_N^{(2i-1)}$ and even index

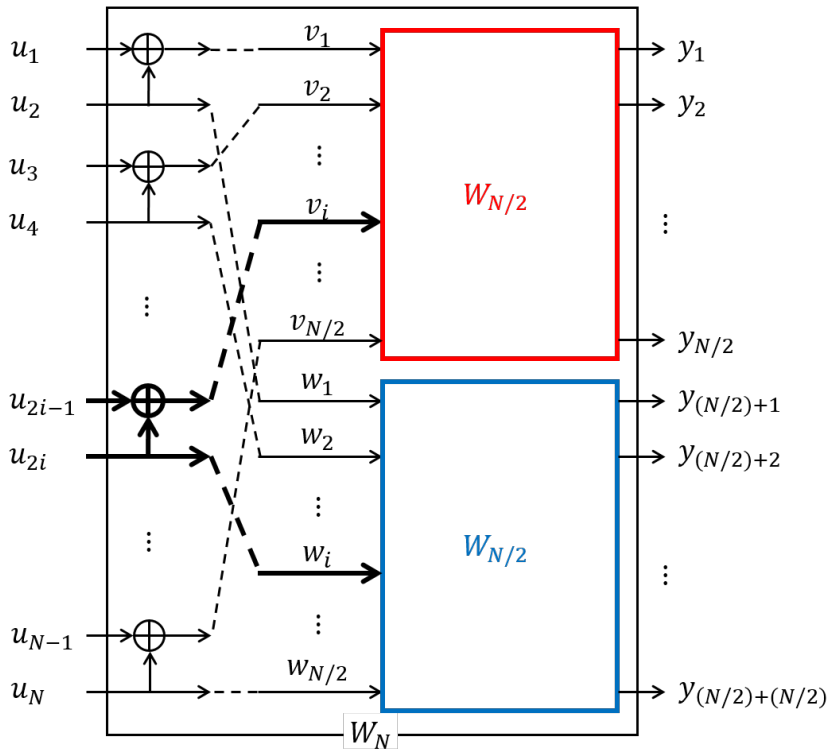

Figure 2.5: Channel splitting at the n-th level.

$W_N^{(2i)}$ can be expressed by $W_{N/2}^{(i)}$ as

$$W_N^{(2i-1)}(y_1^N, u_1^{2i-2}|u_{2i-1}) = \sum_{u_{2i}} \frac{1}{2} W_{N/2}^{(i)}(y_1^{N/2}, v_1^{i-1}|v_i) \cdot W_{N/2}^{(i)}(y_{N/2+1}^N, w_1^{i-1}|w_i)$$
$$W_N^{(2i)}(y_1^N, u_1^{2i-1}|u_{2i}) = \frac{1}{2} W_{N/2}^{(i)}(y_1^{N/2}, v_1^{i-1}|v_i) \cdot W_{N/2}^{(i)}(y_{N/2+1}^N, w_1^{i-1}|w_i), \tag{2.23}$$

where $v_i = u_{2i-1} \oplus u_{2i}$ and $w_i = u_{2i}$ for i, $1 \leq i \leq (N/2)$. Figure 2.5 helps understanding the recursive structure of the channel splitting at the n-th level.

Recall that $W_2^{(1)}$ and $W_2^{(2)}$ generated by (2.22) satisfy (2.6)–(2.9). Motivating from the similarity between (2.22) and (2.23), the bit-channels with odd index $W_N^{(2i-1)}$ and even index $W_N^{(2i)}$ can be measured by the symmetric capacity of $W_{N/2}^{(i)}$ as

$$I(W_N^{(2i-1)}) + I(W_N^{(2i)}) = 2I(W_{N/2}^{(i)}) \tag{2.24}$$

and

$$I(W_N^{(2i-1)}) \leq 2I(W_{N/2}^{(i)}) \leq I(W_N^{(2i)}) \tag{2.25}$$

for i, $1 \leq i \leq (N/2)$ with equality in (2.25) if and only if $I(W_{N/2}^{(i)})$ equals 0 or 1. And they can also be measured by the Bhattacharyya parameter of $W_{N/2}^{(i)}$ as

$$Z(W_N^{(2i-1)}) \leq 2Z(W_{N/2}^{(i)}) - Z(W_{N/2}^{(i)})^2 \tag{2.26}$$

and

$$Z(W_N^{(2i)}) = Z(W_{N/2}^{(i)})^2 \tag{2.27}$$

for i, $1 \leq i \leq (N/2)$ with equality in (2.26) if and only if W is a BEC. These four properties of bit-channels (2.24)–(2.27) underlie the channel polarization theorem. The details are proved in [18].

The concept of the channel combining and splitting stages is the theoretical basis of the construction and the fundamental decoding scheme of polar codes. Note that the recursive structures of these two phases help to reduce the encoding and decoding complexities of polar codes. Both of them are proportional to $N\log N$, where N is the code length of polar codes.

2.1.2 Systematic Encoding of Polar Codes

Before introducing the systematic encoding scheme of polar codes, the standard non-systematic encoding scheme is reviewed first. Consider a generator matrix of size $N \times N$, where $N = 2^n$, without the bit-reversal permutation. Note that this permutation can be taken into the decoding stage. Then, the generator matrix can be written as $\mathbf{G}_N = \mathbf{F}^{\otimes n}$, where $\mathbf{F} = \left[\begin{smallmatrix} 1 & 0 \\ 1 & 1 \end{smallmatrix}\right]$ is the 2×2 matrix. Consider an index set $\mathcal{A} \subset \{1, 2, \cdots, N\}$ as a set of information indices. Note that $|\mathcal{A}| = K$, where K is the message length of polar codes. The encoding scheme of non-systematic polar codes can be written as

$$x_1^N = v_1^N \mathbf{G}_N \tag{2.28}$$

and by setting $v_{\mathcal{A}^c} = \mathbf{0}$, it can also be written as

$$x_1^N = v_{\mathcal{A}}\mathbf{G}_{\mathcal{A}}. \tag{2.29}$$

Although there are a lot of systematic encoding algorithms of polar codes, this dissertation introduces E. Arikan's algorithm [37]. Consider the encoding scheme of non-systematic polar codes $x_1^N = v_{\mathcal{A}}\mathbf{G}_{\mathcal{A}}$. The codeword x_1^N can be split into two parts $\{x_{\mathcal{A}}, x_{\mathcal{A}^c}\}$ and they can be written as

$$\begin{cases} x_{\mathcal{A}} = v_{\mathcal{A}}\mathbf{G}_{\mathcal{A}\mathcal{A}} \\ x_{\mathcal{A}^c} = v_{\mathcal{A}}\mathbf{G}_{\mathcal{A}\mathcal{A}^c}, \end{cases} \tag{2.30}$$

where $x_{\mathcal{A}}$ and $x_{\mathcal{A}^c}$ denote the systematic part and the parity part of the codeword, respectively. Also $\mathbf{G}_{\mathcal{A}\mathcal{A}}$ and $\mathbf{G}_{\mathcal{A}\mathcal{A}^c}$ denote the submatrices of $\mathbf{G}_N$ with the row index set $\mathcal{A}$, both and the column index set $\mathcal{A}$ and $\mathcal{A}^{\mathcal{C}}$, respectively.

It is proved that $\mathbf{G}_{\mathcal{A}\mathcal{A}}$ is self-invertible, i.e., $\mathbf{G}_{\mathcal{A}\mathcal{A}} = \mathbf{G}_{\mathcal{A}\mathcal{A}}^{-1}$, for any subset $\mathcal{A} \subset \{1, 2, \cdots, N\}$. By mapping $v_{\mathcal{A}} = u_{\mathcal{A}}\mathbf{G}_{\mathcal{A}\mathcal{A}}$, the encoding scheme of systematic polar codes is obtained and it can be written as

$$\begin{cases} x_{\mathcal{A}} = v_{\mathcal{A}}\mathbf{G}_{\mathcal{A}\mathcal{A}} = u_{\mathcal{A}}\mathbf{G}_{\mathcal{A}\mathcal{A}}\mathbf{G}_{\mathcal{A}\mathcal{A}} = u_{\mathcal{A}}\mathbf{I}_K \\ x_{\mathcal{A}^c = v_{\mathcal{A}}\mathbf{G}_{\mathcal{A}\mathcal{A}^c} = u_{\mathcal{A}}\mathbf{G}_{\mathcal{A}\mathcal{A}}\mathbf{G}_{\mathcal{A}\mathcal{A}^c} = u_{\mathcal{A}}\mathbf{P}}, \end{cases} \tag{2.31}$$

where $\mathbf{I}_K$ is the $K \times K$ identity matrix and $\mathbf{P} = \mathbf{G}_{\mathcal{A}\mathcal{A}}\mathbf{G}_{\mathcal{A}\mathcal{A}^c}$ is the $K \times (N-K)$ parity matrix. Thus, by multiplying $\mathbf{G}_{\mathcal{A}\mathcal{A}}$ twice, which means non-systematic encoding twice consecutively, it is possible to represent information bits explicitly in the codeword.

2.1.3 Decoding Schemes of Polar Codes

The SC decoding algorithm, the fundamental decoding algorithm of polar codes, was proposed by E. Arikan based on (2.21) [18]. Consider the encoding scheme of non-systematic polar codes $x_1^N = v_1^N\mathbf{G}_N$ and denote $\hat{v}_1^N$ as the estimation of v_1^N. For each

integer i, $1 \leq i \leq N$ and the set of information indices $\mathcal{A}$, $\hat{v}_i$ is determined as

$$\hat{v}_i = \begin{cases} h_i(y_1^N, \hat{v}_1^{i-1}), & \text{if } i \in \mathcal{A} \\ 0, & \text{if } i \in \mathcal{A}^{\mathcal{C}}, \end{cases} \tag{2.32}$$

where the decision functions $h_i : \mathcal{Y}^N \times \mathcal{X}^{i-1} \to \mathcal{X}, i \in \mathcal{A}$ are defined as

$$h_i(y_1^N, \hat{v}_1^{i-1}) \triangleq \begin{cases} 0, & \text{if } W_N^i(y_1^N, \hat{v}_1^{i-1}|0) \geq W_N^i(y_1^N, \hat{v}_1^{i-1}|1) \\ 1, & \text{otherwise.} \end{cases} \tag{2.33}$$

The SCL decoding algorithm was proposed by I. Tal and A. Vardy to complement the SC decoding algorithm in [30]. Unlike the SC decoder, the SCL decoder stores at most $\mathcal{L}$ candidates of the input path in the decoding tree at each decoding stage. Note that the special case $\mathcal{L} = 2^K$ of the SCL decoder is the ML decoder. In [30], they verified that the error performance of the SCL decoder with small $\mathcal{L}$, such as $\mathcal{L} = 32$, approaches that of the ML decoder over the AWGN channel when SNR is high enough.

They also proposed the CRC concatenated polar codes and the CASCL decoding algorithm, which is very similar to the SCL decoding algorithm, except that it checks whether the final path in the list satisfies the CRC. The concept of this algorithm is illustrated in Figure 2.6. It is already known that the ML decoding performance of a linear block code depends on the minimum distance of that code. Also, by concatenating some fixed CRC code as an outer code, a code with large minimum distance can be obtained. As the minimum distance of the concatenated code is increased, the performance of the CASCL decoding algorithm as well as the optimal ML decoding is improved.

There are a number of decoding algorithms of polar codes, such as successive cancellation stack (SCS) decoding algorithm [38] and soft-cancellation (SCAN) algorithm [39]. These algorithms are based on the stack decoding algorithm and the belief propagation (BP) algorithm, respectively. But this dissertation concentrates on the SCL decoding algorithm only.

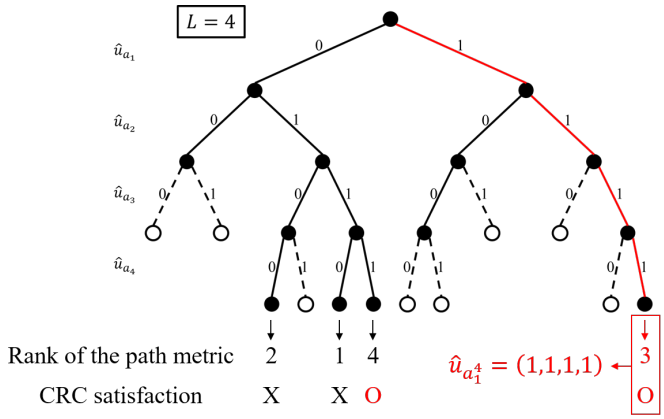

Figure 2.6: Concept of the CASCL decoding algorithm.

2.2 Review of PIC Polar Codes

In this section, there are four subsections to review the PIC polar codes in [36]. First, the code structure of PIC polar codes is introduced. Second, the decoding scheme of polar CB is presented. Third, the inter-CB decoding schemes of PIC polar codes are introduced. In [36], X. Wu *et al.* proposed a look-back and go-back inter-CB decoding scheme to reduce the decoding complexity without loss of TBER performance rather than the conventional sequential inter-CB decoding scheme. Finally, the performance analysis of the look-back and go-back inter-CB decoding scheme is introduced at the fourth subsection.

2.2.1 Encoding Structure of PIC Polar Codes

In this subsection, the construction method of PIC polar codes is reviewed. These codes can be constructed by segmenting long binary $\{0, 1\}$ message bits into the several message blocks with the same length and encoding each message blocks into a systematic polar codeword. Note that each segmented message block is in a line and shares some message bits with neighboring blocks. Note that, two terminal blocks have only one neighboring block. Therefore, each of the sharing bits in the terminal

blocks is 0-padded for the successful decoding performance and homogeneity. In this way, partially information coupling is achieved by sharing some message bits between neighboring blocks. In addition, by encoding each message block into a systematic codeword, it is possible to couple not only the message blocks but also the CBs. This is possible because the systematic codeword contains the coupled message bits explicitly.

The encoding scheme of PIC polar codes consists of three stages:

i) Message segmentation and coupling

ii) Systematic polar CB encoding

iii) CB concatenation.

Figure 2.7 illustrates this encoding scheme.

Let $\mathbf{u}$ be the long binary $\{0, 1\}$ message bits and L be the number of CBs, called the chain length. There are three steps in the message block segmentation and coupling stage. At the first step, called the message segmentation step, $\mathbf{u}$ is segmented into L uncoupled blocks notated as $\{\mathbf{u}_l\}_{1\leq l\leq L}$ and $(L-1)$ coupled blocks notated as $\{\mathbf{u}_l^{\mathrm{c}}\}_{1\leq l\leq (L-1)}$. Let K_{u} and K_{c} be the length of these two types of blocks, respectively. At the second step, called the dummy message insertion step, two all-zero padded dummy message blocks notated as $\mathbf{u}_0^{\mathrm{c}}$ and $\mathbf{u}_L^{\mathrm{c}}$ are attached to the head of $\mathbf{u}_1$ and the tail of $\mathbf{u}_L$, respectively. The length of each dummy message block is K_{c}. At the third step, called the message coupling step, a group of message blocks $\{\mathbf{u}_{l-1}^{\mathrm{c}}, \mathbf{u}_l, \mathbf{u}_l^{\mathrm{c}}\}$ becomes the l-th message block for l, $1 \leq l \leq L$. Thus, the message vector of PIC polar codes is represented as

$$\mathbf{u} = \begin{bmatrix} \mathbf{u}_1 & \mathbf{u}_1^{\mathrm{c}} & \cdots & \mathbf{u}_{l-1}^{\mathrm{c}} & \mathbf{u}_l & \mathbf{u}_l^{\mathrm{c}} & \mathbf{u}_{l+1} & \mathbf{u}_{l+1}^{\mathrm{c}} & \cdots \mathbf{u}_{L-1}^{\mathrm{c}} & \mathbf{u}_L \end{bmatrix}. \tag{2.34}$$

The systematic polar CB encoding stage also consists of the three steps. At the first step, called the CRC attachment step, the K_{CRC}-bit CRC denoted by $\mathbf{c}_l$ is computed and attached to the l-th message block as $\{\mathbf{u}_{l-1}^{\mathrm{c}}, \mathbf{u}_l, \mathbf{u}_l^{\mathrm{c}}, \mathbf{c}_l\}$ for l, $1 \leq l \leq L$. At the

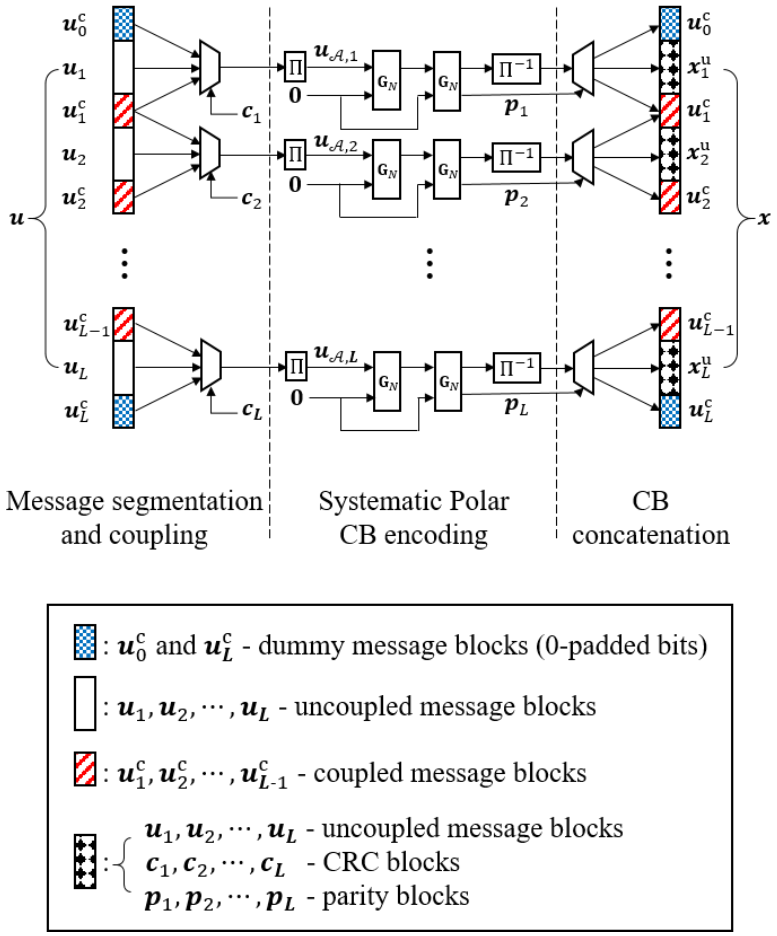

Figure 2.7: Encoding structure of PIC polar codes.

second step, called the interleaving step, the l-th CRC attached message block is interleaved into $u_{\mathcal{A},l}$ for l, $1 \leq l \leq L$, where $\mathcal{A}$ is a set of information indices. Basically, similar to the conventional polar codes, information is sent through the reliable indices while the rest indices are frozen to be zero-padded, where the reliable indices means the indices with good bit-channels and the unreliable indices means the indices with bad bit-channels. Thus, proper allocation from those coupled message blocks, uncoupled message blocks, and CRC blocks to the reliable indices is required. X. Wu *et al.* [36] showed that the decoding performance with interleaving two coupled message

Table 2.1: Three stages of encoding PIC polar codes

Stages	Steps
Message segmentation and coupling	a) Message segmentation b) Dummy message insertion c) Message coupling
Systematic polar CB encoding	a) CRC attachment b) Interleaving c) Systematic polar encoding
CB concatenation	CB concatenation

blocks into the most unreliable index set among the unfrozen index set is better than that with interleaving into the most reliable indices. At the third step, called the systematic encoding step, each $u_{\mathcal{A},l}$'s is encoded by a systematic polar code encoder. As introduced in Subsection 2.1.2, the systematic codeword of each CB can be obtained by multiplying the generator matrix $\mathbf{G}_N$ twice with adequate bit-freezing.

The systematic codeword in the l-th CB can be represented as $\{\mathbf{u}_{l-1}^{\mathrm{c}}, \mathbf{x}_l, \mathbf{u}_l^{\mathrm{c}}\}$, where $\mathbf{u}_{l-1}^{\mathrm{c}}$ and $\mathbf{u}_l^{\mathrm{c}}$ are the head and tail coupled message blocks, respectively and $\mathbf{x}_l$ is the rest part of the codewords in the l-th CB for l, $1 \leq l \leq L$. In the CB concatenation stage, all CBs are concatenated such that coupled message blocks are contained once and dummy message blocks are omitted. Thus, the concatenated codeword of PIC polar codes is represented as

$$\mathbf{x} = \begin{bmatrix} \mathbf{x}_1 & \mathbf{u}_1^{\mathrm{c}} & \cdots & \mathbf{u}_{l-1}^{\mathrm{c}} & \mathbf{x}_l & \mathbf{u}_l^{\mathrm{c}} & \mathbf{x}_{l+1} & \mathbf{u}_{l+1}^{\mathrm{c}} & \cdots \mathbf{u}_{L-1}^{\mathrm{c}} & \mathbf{x}_L \end{bmatrix}. \tag{2.35}$$

Those three stages of encoding PIC polar codes are summarized in Table 2.1

Let K be the total message length of each message block given as

$$K = K_{\mathrm{u}} + 2K_{\mathrm{c}}. \tag{2.36}$$

After PIC polar encoding, the total message length K_{eff} is calculated as

$$K_{\mathrm{eff}} = LK - (L+1)K_{\mathrm{c}}, \tag{2.37}$$

and the total code length N_{eff} is also calculated as

$$N_{\text{eff}} = LN - (L+1)K_{\text{c}}. \tag{2.38}$$

Therefore, the effective code rate R_{eff} is given as

$$R_{\text{eff}} = \frac{LK - (L+1)K_{\text{c}}}{LN - (L+1)K_{\text{c}}}. \tag{2.39}$$

The *coupling ratio* r_c of PIC polar codes is also defined in [36] as

$$r_{\text{c}} = \frac{K_{\text{c}}}{K}. \tag{2.40}$$

As mentioned in Subsection 2.1.2, the interleaved information bits $\mathbf{u}_{\mathcal{A}}$ are explicitly shown in codeword x as a subvector $x_{\mathcal{A}}$. Consider a permutation Π: $\mathbf{u}_1^K \rightarrow \mathbf{u}_{\mathcal{A}}$ and its matrix expression $\mathbf{\Pi}$. By multiplying $\mathbf{\Pi}$ to the left and $\mathbf{\Pi}^{-1}$ to the right of the generator matrix of the systematic encoder $\mathbf{G}_{N,\text{sys}}$, the aligned matrix $\mathbf{G'}_{N,\text{sys}}$ can be written as

$$\begin{aligned} \mathbf{G'}_{N,\text{sys}} &= \mathbf{\Pi}\mathbf{G}_{N,\text{sys}}\mathbf{\Pi}^{-1} \\ &= \begin{bmatrix} \mathbf{I}_{K_c} & \mathbf{0} & \mathbf{0} & \mathbf{P}_1 \\ \mathbf{0} & \mathbf{I}_{K_u} & \mathbf{0} & \mathbf{P}_2 \\ \mathbf{0} & \mathbf{0} & \mathbf{I}_{K_c} & \mathbf{P}_3 \end{bmatrix}, \end{aligned} \tag{2.41}$$

where $\mathbf{P}_1$, $\mathbf{P}_2$, and $\mathbf{P}_3$ are the partial parity matrix of $\mathbf{u}_{l-1}^{\text{c}}$, $\mathbf{u}_l$, and $\mathbf{u}_l^{\text{c}}$, respectively for all l, $1 \leq l \leq L$. This aligned generator matrix $\mathbf{G'}_{N,\text{sys}}$ can be transformed into $\mathbf{G''}_{N,\text{sys}}$ by permuting columns as

$$\mathbf{G''}_{N,\text{sys}} = \begin{bmatrix} \mathbf{I}_{K_c} & \mathbf{0} & \mathbf{P}_1 & \mathbf{0} \\ \mathbf{0} & \mathbf{I}_{K_u} & \mathbf{P}_2 & \mathbf{0} \\ \mathbf{0} & \mathbf{0} & \mathbf{P}_3 & \mathbf{I}_{K_c} \end{bmatrix}. \tag{2.42}$$

Therefore, the encoding of PIC polar codes with generator matrix $\mathbf{G}_{\text{PIC}}$ is expressed

as

$$\mathbf{u}\mathbf{G}_{\mathrm{PIC}} = \mathbf{u}\begin{bmatrix} \ddots & & & & & & & & \\ & \mathbf{I}_{K_c} & \mathbf{0} & \mathbf{P}_1 & \mathbf{0} & & & & \\ & \mathbf{0} & \mathbf{I}_{K_u} & \mathbf{P}_2 & \mathbf{0} & & & & \\ & \mathbf{0} & \mathbf{0} & \mathbf{P}_3 & \mathbf{I}_{K_c} & \mathbf{0} & \mathbf{P}_1 & \mathbf{0} & \\ & & & & \mathbf{0} & \mathbf{I}_{K_u} & \mathbf{P}_2 & \mathbf{0} & \\ & & & & \mathbf{0} & \mathbf{0} & \mathbf{P}_3 & \mathbf{I}_{K_c} & \\ & & & & & & & & \ddots \end{bmatrix}, \tag{2.43}$$

where $\mathbf{u}$ is given in (2.34).

2.2.2 Polar CB Decoding Scheme

In this subsection, the decoding scheme of a PIC polar CB is reviewed. Suppose that binary AWGN channel is used. Then the transmitted signal $\mathbf{t}$ is represented as

$$\mathbf{t} = \mathbf{1} - 2\mathbf{x}, \tag{2.44}$$

where $\mathbf{x}$ is the PIC polar codeword given in (2.35). Also the received signal $\mathbf{r}$ is represented as

$$\mathbf{r} = \mathbf{t} + \mathbf{n}, \tag{2.45}$$

where $\mathbf{n}$ is a white Gaussian noise vector. Let $\mathbf{y}$ be the sequence of the log-likelihood-ratio (LLR) from the received signal $\mathbf{r}$. Note that the sequences of the LLR from the zero-padded blocks, $\mathbf{u}_0^{\mathrm{c}}$ and $\mathbf{u}_L^{\mathrm{c}}$, are given as the sequences of $+\infty$, both.

Recall (2.28)–(2.31) of the systematic polar encoding scheme. The decoded output $\hat{u}_{\mathcal{A}}$ can be obtained by multiplying the submatirx of the generator matrix $\mathbf{G}_N$ as

$$\hat{u}_{\mathcal{A}} = \hat{v}_{\mathcal{A}}\mathbf{G}_{\mathcal{A}\mathcal{A}}. \tag{2.46}$$

where, $\mathbf{G}_{\mathcal{A}\mathcal{A}}$ denotes the submatrix of $\mathbf{G}_N$ with the row index set $\mathcal{A}$ and the column index set $\mathcal{A}$, respectively. The hard-decision decoded output $\hat{v}_{\mathcal{A}}$ can be obtained by applying the CASCL decoder from the sequence of LLR y_1^N.

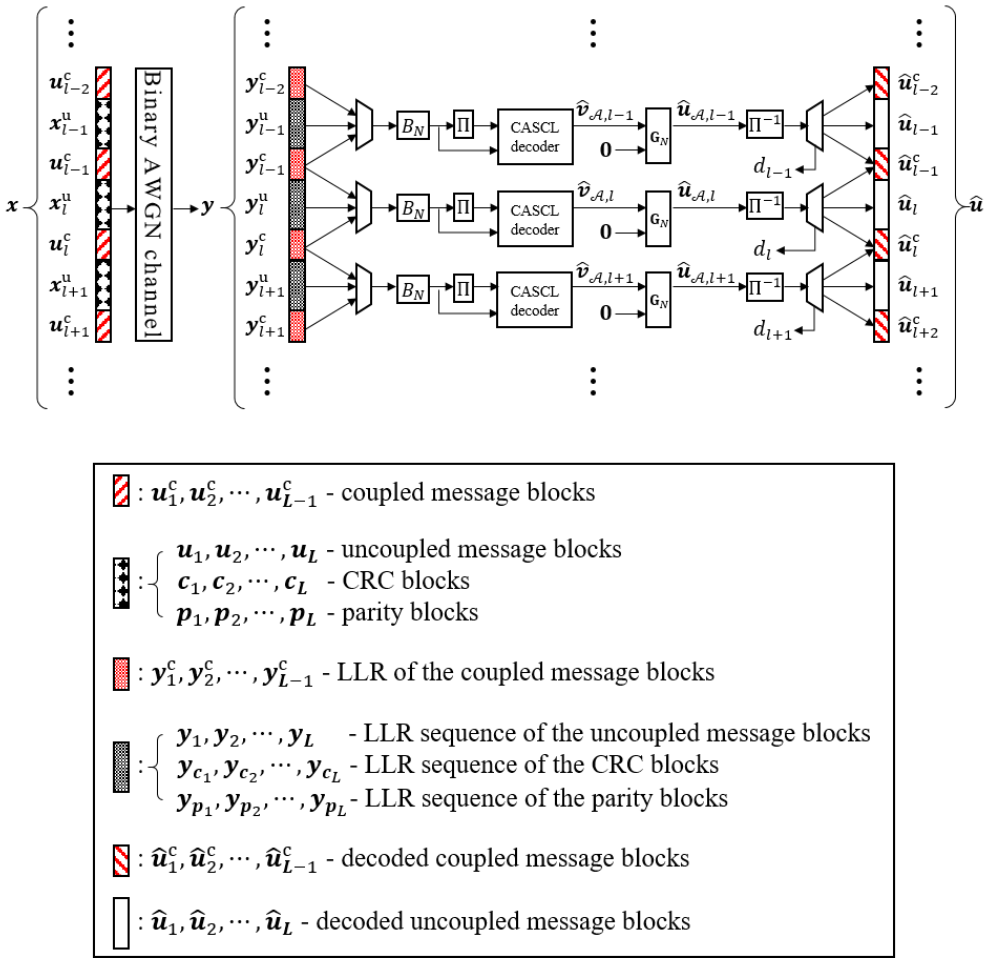

Figure 2.8: Decoding scheme of the l-th polar CB.

For any spatially coupled codes, if the decoding result of any coupled CB is successful, the extrinsic information obtained from the coupled CB can also increase the successful CB decoding probability. Especially for PIC polar codes, it is assumed that the extrinsic information is nearly perfect with the aid of long-enough CRC.

Let d_l be the decoding indicator of the l-th CB decoding result for l, $1 \leq l \leq L$.

For PIC polar codes, it is determined as

$$d_l = \begin{cases} 1, & \text{if CRC does not detect errors} \\ 0, & \text{otherwise.} \end{cases} \tag{2.47}$$

The input LLR y_1^N of the l-th polar CB can be partitioned into $\{\mathbf{y}_{l-1}^{\mathrm{c}}, \mathbf{y}_l, \mathbf{y}_l^{\mathrm{c}}\}$, where $\mathbf{y}_{l-1}^{\mathrm{c}}$ and $\mathbf{y}_l^{\mathrm{c}}$ represent the LLR sequence of the head and tail coupled message blocks $\mathbf{u}_{l-1}^{\mathrm{c}}$ and $\mathbf{u}_l^{\mathrm{c}}$, respectively. Also $\mathbf{y}_l$ represents the LLR sequence of the uncoupled message blocks, CRC blocks, and parity blocks. Figure 2.8 illustrates the decoding scheme of the l-th polar CB.

The input LLR sequences $\mathbf{y}_{l-1}^{\mathrm{c}}$ and $\mathbf{y}_l^{\mathrm{c}}$ of the coupled message blocks can be updated by

$$\mathbf{y}_{l-1}^{\mathrm{c}} = \begin{cases} \infty \cdot (\mathbf{1} - 2\hat{\mathbf{u}}_{l-1}^{\mathrm{c}}), & \text{if } d_{l-1} = 1 \\ \mathbf{y}_{l-1}^{\mathrm{c}}, & \text{if } d_{l-1} = 0 \end{cases} \tag{2.48}$$

and

$$\mathbf{y}_l^{\mathrm{c}} = \begin{cases} \infty \cdot (\mathbf{1} - 2\hat{\mathbf{u}}_l^{\mathrm{c}}), & \text{if } d_{l+1} = 1 \\ \mathbf{y}_l^{\mathrm{c}}, & \text{if } d_{l+1} = 0, \end{cases} \tag{2.49}$$

where $\hat{\mathbf{u}}_{l-1}^{\mathrm{c}}$ and $\hat{\mathbf{u}}_l^{\mathrm{c}}$ are the decoded message blocks of the input coupled message blocks $\mathbf{u}_{l-1}^{\mathrm{c}}$ and $\mathbf{u}_l^{\mathrm{c}}$ obtained by using the systematic CASCL decoder. These extrinsic information updates improve the l-th CB decoding performance for $d_{l-1} = 1$ or $d_{l+1} = 1$.

2.2.3 Inter-CB Decoding Schemes

Inter-CB decoding means a rule for determining a CB to be decoded next according to the decoding indicators $\{d_l\}_{1 \le l \le L}$ of all CBs. The conventional parallel and sequential inter-CB decoding schemes are introduced as in Figure 2.9 and their complexity and latency are derived in [36]. Note that the blocks in (b) and (c) correspond to the blocks in (a) in Figure 2.9. Based on the sequential inter-CB decoding scheme, they also proposed and concentrated on the look-back and go-back inter-CB decoding scheme,

which is superior to the sequential inter-CB decoding scheme in terms of decoding latency and complexity without sacrificing the TBER performance.

In the conventional sequential inter-CB decoding scheme, PIC polar CBs are decoded sequentially from the head $(l = 1)$ to the tail $(l = L)$, which is called the feed-forward (FF) decoding process, and then the feed-back (FB) decoding process is performed in the opposite direction.

As in Figure 2.10, on the other hand, in the look-back and go-back inter-CB decoding scheme, the FB decoding process can be performed until $d_l = 1$ and $d_{l-1} = 0$ for any l for $1 \leq l \leq L$. The look-back and go-back inter-CB decoding algorithm is given in Algorithm 2.1 and its flowchart is illustrated in Figure 2.11. By quickly converting from the FF decoding process to the FB decoding process, it is possible to fine the undecodable but detectable errors in the middle of inter-CB decoding process, and thus declare a transport block (TB) error. Note that a TB error is an event as

$$\hat{\mathbf{u}} \neq \mathbf{u}, \tag{2.50}$$

where $\hat{\mathbf{u}}$ and $\mathbf{u}$ are the decoded and transmitted message vectors, respectively. It is recommended to read the conditions for **early conversion** and **early termination** carefully. These conditions will be modified in Section 4.4 for the modified look-back and go-back inter-CB decoding scheme of proposed PIC polar codes.

2.2.4 Performance Analysis of PIC Polar Codes

They defined four CB error events in [36] that the decoding of the l-th polar CB fails with:

i) No coupling information available

ii) Only head coupling information available

iii) Only tail coupling information available

iv) Both head and tail coupling information available.

The probabilities of these four events are denoted by P_0, $P_{1\mathrm{h}}$, $P_{1\mathrm{t}}$, and P_2, respectively. Over the AWGN channel, these probabilities can be accessed by using Gaussian approximation [22] for $\mathcal{L} = 1$, i.e., SC decoding, or by Monte-Carlo simulations for arbitrary $\mathcal{L}$.

Using these four probabilities, the code block error rate (CBER) of the l-th polar CB in the FF decoding process, $\mathrm{Pr}_l\{\mathrm{FF\ fail}\}$, can be derived. $\mathrm{Pr}_l\{\mathrm{FB\ success}|\mathrm{FF\ fail}\}$ was also derived, which represents the conditional probability that the polar CB is successfully decoded in the FB decoding process given that it was not successfully decoded in the FF decoding process. Using these two probabilities, the CBER of the l-th CB in the FB decoding process denoted by $\mathrm{Pr}_l\{\mathrm{FB\ fail}\}$ can be written as

$$\mathrm{Pr}_l\{\mathrm{FB\ fail}\} = \mathrm{Pr}_l\{\mathrm{FF\ fail}\} - \mathrm{Pr}_l\{\mathrm{FB\ success}|\mathrm{FF\ fail}\}. \tag{2.51}$$

They notated $\mathrm{Pr}_l\{\mathrm{FB\ fail}\}$ shortly as P_l^{B}. Under the assumption that the all CB error events are independent each other, the TBER of the PIC polar codes under the look-back and go-back inter-CB decoding scheme can be written as

$$P_f = 1 - \prod_{1 \le l \le L} (1 - P_l^{\mathrm{B}}). \tag{2.52}$$

Using (2.52), they showed that coupling with unreliable message blocks each other is better than that with reliable message blocks, in terms of TBER performance. They also confirmed it using Monte-Carlo simulation. Detailed explanations and derivations are described in [36].

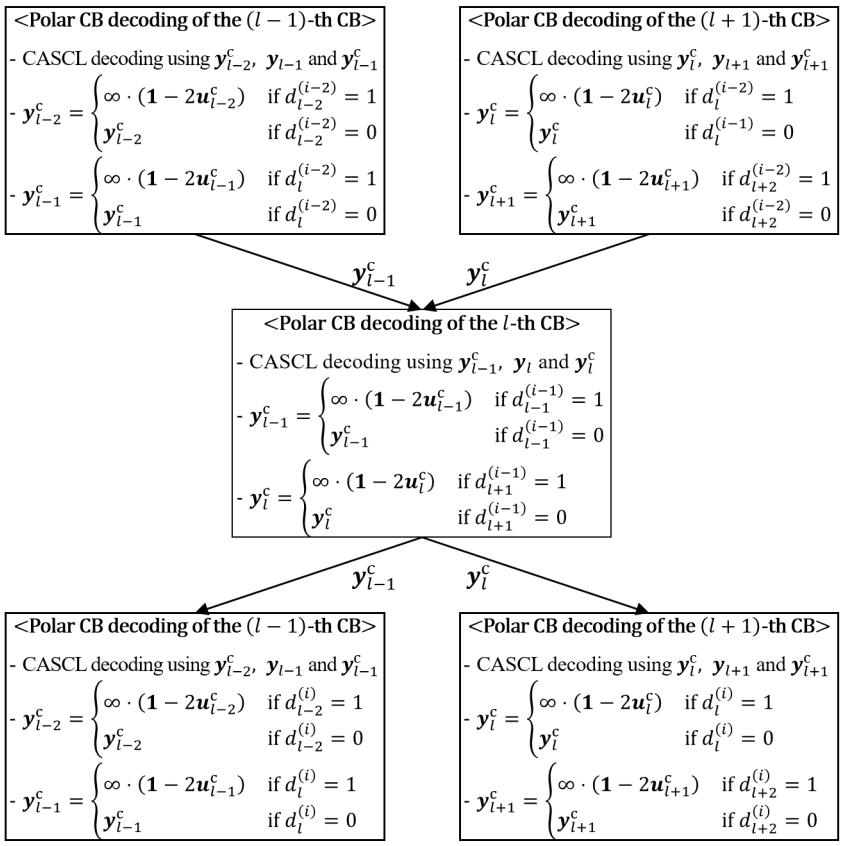

(a) Concept of the inter-CB decoding

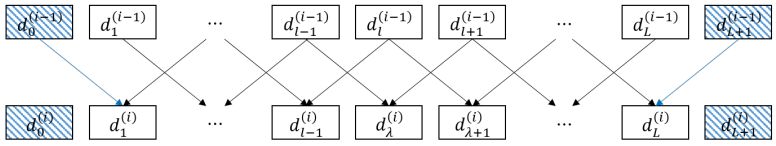

(b) Parallel inter-CB decoding scheme

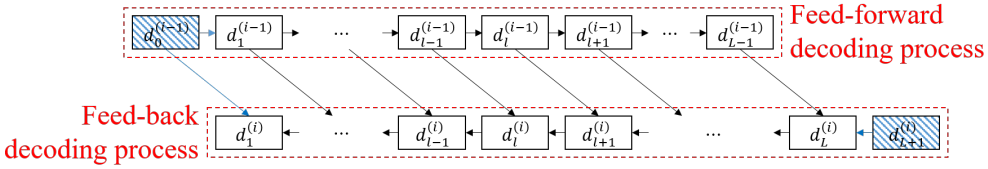

(c) Sequential inter-CB decoding scheme

Figure 2.9: Two main inter-CB decoding schemes of PIC polar codes.

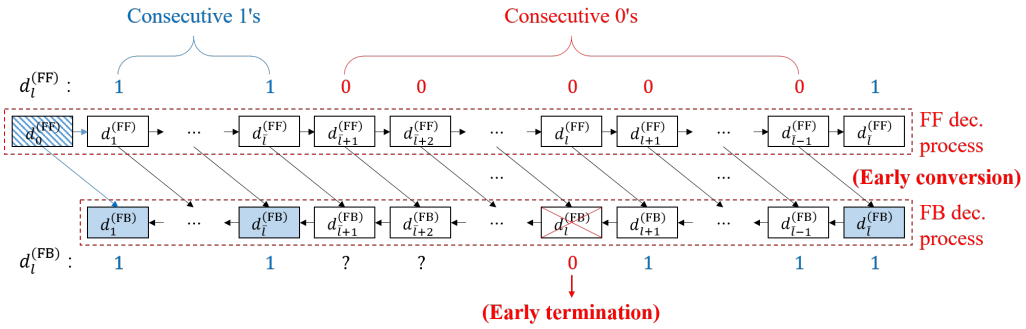

(a) Early termination scenario of the look-back and go-back inter-CB decoding scheme

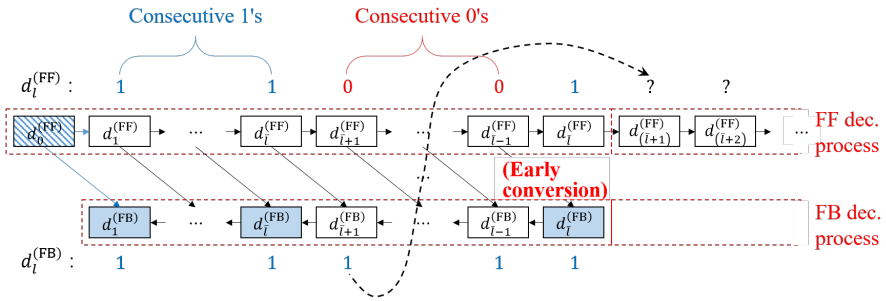

- Note that the dashed block represents the aid of the dummy message block.
- Note that the colored block represents the correctly decoded CB in the FF decoding process.
- If the decoding result of the $(\tilde{l}+1)$-th block is successful in the FB decoding process, that is, $d_{\tilde{l}+1}^{(\mathrm{FB})} = 1$, then set $l \leftarrow (\tilde{l}+1)$ and proceed the FF decoding process.

(b) Process conversion scenario of the look-back and go-back inter-CB decoding scheme

Figure 2.10: Look-back and go-back inter-CB decoding scheme.

Algorithm 2.1 Look-back and go-back inter-CB decoding algorithm [36]

Input: $\{\mathbf{y}_{l-1}^{\mathrm{c}}, \mathbf{y}_l, \mathbf{y}_l^{\mathrm{c}}\}_{l=1}^{L}$

1: **Initialization**:
$$\begin{cases} \mathbf{y}_0^{\mathrm{c}} = \mathbf{y}_L^{\mathrm{c}} = \infty \cdot \mathbf{1} \\ d_0 = d_{L+1} = 1 \\ \tilde{l} = 0, \text{ and } l = (\tilde{l} + 1). \end{cases}$$

2: **while do**

3: **FF decoding**:

4: **while** $l \leq L$ **do**

5: Decode the l-th CB using the polar CB decoder, if $d_l = 0$.

a) If $d_l = 1$ for all $1 \leq l \leq L$
go to **Message concatenation** process.

b) If $d_l = 1$ and $d_{l-1} = 0$
update $\tilde{l} \leftarrow l$ and $l \leftarrow (\tilde{l} - 1)$, then go to **FB decoding** process. (**early conversion**)

c) If $l = L$ and $d_L = 0$
exit decoding and declare a TB error.

d) Else
update $l \leftarrow (l + 1)$ continue **FF decoding** process.

6: **end while**

7: **FB decoding**:

8: **while** $1 \leq l$ **do**

9: Decode the l-th CB using the polar CB decoder, if $d_l = 0$.

a) If $d_l = 1$ for all $1 \leq l \leq L$
go to **Message concatenation** process.

b) If $d_l = 0$
exit decoding and declare a TB error. (**early termination**)

c) If $d_l = 1$ and $d_{l-1} = 1$
update $l \leftarrow (\tilde{l} + 1)$, then go to **FF decoding** process.

d) Else
update $l \leftarrow (l - 1)$ and continue **FB decoding** process.

10: **end while**

11: **end while**

12: **Message concatenation**: Concatenate all decoded uncoupled message blocks $\{\hat{\mathbf{u}}_l\}_{1 \leq l \leq L}$ and decoded coupled message blocks $\{\hat{\mathbf{u}}_l^{\mathrm{c}}\}_{1 \leq l \leq L-1}$ to obtain the decoded output $\hat{\mathbf{u}}$.

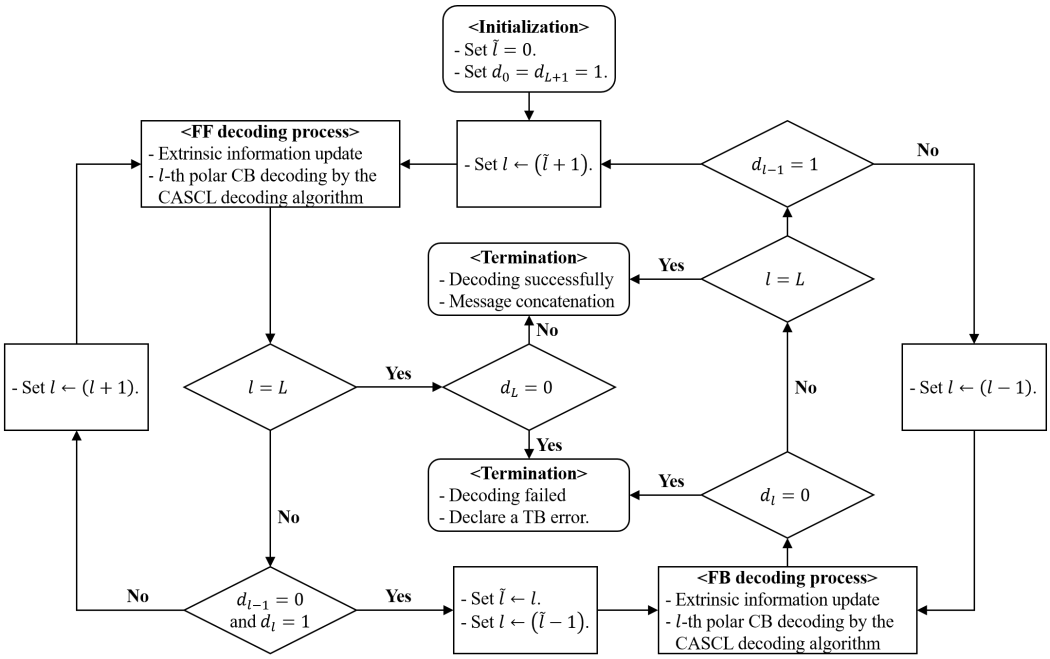

Figure 2.11: Flowchart of the look-back and go-back inter-CB decoding algorithm.

Chapter 3

Encoding Structure of PIC Polar Codes with Coupling Depth J

As reviewed in Subsection 2.2.2, the performance gain of information coupling is due to the extrinsic information update obtained from the successfully decoded adjacent CBs. If more than two CBs could deliver the extrinsic information, can PIC polar codes obtain more coding gain from the coupling diversity? This question becomes the motivation to improve the performance of PIC polar codes in this dissertation. In the conventional PIC polar codes [36], each CB is coupled with only the adjacent immediate CBs. On the other hands, in our proposed codes, each CB can be coupled with more than one CB to obtain the coupling diversity.

This chapter consists of three sections. In the first section, the generalized coupling method of the proposed PIC polar codes is introduced. In the second section, the generalized message segmentation and coupling stage is proposed. Based on the generalized step, the encoding structure of the proposed PIC polar codes is introduced in the third section. Since the structure of the proposed PIC polar codes is very similar to that of the conventional PIC polar codes, it is recommended to concentrate on the different notations and encoding structures between the conventional and the proposed PIC polar codes.

3.1 Coupling Method of the Proposed PIC Polar Codes

The coupling depth in the proposed PIC polar codes is defined as follows.

Definition 1. *Let J_l^{h} and J_l^{t}, $1 \leq l \leq L$, be the l-th head coupling depth and l-th tail coupling depth, which are the numbers of CBs coupled with the l-th CB in the head and tail directions, respectively.*

Considering homogeneity for easy analysis, this dissertation only focuses on the case that all J_l^{h}'s and J_l^{t}'s are equal to J. These PIC polar codes are called PIC polar codes with coupling depth J. The segmented message blocks of the proposed PIC polar codes are illustrated in Figure 3.1. Note that the conventional PIC polar codes are the special case $J = 1$ of the proposed generalization of PIC polar codes.

Unlike the conventional PIC codes, i.e., for $J \geq 2$, it is not possible to segment the message bits so that the coupled and uncoupled message blocks appear alternately. Thus, a method of message segmentation for the PIC polar codes with coupling depth J is proposed in the next section. The proposed message segmentation structure also affects to the extrinsic information update stage at the polar CB decoding scheme, which further improve the performance of the proposed PIC polar codes. It is recommended to understand the relationship between the encoding structure of the conventional PIC polar codes and their extrinsic information updates in (2.47)–(2.49). In addition, the effective message length, code length, code rate, and coupling ratio of the proposed PIC polar codes are also derived.

3.2 Message Segmentation and Coupling

In this section, a new method of message segmentation and coupling for the PIC polar codes with coupling depth J is proposed. The message block of the l-th CB is segmented into $\mathbf{u}_l^{\mathrm{h}}$, $\mathbf{u}_l$, and $\mathbf{u}_l^{\mathrm{t}}$ for l, $1 \leq l \leq L$. The coupled message blocks $\mathbf{u}_l^{\mathrm{h}}$ and $\mathbf{u}_l^{\mathrm{t}}$ are also segmented into $\{\mathbf{u}_{l,1}^{\mathrm{h}}, \mathbf{u}_{l,2}^{\mathrm{h}}, \cdots, \mathbf{u}_{l,J}^{\mathrm{h}}\}$ and $\{\mathbf{u}_{l,1}^{\mathrm{t}}, \mathbf{u}_{l,2}^{\mathrm{t}}, \cdots, \mathbf{u}_{l,J}^{\mathrm{t}}\}$, respectively, as in Figure 3.1.

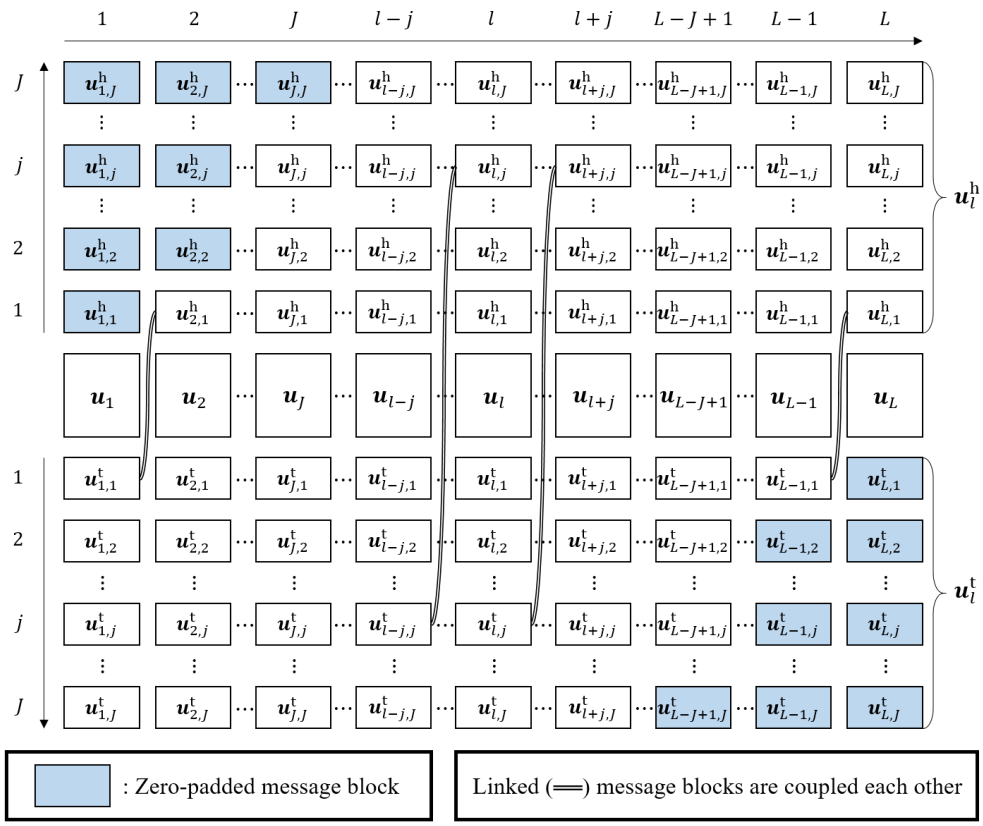

Figure 3.1: Segmented and coupled message blocks for chain length L and coupling depth J.

The coupled message blocks $\{\mathbf{u}^{\mathrm{h}}_{l,1}, \mathbf{u}^{\mathrm{h}}_{l,2}, \cdots, \mathbf{u}^{\mathrm{h}}_{l,J}\}$ and $\{\mathbf{u}^{\mathrm{t}}_{l,1}, \mathbf{u}^{\mathrm{t}}_{l,2}, \cdots, \mathbf{u}^{\mathrm{t}}_{l,J}\}$ are duplicated or zero-padded, because of the coupling or dummy message insertion. For l, $1 \leq l \leq L$, and j, $1 \leq j \leq J$, the head coupled message block $\mathbf{u}^{\mathrm{h}}_{l,j}$ is given by

$$\mathbf{u}^{\mathrm{h}}_{l,j} = \begin{cases} \mathbf{0}, & \text{if } l \leq j \\ \mathbf{u}^{\mathrm{t}}_{l-j,j}, & \text{otherwise} \end{cases} \tag{3.1}$$

and the tail coupled message block $\mathbf{u}^{\mathrm{t}}_{l,j}$ is given by

$$\mathbf{u}^{\mathrm{t}}_{l,j} = \begin{cases} \mathbf{0}, & \text{if } l \geq L + 1 - j \\ \mathbf{u}^{\mathrm{h}}_{l+j,j}, & \text{otherwise,} \end{cases} \tag{3.2}$$

where $\mathbf{0}$ means the zero-padded message block with length K_{c}. Figure 3.1 helps to understand (3.1) and (3.2).

3.3 Encoding Structure of the Proposed PIC Polar Codes with Coupling Depth J

In this section, the encoding structure of the proposed PIC polar codes with coupling depth J is introduced. Similar to the encoding structure of the conventional PIC polar codes, the encoding structure of the proposed PIC polar codes also consists of three stages:

i) Message segmentation and coupling

ii) Systematic polar CB encoding

iii) CB concatenation.

Figure 3.2 shows the encoding structure of the proposed PIC polar codes. Most of this figure are similar to Figure 2.7 except some notations and message segmentation and CB concatenation stages.

As discussed in the previous section, a long binary $\{0, 1\}$ message bits $\mathbf{u}$ is segmented and zero-padded into L message blocks in the message segmentation and coupling stage, which is the first stage of the proposed PIC polar encoding. The l-th message block is expressed as $\{\mathbf{u}_l^{\mathrm{h}}, \mathbf{u}_l, \mathbf{u}_l^{\mathrm{t}}\}$ for l, $1 \leq l \leq L$, where $\mathbf{u}_l^{\mathrm{h}}$, $\mathbf{u}_l$, and $\mathbf{u}_l^{\mathrm{t}}$ are the head coupled, the uncoupled, and tail coupled message blocks of the l-th message block, respectively. The coupled message blocks $\mathbf{u}_l^{\mathrm{h}}$ and $\mathbf{u}_l^{\mathrm{t}}$ are segmented into $\{\mathbf{u}_{l,1}^{\mathrm{h}}, \mathbf{u}_{l,2}^{\mathrm{h}}, \cdots, \mathbf{u}_{l,J}^{\mathrm{h}}\}$ and $\{\mathbf{u}_{l,1}^{\mathrm{t}}, \mathbf{u}_{l,2}^{\mathrm{t}}, \cdots, \mathbf{u}_{l,J}^{\mathrm{t}}\}$, respectively as in Figure 3.1.

The systematic polar CB encoding stage of the proposed PIC polar codes is the same as the systematic polar CB encoding stage of the conventional PIC polar codes. Thus, this stage also consists of the three steps. At the first step, called the CRC attachment step, each message block is encoded by some fixed CRC with length K_{CRC}.

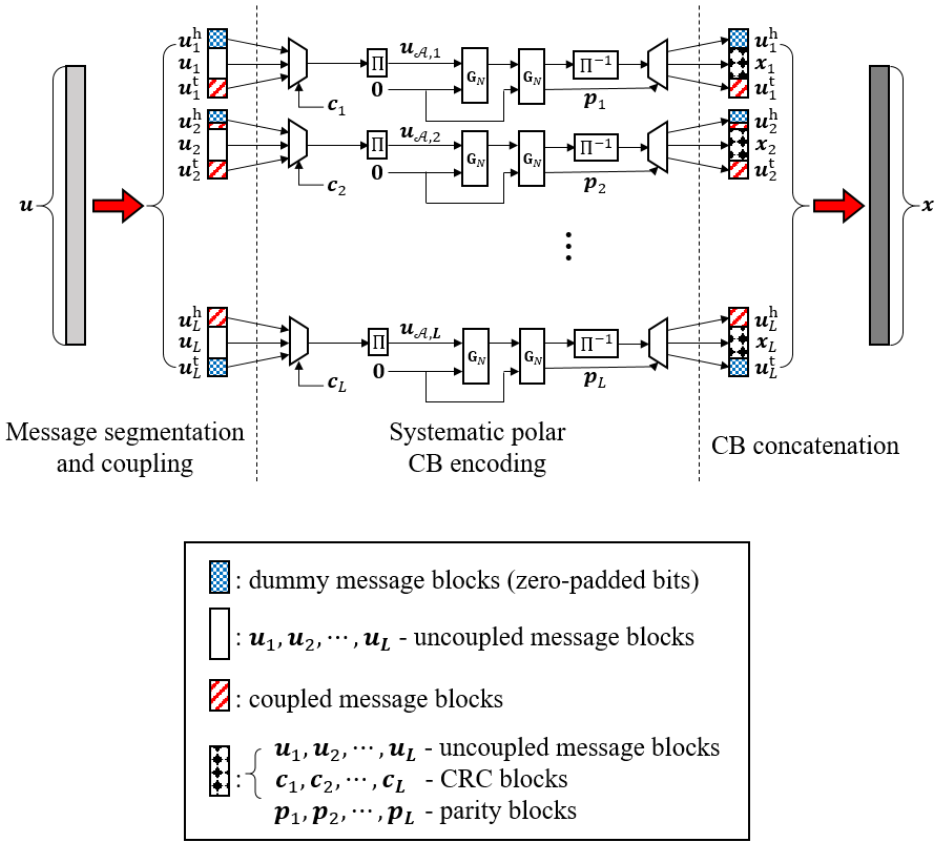

Figure 3.2: Encoding structure of the proposed PIC polar codes.

Let $\mathbf{c}_l$ be the K_{CRC}-bit CRC for the l-th message block. This CRC is appended as $\{\mathbf{u}_l^{\mathrm{h}}, \mathbf{u}_l, \mathbf{u}_l^{\mathrm{t}}, \mathbf{c}_l\}$ for l, $1 \leq l \leq L$. At the second step, called the interleaving step, the l-th CRC encoded information $\{\mathbf{u}_l^{\mathrm{h}}, \mathbf{u}_l, \mathbf{u}_l^{\mathrm{t}}, \mathbf{c}_l\}$ is interleaved into $u_{\mathcal{A},l}$ for l, $1 \leq l \leq L$. Note that $\mathcal{A}$ is used as a set of information indices of the polar codes, where the reliability of each index in $\mathcal{A}$ is different. As the optimization result of the coupling scheme in [36], the coupled message blocks are interleaved into the unreliable indices of $\mathcal{A}$, whereas the uncoupled one is interleaved into the reliable indices. At the third step, called the systematic encoding step, each $u_{\mathcal{A},l}$ is systematically encoded by the systematic polar encoder, for all l, $1 \leq l \leq L$.

In the CB concatenation stage, the individual CBs are concatenated except for

the overlapped codewords due to the coupling or dummy message insertion. That is, from (3.1) and (3.2), the head coupled message blocks are exactly the same as the tail coupled message blocks, and thus, only one kind of blocks of them are included in the codeword. The concatenated codeword $\mathbf{x}$ can be represented as

$$\mathbf{x} = \{x_1, u_1^{\mathrm{t}}, x_2, u_2^{\mathrm{t}}, \cdots, x_{L-1}, u_{L-1}^{\mathrm{t}}, x_L\}, \tag{3.3}$$

where the zero-padded tail coupled message blocks are omitted in $u_{L-J+1}^{\mathrm{t}}, \cdots, u_{L-1}^{\mathrm{t}}, u_L^{\mathrm{t}}$ from (3.2). Clearly, u_L^{t} is composed of all zero-padded block and thus, it is deleted. Also, the i-th element of the l-th uncoupled CB $\mathbf{x}_l$ denoted by $(\mathbf{x}_l)_i$ is given as

$$(\mathbf{x}_l)_i = \begin{cases} (\mathbf{u}_l)_i, & \text{if } 1 \le i \le K_{\mathrm{u}} \\ (\mathbf{c}_l)_{i-K_{\mathrm{u}}}, & \text{if } K_{\mathrm{u}}+1 \le i \le K_{\mathrm{u}}+K_{\mathrm{CRC}} \\ (\mathbf{p}_l)_{i-K_{\mathrm{u}}-K_{\mathrm{CRC}}}, & \text{if } K_{\mathrm{u}}+K_{\mathrm{CRC}}+1 \le i \le N-2K_{\mathrm{c}}, \end{cases} \tag{3.4}$$

where $\mathbf{p}_l$ is the parity block of the l-th CB.

Since the more dummy blocks are used as J increases, the effective message and code length of the proposed PIC polar codes are slightly different from the values in the conventional PIC polar codes. Let N be the code length of each CB and let K be the total message length of each CB. Note that the total message length K can be expressed as

$$K = K_{\mathrm{u}} + 2JK_{\mathrm{c}}, \tag{3.5}$$

where K_{u} and K_{c} are the lengths of the uncoupled message block $\mathbf{u}_l$ and the coupled message block $\mathbf{u}_{l,j}^{\mathrm{h}}$ or $\mathbf{u}_{l,j}^{\mathrm{t}}$, respectively.

As shown in Figure 3.1, the $\frac{J(J+1)}{2}$ coupled message blocks with length K_{c} are zero-padded and $LJ - \frac{J(J+1)}{2}$ coupled message blocks with length K_{c} are coupled in the head and tail directions, respectively. Therefore, the effective message length K_{eff} of the proposed PIC polar codes with coupling depth J is given as

$$\begin{aligned} K_{\mathrm{eff}} &= LK_{\mathrm{u}} + (LJ - \frac{J(J+1)}{2})K_{\mathrm{c}} \\ &= LK - (LJ + \frac{J(J+1)}{2})K_{\mathrm{c}}, \end{aligned} \tag{3.6}$$

where the head coupled message blocks are exactly duplicated to the tail coupled message blocks from (3.1) and (3.2). The effective code length N_{eff} is given as

$$N_{\text{eff}} = LN - (LJ + \frac{J(J+1)}{2})K_{\text{c}}, \tag{3.7}$$

where the duplicated blocks in the codewords are exactly the same as those in the message. Then the effective code rate R_{eff} is derived as

$$R_{\text{eff}} = \frac{LK - (LJ + \frac{J(J+1)}{2})K_{\text{c}}}{LN - (LJ + \frac{J(J+1)}{2})K_{\text{c}}}. \tag{3.8}$$

Also, the coupling ratio in (2.40) is given as

$$r_{\text{c}} = \frac{JK_{\text{c}}}{K}. \tag{3.9}$$

Chapter 4

Decoding Schemes of PIC Polar Codes with Coupling Depth J

There are two main decoding stages in the decoding algorithm of PIC polar codes with coupling depth J, called polar CB decoding stage and inter-CB decoding stage. In the polar CB decoding stage, the l-th CB is decoded under the CASCL decoding algorithm with the aid of extrinsic information from the coupled CBs for l, $1 \leq l \leq L$. Then, the l-th decoding indicator d_l and the decoded message block are returned to the inter-CB decoding stage. In the inter-CB decoding stage, the CB to be decoded is selected under the inter-CB decoding algorithm with the sequence of the decoding indicators $\{d_l\}_{l=1}^{L}$. Then, the index l is returned to the polar CB decoding stage. The relationship between these two maid decoding stages of the PIC polar decoding is shown in Figure 4.1.

The remainder of this chapter consists of five sections. In the first section, the polar CB decoding stage of the proposed PIC polar codes with coupling depth J is proposed. In the second section, the parallel inter-CB decoding schemes and the modified parallel inter-CB decoding scheme of the proposed PIC polar codes with coupling depth J are proposed. In the third section, the sequential inter-CB decoding schemes and the modified parallel inter-CB decoding scheme of the proposed PIC polar codes with coupling depth J are proposed. In the fourth section, the look-back and go-back inter-

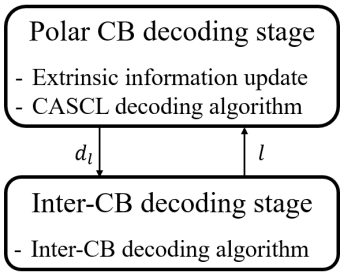

Figure 4.1: Two main decoding stages of the PIC polar decoding.

CB decoding scheme in [36] is modified to apply the coupling depth $J = 2$. In the fifth section, a new inter-CB decoding scheme is proposed, which is called the sequential and probabilistic re-decoding inter-CB decoding scheme.

4.1 Polar CB Decoding of the Proposed PIC Polar Codes with Coupling Depth J

In this section, a polar CB decoding of the proposed PIC polar codes with coupling depth J is proposed. The basic concept of the proposed polar CB decoding is similar to that of the conventional one. The proposed polar CB decoding also consists of the extrinsic information update stage and the systematic decoding stage using the CASCL decoder. The difference of the proposed and conventional polar CB decoding is in the extrinsic information update stage, because the message segmentation and coupling schemes of the conventional and proposed PIC polar codes are different, due to the coupling depth J.

Let d_l be the decoding indicator of the l-th CB in (2.47) for l, $1 \leq l \leq L$. To express the aids of the dummy message blocks (zero-padded bits), the decoding indicator d_l is given as

$$d_l = 1, \quad \text{if } l < 1 \text{ or } l > L. \tag{4.1}$$

The input LLR y_1^N of the l-th polar CB can be partitioned into $\{\mathbf{y}_{l,1}^{\mathrm{h}}, \mathbf{y}_{l,2}^{\mathrm{h}}, \cdots, \mathbf{y}_{l,J}^{\mathrm{h}}, \mathbf{y}_l, \mathbf{y}_{l,1}^{\mathrm{t}}, \mathbf{y}_{l,2}^{\mathrm{t}}, \cdots, \mathbf{y}_{l,J}^{\mathrm{t}}\}$, where $\mathbf{y}_{l,j}^{\mathrm{h}}$ and $\mathbf{y}_{l,j}^{\mathrm{t}}$ represent the LLR sequence of the j-th head and tail coupled message blocks $\mathbf{u}_{l,j}^{\mathrm{h}}$ and $\mathbf{u}_{l,j}^{\mathrm{t}}$, respectively for all j, $1 \leq j \leq J$. The LLR sequence $\mathbf{y}_l$ corresponds to the rest blocks, such as the uncoupled message blocks, CRC blocks, and parity blocks of the l-th CB.

From (3.1), (3.2), and (4.1), the input LLR sequences $\mathbf{y}_{l,j}^{\mathrm{h}}$ and $\mathbf{y}_{l,j}^{\mathrm{t}}$ of the coupled message blocks in the proposed PIC polar codes can be updated by

$$\mathbf{y}_{l,j}^{\mathrm{h}} = \begin{cases} \infty \cdot \mathbf{1}, & \text{if } 1 \leq l \leq j \\ \infty \cdot (\mathbf{1} - 2\hat{\mathbf{u}}_{l-j,j}^{\mathrm{t}}), & \text{if } j < l \leq L \text{ and } d_{l-j} = 1 \\ \mathbf{y}_{l,j}^{\mathrm{h}}, & \text{if } j < l \leq L \text{ and } d_{l-j} = 0 \end{cases} \tag{4.2}$$

and

$$\mathbf{y}_{l,j}^{\mathrm{t}} = \begin{cases} \infty \cdot \mathbf{1}, & \text{if } L+1-j \leq l \leq L \\ \infty \cdot (\mathbf{1} - 2\hat{\mathbf{u}}_{l+j,j}^{\mathrm{h}}), & \text{if } 1 \leq l < L+1-j \text{ and } d_{l+j} = 1 \\ \mathbf{y}_{l,j}^{\mathrm{t}}, & \text{if } 1 \leq l < L+1-j \text{ and } d_{l+j} = 0. \end{cases} \tag{4.3}$$

The remaining of the proposed polar CB decoding stage is the same as that of the conventional one.

4.2 Parallel Inter-CB Decoding Schemes of the Proposed PIC Polar Codes with Coupling Depth J

In this section, two parallel inter-CB decoding schemes of the proposed PIC polar codes with coupling depth J are generalized and a modified parallel inter-CB decoding scheme of the same codes is proposed. Also, the advantages and disadvantages of the parallel inter-CB decoding scheme are presented.

The one-shot parallel inter-CB decoding algorithm of the proposed PIC polar codes with coupling depth J in Algorithm 4.1 is similar to the one-shot parallel inter-CB decoding algorithm in [36] except **Input**, **Initialization**, and **Message concatenation**

Algorithm 4.1 One-shot parallel inter-CB decoding algorithm of the proposed PIC polar codes with coupling depth J

Input: $\{\mathbf{y}_{l,1}^{\mathrm{h}}, \mathbf{y}_{l,2}^{\mathrm{h}}, \cdots, \mathbf{y}_{l,J}^{\mathrm{h}}, \mathbf{y}_l, \mathbf{y}_{l,1}^{\mathrm{t}}, \mathbf{y}_{l,2}^{\mathrm{t}}, \cdots, \mathbf{y}_{l,J}^{\mathrm{t}}\}_{l=1}^{L}$

1: **Initialization**:
$$\begin{cases} \mathbf{y}_{l,j}^{\mathrm{h}} = \infty \cdot \mathbf{1}, \text{ if } 1 \le l \le j \\ \mathbf{y}_{l,j}^{\mathrm{t}} = \infty \cdot \mathbf{1}, \text{ if } L+1-j \le l \le L \\ \{d_l\}_{1 \le l \le L} = \mathbf{0}, \{d_l\}_{l<1} = \mathbf{1}, \text{ and } \{d_l\}_{l>L} = \mathbf{1} \\ l = 1. \end{cases}$$

2: **while** $l \le L$ **do**

3: **CB decoding**: Decode the l-th CB using the CASCL decoder.

4: **CB index updating**: $l \leftarrow (l+1)$.

5: **end while**

6: **Message concatenation**: Concatenate all $\hat{\mathbf{u}}_l$ and $\hat{\mathbf{u}}_l^{\mathrm{t}}$ to obtain the decoded output $\hat{\mathbf{u}}$ for all l, $1 \le l \le L$.

stages. This decoding algorithm is the simplest inter-CB decoding algorithm, but the performance of this decoding algorithm is far degraded because the extrinsic information from the coupled message blocks is not used in Algorithm 4.1. Further, only the estimated tail coupled message blocks $\hat{\mathbf{u}}_l^{\mathrm{t}}$ and the estimated uncoupled message blocks $\hat{\mathbf{u}}_l$ are used in **Message concatenation** stage for all l, $1 \le l \le L$ to avoid the mismatches of the estimated head coupled message blocks and the estimated tail coupled message blocks.

The conventional parallel inter-CB decoding algorithm of the proposed PIC polar codes with coupling depth J in Algorithm 4.2 is also similar to the one-shot parallel inter-CB decoding algorithm in [36] except **Input**, **Initialization**, **Extrinsic information updating**, and **Message concatenation** stages. In this algorithm, all CBs are simultaneously decoded using the polar CB decoder in the **CB decoding** stage and then the extrinsic information of all CBs is simultaneously updated in **Extrinsic information updating** stage. These two stages are alternatively repeated until all decoding

indicators are equal to 1, which means that the decoding is successful, or all indicators are unchanged, which means that the decoding is failed.

Though the parallel inter-CB decoding algorithm requires higher decoding-complexity than the sequential inter-CB decoding algorithms in [36], it has three advantages as follows. The first one is versatility. The parallel inter-CB decoding algorithm can be applied not only to the proposed PIC polar codes with coupling depth J, but also to any PIC polar codes with the generalized coupling schemes. Note that in the PIC polar codes with the generalized coupling schemes, it is not necessary to couple the J nearest CBs.

The second one is analyzability from the homogeneity of the parallel inter-CB decoding algorithm. The successful decoding probability of the l-th CB at the i-th iteration is only determined by $d_{l-J}^{(i-1)}, \cdots, d_{l+J}^{(i-1)}$. Therefore, the successful decoding probability of the conventional parallel inter-CB decoding algorithm can be analyzed if the joint distributions of the decoding indicators of the $(2J+1)$ consecutive CBs are known.

The third advantage is low-latency. In contrast to the sequential inter-CB decoding algorithm, all CBs can be decoded simultaneously in the parallel inter-CB decoding algorithm. Therefore, with L parallel computation capabilities, the latency of the parallel inter-CB decoding algorithm can be reduced.

Now a simple method is proposed to reduce the decoding complexity of the parallel inter-CB decoding algorithm, called the modified parallel inter-CB decoding algorithm of the proposed PIC polar codes with coupling depth J. Before describing the modified decoding algorithm, the *decoding state* D_l of the l-th CB should be defined first for all $l, 1 \leq l \leq L$.

Definition 2. *The decoding state D_l is the decimal number of the binary expression of $2J$ decoding indicators of the CBs which are coupled with the l-th CB given as*

$$D_l = \overline{d_{l-1}d_{l+1}\cdots d_{l-J}d_{l+J}}_{(2)}. \tag{4.4}$$

where $\overline{d_{l-1}d_{l+1}\cdots d_{l-J}d_{l+J}}_{(2)}$ *denotes the binary number with binary digits* d_{l-1}, $d_{l+1}, \cdots, d_{l-J}, d_{l+J}$.

According to the definition, the decoding state D_l is an integer satisfying $0 \leq D_l < 2^{2J}$ and $D_l = 2^{2J} - 1$ means that all CBs which are coupled with the l-th CB are successfully decoded.

The differences between Algorithms 4.2 and 4.3 are in **CB decoding** and **Extrinsic information updating** stages. By decoding the l-th CB only satisfying $d_l^{(i-1)} = 0$ and $D_l^{(i-1)} \neq D_l^{(i-2)}$ for all l and i, $1 \leq l \leq L$ and $i \geq 2$, the decoding complexity can be reduced dramatically. Moreover, by updating the l-th CB only satisfying $D_l^{(i)} \neq D_l^{(i-1)}$ for all l and i, $1 \leq l \leq L$ and $i \geq 1$, the decoding complexity can be reduced dramatically further without sacrificing the decoding performance. The complexity of the proposed modified parallel inter-CB decoding algorithm will be compared with the conventional one in Section 6.9.

4.3 Sequential Inter-CB Decoding Schemes of the Proposed PIC Polar Codes with Coupling Depth J

In this section, two sequential inter-CB decoding schemes of the proposed PIC polar codes with coupling depth J are generalized and a modified sequential inter-CB decoding algorithm is proposed. This section is described similarly to the previous section, except that the sequential inter-CB decoding algorithm is applied.

The one-shot sequential inter-CB decoding algorithm of the proposed PIC polar codes with coupling depth J in Algorithm 4.4 is similar to the one-shot sequential inter-CB decoding algorithm in [36] except **Input**, **Initialization**, **Extrinsic information updating**, and **Message concatenation** stages. Since there is no re-decoding for those CBs with failed decoding results, the decoding performance is slightly degraded.

The conventional sequential inter-CB decoding algorithm of the proposed PIC polar codes with coupling depth J in Algorithm 4.5 is also similar to the one-shot parallel

inter-CB decoding algorithm in [36] except **Input**, **Initialization**, **Extrinsic information updating**, and **Message concatenation** stages. This decoding algorithm consists of the repetition of two processes, alternatively, called **FF decoding** process and **FB decoding** process. In **FF decoding** process, all CBs from the head $(l = 1)$ to the tail $(l = L)$ are decoded sequentially by using the polar CB decoder. Before decoding the l-th CB, extrinsic information of the l-th CB is updated for all l, $1 \leq l \leq L$. In **FB decoding** process, extrinsic information update and polar CB decoding is proceeded in the opposite direction. These two processes are repeated alternatively until all decoding indicators are equal to 1, which means that the decoding is successful, or all decoding indicators are unchanged, which means that the decoding is failed.

Now a simple method is proposed to reduce the decoding complexity of the sequential inter-CB decoding algorithm, called the modified sequential inter-CB decoding algorithm of the proposed PIC polar codes with coupling depth J. This inter-CB decoding algorithm is similar to the modified parallel inter-CB decoding algorithm, except the **CB decoding** and **Decoding state updating** steps in both **FF decoding** and **FB decoding** processes. In the modified sequential inter-CB decoding algorithm, $(2J)$ decoding states $D_{l-J}^{(i)}, \cdots, D_{l-1}^{(i)}, D_{l+1}^{(i)}, \cdots, D_{l+J}^{(i)}$ are updated after the l-th CB is successfully decoded. Since the decoding state $D_l^{(i)}$ is still updated before the l-th CB is decoded, the l-th CB at the i-th iteration is decoded if $d_l^{(i-1)} = 0$ and not $D_l^{(i-1)} \neq D_l^{(i-2)}$, but $D_l^{(i)} \neq D_l^{(i-1)}$. The rest of algorithms are exactly the same as the conventional sequential inter-CB decoding algorithm. Thus, the decoding complexity of the proposed modified sequential inter-CB decoding algorithm is lower than that of the conventional sequential inter-CB decoding algorithm without sacrificing the decoding performance. The complexity of the proposed modified sequential inter-CB decoding algorithm will be compared with the conventional one in Section 6.9.

4.4 Modified Look-Back and Go-Back Inter-CB Decoding Scheme of the Proposed PIC Polar Codes with Coupling Depth $J = 2$

In this section, a modified look-back and go-back inter-CB decoding scheme of the proposed PIC polar codes with coupling depth $J = 2$ is proposed. Recall the conventional look-back and go-back inter-CB decoding algorithm in Algorithm 2.1, which reduces the decoding complexity without sacrificing the TBER performance. The main idea of the conventional look-back and go-back inter-CB decoding algorithm is finding the **early process conversion** condition from the FF decoding process to the FB decoding process and the **early decoding termination** condition in the FB decoding process. Thus, the question would be natural if it is possible to generalize this idea to the PIC polar codes with coupling depth $J \geq 2$.

The **early process conversion** condition can be made by mimicking the conventional look-back and go-back inter-CB decoding algorithm. Let l be the numbering index of the currently decoded CB, $1 \leq l \leq L$. In the conventional decoding algorithm, the **early process conversion** condition in the FF decoding process is $d_{l-1} = 0$ and $d_l = 1$, because the $(l-1)$-th CB can be decoded successfully with the aid of the extrinsic information from the l-th block and the decoding results of those CBs with index larger than l are irrelevant to the decoding result of the $(l-1)$-th CB, if $d_l = 1$. From these reasons, the **early process conversion** condition in the FF decoding process can be generalized to $d_{l-J} = 0$ and $\{d_{l-j}\}_{0 \leq j < J} = \mathbf{1}$ for arbitrary coupling depth J.

On the other hand, it is hard to imitate the **early decoding termination** condition in the FB decoding process of the conventional look-back and go-back inter-CB decoding algorithm. In the conventional decoding algorithm, the decoding process is terminated if $d_l = 0$, where l is the numbering index of the currently decoded CB in the FB decoding process, because no more extrinsic information can be obtained during the

Table 4.1: FF decoding process of the modified look-back and go-back inter-CB decoding algorithm of the proposed PIC polar codes with coupling depth $J = 2$

d_{l-4}	d_{l-3}	d_{l-2}	d_{l-1}	d_l	States
		0	1	1	FB decoding from the $(l-2)$-th CB (**early process conversion**)
		0	1	0	Re-decode the $(l-2)$-th CB (★)
		0 (★)	1	0	Proceed the FF decoding from the $(l+1)$-th CB
0	0	1 (★)	1	0	FB decoding from the $(l-3)$-th CB (**early process conversion**)
	1				FB decoding from the $(l-4)$-th CB (**early process conversion**)
1	1				Proceed the FF decoding from the l-th CB

l-th CB decoding.

But for $J \geq 2$, it is possible to obtain more extrinsic information during the l-th CB decoding in the FB decoding process, because the decoding results of the FF decoding process can be changed during the l-th CB decoding. Thus, it is necessary to modify the FF decoding process to use the **early decoding termination** condition in the FB decoding process.

For $J = 2$, it is possible to use the **early decoding termination** condition by modifying the FF decoding process in the look-back and go-back inter-CB decoding. In the modified FF decoding process, when $d_{l-1} = 0$ and $d_l = 1$, the $(l-1)$-th CB should be re-decoded but not immediately. In this case, the $(l+1)$-th CB is decoded first and then l is updated by $(l-1)$ to represent the numbering index of the lately decoded CB l. Then, the modified FF decoding process is described as follows:

i) If $d_{l-2} = 0$, $d_{l-1} = 1$, and $d_l = 1$;

The FF decoding process is converted into the FB decoding process (**early process conversion**) from the $(l-2)$-th CB.

ii) If $d_{l-2}=0$, $d_{l-1}=1$, and $d_l=0$;

The $(l-2)$-th CB is re-decoded using the extra extrinsic information from the $(l-1)$-th CB.

1) If $d_{l-2}=0$;

The FF decoding process is proceeded from the $(l+1)$-th CB.

2) If $d_{l-2}=1$;

a) $d_{l-3}=0$;

Since $d_{l-3}=0$, $d_{l-2}=1$, and $d_{l-1}=1$, the FF decoding process is converted into the FB decoding process (**early process conversion**) from the $(l-3)$-th CB.

b) $d_{l-3}=1$ and $d_{l-4}=0$;

Since $d_{l-4}=0$, $d_{l-3}=1$, and $d_{l-2}=1$, the FF decoding process is converted into the FB decoding process (**early process conversion**) from the $(l-4)$-th CB.

c) $d_{l-3}=1$ and $d_{l-4}=1$;

If $d_{l'}=0$ for some l', $1 \le l' \le l-4$, the decoding process had to be converted into the FB decoding process from the l'-th CB before the $(l-2)$-th CB is decoded in the FF decoding process. Thus, all decoding indicators with index below l must be 1 and the FF decoding process is proceeded from the l-th CB.

The modified FF decoding process of the proposed modified look-back and go-back inter-CB decoding algorithm of the proposed PIC polar codes with coupling depth $J=2$ is described in Table 4.1. In this decoding algorithm, the FB decoding process also has to be modified. Basically, if consecutive CBs are failed to be decoded,

that is, $d_l = 0$ and $d_{l+1} = 0$, it is possible to terminate decoding and declare a TB error (**early decoding termination**). But this condition is not sufficient.

If $d_{l-1} = 1$, $d_l = 0$, and $d_{l+1} = 1$, it is also possible to terminate decoding and declare a TB error (**early decoding termination**), because no more extrinsic information can be updated from both the head and tail directions. If the current CB decoding result is successful but the previous CB decoding result is failed, that is, $d_l = 1$, and $d_{l+1} = 0$, re-decode the previous CB and update the d_{l+1}. If the result of re-decoding is also failed, then it is also possible to terminate decoding and declare a TB error (**early decoding termination**).

If the result of re-decoding is successful, there are three options left. Before describing these three options, let $l_{\max}$ be the smallest index of the non-successfully decoded CB such that $d_{l_{\max}} = 0$, $d_{l<l_{\max}} = \mathbf{1}$, and $1 \leq l_{\max} \leq L$. The three options are as follows:

i) If $l_{\max}$ does not exist;

   Since all CBs are successfully decoded, the FB decoding process is converted into the message concatenation process.

ii) If $l_{\max}$ exists and $l_{\max} > l$;

   Since all CBs in the FB decoding process are successfully decoded, the FB decoding process is converted into the FF decoding process.

iii) Else;

   There exists a CB to be decoded in the FB decoding process, the FB decoding process is proceeded.

These three options are also considered when $d_{l-2} = 1$, $d_{l-1} = 1$, and $d_l = 1$. Otherwise, the FB decoding process is proceeded.

The modified look-back and go-back inter-CB decoding algorithm of the proposed PIC polar codes with coupling depth $J = 2$ is described in Algorithm 4.7. Its decoding performance and complexity will be compared with the other inter-CB decoding

algorithms in Algorithms 4.1–4.6 in Section 6.9.

4.5 Sequential and Probabilistic Re-Decoding Inter-CB Decoding Scheme of the Proposed PIC Polar Codes with Coupling Depth J

In this section, a new efficient inter-CB decoding scheme of the proposed PIC polar codes with coupling depth J. In this decoding scheme, all CBs are sequentially decoded from the first to the L-th CB and then re-decode the CB with the successfully decodable order. Thus, this algorithm is called the sequential and probabilistic re-decoding inter-CB decoding algorithm.

Let S_l be the summation of the decoding indicators of the coupled CBs with the l-th CB, which can be expressed as

$$S_l = d_{l-J} + \cdots + d_{l-1} + d_{l+1} + \cdots + d_{l+J} \tag{4.5}$$

for l, $1 \leq l \leq L$. As S_l becomes larger, there exist more CBs which can deliver the correct extrinsic information and thus the l-th CB becomes more successfully decodable.

In order to describe the proposed sequential and probabilistic re-decoding inter-CB decoding algorithm, the CB indices $l_{\min}$ and $l_{\max}$ are defined first. The $l_{\min}$ is the CB index satisfying $d_{l_{\min}} = 0$ and $d_{l<l_{\min}} = \mathbf{1}$. Likewise, $l_{\max}$ is the CB index satisfying $d_{l_{\max}} = 0$ and $d_{l>l_{\max}} = \mathbf{1}$. If $l_{\min}$ and $l_{\max}$ do not exist, then all CBs are successfully decoded and the decoding process is converted into the message concatenation process.

In the re-decoding process, all CBs with indices from $l_{\min}$ to $l_{\max}$ are decoded by the decreasing order sorted by S_l. If any CB is successfully re-decoded, $l_{\min}$, $l_{\max}$, and S_l should be updated. The re-decoding process is repeated until no CBs with indices from $l_{\min}$ to $l_{\max}$ are successfully re-decoded or $l_{\min}$ and $l_{\max}$ do not exist.

The proposed sequential and probabilistic re-decoding inter-CB decoding algo-

rithm of the proposed PIC polar codes with coupling depth J is described in Algorithm 4.8. Since the proposed decoding algorithm has no (**early decoding termination**) condition, the decoding complexity of this decoding algorithm is not as low as the modified sequential inter-CB decoding algorithm at low $\frac{E_{\mathrm{b}}}{N_0}$. In contrast, the proposed decoding algorithm has relatively low decoding complexity at high $\frac{E_{\mathrm{b}}}{N_0}$ with large coupling depth J, because the probabilistic re-decoding is efficient at high $\frac{E_{\mathrm{b}}}{N_0}$ with large coupling depth J. Moreover, the proposed decoding algorithm can be applied to arbitrary coupling depth J. Its decoding performance and complexity will be compared with the other algorithms in Algorithms 4.1–4.6 in Section 6.9.

Algorithm 4.2 Conventional parallel inter-CB decoding algorithm of the proposed PIC polar codes with coupling depth J

Input: $\{\mathbf{y}_{l,1}^{\mathrm{h}}, \mathbf{y}_{l,2}^{\mathrm{h}}, \cdots, \mathbf{y}_{l,J}^{\mathrm{h}}, \mathbf{y}_l, \mathbf{y}_{l,1}^{\mathrm{t}}, \mathbf{y}_{l,2}^{\mathrm{t}}, \cdots, \mathbf{y}_{l,J}^{\mathrm{t}}\}_{l=1}^{L}$

1: **Initialization**:
$$\begin{cases} \mathbf{y}_{l,j}^{\mathrm{h}} = \infty \cdot \mathbf{1}, \text{ if } 1 \le l \le j \\ \mathbf{y}_{l,j}^{\mathrm{t}} = \infty \cdot \mathbf{1}, \text{ if } L+1-j \le l \le L \\ \{d_l^{(0)}\}_{1 \le l \le L} = \mathbf{0}, \{d_l^{(i)}\}_{l<1} = \mathbf{1}, \text{ and } \{d_l^{(i)}\}_{l>L} = \mathbf{1} \text{ for all } i \\ l = 1, \text{ and } i = 1. \end{cases}$$

2: **while** $\{d_l^{(i)}\}_{1 \le l \le L} \neq \mathbf{1}$ or $\{d_l^{(i)}\}_{1 \le l \le L} \neq \{d_l^{(i-1)}\}_{1 \le l \le L}$ **do**

3: **while** $l \le L$ **do**

4: **CB decoding**: Decode the l-th CB using the polar CB decoder if $d_l^{(i-1)} = 0$.

5: **CB index updating**: $l \leftarrow (l+1)$.

6: **end while**

7: $l = 1$

8: **while** $l \le L$ **do**

9: **Decoding indicator updating**: Update the decoding indicator $d_l^{(i)}$.

10: **CB index updating**: $l \leftarrow (l+1)$.

11: **end while**

12: $l = 1$

13: **while** $l \le L$ **do**

14: **Extrinsic information updating**: Update the extrinsic information of the l-th CB by (4.2) and (4.3).

15: **CB index updating**: $l \leftarrow (l+1)$.

16: **end while**

17: $l = 1$

18: **Iteration index updating**: $i \leftarrow (i+1)$

19: **end while**

20: **Message concatenation**: Concatenate all $\hat{\mathbf{u}}_l^{\mathrm{h}}$, $\hat{\mathbf{u}}_l$, and $\hat{\mathbf{u}}_l^{\mathrm{t}}$ to obtain the decoded output $\hat{\mathbf{u}}$ for all l, $1 \le l \le L$.

Algorithm 4.3 Modified parallel inter-CB decoding algorithm of the proposed PIC polar codes with coupling depth J

Input: $\{\mathbf{y}_{l,1}^{\mathrm{h}}, \mathbf{y}_{l,2}^{\mathrm{h}}, \cdots, \mathbf{y}_{l,J}^{\mathrm{h}}, \mathbf{y}_l, \mathbf{y}_{l,1}^{\mathrm{t}}, \mathbf{y}_{l,2}^{\mathrm{t}}, \cdots, \mathbf{y}_{l,J}^{\mathrm{t}}\}_{l=1}^{L}$

1: **Initialization**:
$$\begin{cases} \mathbf{y}_{l,j}^{\mathrm{h}} = \infty \cdot \mathbf{1}, \text{ if } 1 \le l \le j \\ \mathbf{y}_{l,j}^{\mathrm{t}} = \infty \cdot \mathbf{1}, \text{ if } L+1-j \le l \le L \\ \{d_l^{(0)}\}_{1\le l\le L} = \mathbf{0}, \{d_l^{(i)}\}_{l<1} = \mathbf{1}, \text{ and } \{d_l^{(i)}\}_{l>L} = \mathbf{1} \text{ for all } i \\ \{D_l^{(0)}\}_{1\le l\le L} \text{ is defined by } \{d_l^{(0)}\}_{-J+1\le l\le L+J} \\ l = 1, \text{ and } i = 1. \end{cases}$$

2: **while** $\{d_l^{(i)}\}_{1\le l\le L} \neq \mathbf{1}$ or $\{d_l^{(i)}\}_{1\le l\le L} \neq \{d_l^{(i-1)}\}_{1\le l\le L}$ **do**

3: **while** $l \le L$ **do**

4: **CB decoding**: Decode the l-th CB using the polar CB decoder if $d_l^{(i-1)} = 0$ and $D_l^{(i-1)} \neq D_l^{(i-2)}$ when $i \ge 2$.

5: **CB index updating**: $l \leftarrow (l+1)$.

6: **end while**

7: $l = 1$

8: **while** $l \le L$ **do**

9: **Decoding indicator updating**: Update the decoding indicator $d_l^{(i)}$.

10: **CB index updating**: $l \leftarrow (l+1)$.

11: **end while**

12: $l = 1$

13: **while** $l \le L$ **do**

14: **Decoding state updating**: Update the decoding state $D_l^{(i)}$ from Definition 2.

15: **CB index updating**: $l \leftarrow (l+1)$.

16: **end while**

17: $l = 1$

18: **while** $l \le L$ **do**

19: **Extrinsic information updating**: Update the extrinsic information of the l-th CB by (4.2) and (4.3), if $D_l^{(i)} \neq D_l^{(i-1)}$.

20: **CB index updating**: $l \leftarrow (l+1)$.

21: **end while**

22: $l = 1$

23: **Iteration index updating**: $i \leftarrow (i+1)$

24: **end while**

25: **Message concatenation**: Concatenate all $\hat{\mathbf{u}}_l^{\mathrm{h}}$, $\hat{\mathbf{u}}_l$, and $\hat{\mathbf{u}}_l^{\mathrm{t}}$ to obtain the decoded output $\hat{\mathbf{u}}$ for all l, $1 \le l \le L$.

Algorithm 4.4 One-shot sequential inter-CB decoding algorithm of the proposed PIC polar codes with coupling depth J

Input: $\{\mathbf{y}_{l,1}^{\mathrm{h}}, \mathbf{y}_{l,2}^{\mathrm{h}}, \cdots, \mathbf{y}_{l,J}^{\mathrm{h}}, \mathbf{y}_l, \mathbf{y}_{l,1}^{\mathrm{t}}, \mathbf{y}_{l,2}^{\mathrm{t}}, \cdots, \mathbf{y}_{l,J}^{\mathrm{t}}\}_{l=1}^{L}$

1: **Initialization**:
$$\begin{cases} \mathbf{y}_{l,j}^{\mathrm{h}} = \infty \cdot \mathbf{1}, \text{ if } 1 \leq l \leq j \\ \mathbf{y}_{l,j}^{\mathrm{t}} = \infty \cdot \mathbf{1}, \text{ if } L+1-j \leq l \leq L \\ \{d_l\}_{1 \leq l \leq L} = \mathbf{0}, \{d_l\}_{l<1} = \mathbf{1}, \text{ and } \{d_l\}_{l>L} = \mathbf{1} \\ l = 1. \end{cases}$$

2: **while** $l \leq L$ **do**

3: **Extrinsic information updating**: Update the extrinsic information of the l-th CB by (4.2) and (4.3).

4: **CB decoding**: Decode the l-th CB using the polar CB decoder.

5: **Decoding indicator updating**: Update the decoding indicator d_l.

6: **CB index updating**: $l \leftarrow (l+1)$.

7: **end while**

8: **Message concatenation**: Concatenate all $\hat{\mathbf{u}}_l^{\mathrm{h}}$, $\hat{\mathbf{u}}_l$, and $\hat{\mathbf{u}}_l^{\mathrm{t}}$ to obtain the decoded output $\hat{\mathbf{u}}$ for all l, $1 \leq l \leq L$.

Algorithm 4.5 Conventional sequential inter-CB decoding algorithm of the proposed PIC polar codes with coupling depth J

Input: $\{\mathbf{y}_{l,1}^{\mathrm{h}}, \mathbf{y}_{l,2}^{\mathrm{h}}, \cdots, \mathbf{y}_{l,J}^{\mathrm{h}}, \mathbf{y}_l, \mathbf{y}_{l,1}^{\mathrm{t}}, \mathbf{y}_{l,2}^{\mathrm{t}}, \cdots, \mathbf{y}_{l,J}^{\mathrm{t}}\}_{l=1}^{L}$

1: **Initialization**:
$$\begin{cases} \mathbf{y}_{l,j}^{\mathrm{h}} = \infty \cdot \mathbf{1}, \text{ if } 1 \le l \le j \\ \mathbf{y}_{l,j}^{\mathrm{t}} = \infty \cdot \mathbf{1}, \text{ if } L+1-j \le l \le L \\ \{d_l^{(0)}\}_{1 \le l \le L} = \mathbf{0}, \{d_l^{(i)}\}_{l<1} = \mathbf{1}, \text{ and } \{d_l^{(i)}\}_{l>L} = \mathbf{1} \text{ for all } i \\ i = 1. \end{cases}$$

2: **while** $\{d_l^{(i)}\}_{1 \le l \le L} \neq \mathbf{1}$ or $\{d_l^{(i)}\}_{1 \le l \le L} \neq \{d_l^{(i-1)}\}_{1 \le l \le L}$ **do**

3: **FF decoding**:

4: $l = 1$

5: **while** $l \le L$ **do**

6: **Extrinsic information updating**: Update the extrinsic information of the l-th CB by (4.2) and (4.3).

7: **CB decoding**: Decode the l-th CB using the polar CB decoder if $d_l^{(i-1)} = 0$.

8: **Decoding indicator updating**: Update the decoding indicator $d_l^{(i)}$.

9: **CB index updating**: $l \leftarrow (l+1)$.

10: **end while**

11: **Iteration index updating**: $i \leftarrow (i+1)$

12: **FB decoding**:

13: $l = L$

14: **while** $1 \le l$ **do**

15: **Extrinsic information updating**: Update the extrinsic information of the l-th CB by (4.2) and (4.3).

16: **CB decoding**: Decode the l-th CB using the polar CB decoder if $d_l^{(i-1)} = 0$.

17: **Decoding indicator updating**: Update the decoding indicator $d_l^{(i)}$.

18: **CB index updating**: $l \leftarrow (l-1)$.

19: **end while**

20: **Iteration index updating**: $i \leftarrow (i+1)$

21: **end while**

22: **Message concatenation**: Concatenate all $\hat{\mathbf{u}}_l^{\mathrm{h}}$, $\hat{\mathbf{u}}_l$, and $\hat{\mathbf{u}}_l^{\mathrm{t}}$ to obtain the decoded output $\hat{\mathbf{u}}$ for all l, $1 \le l \le L$.

Algorithm 4.6 Modified sequential inter-CB decoding algorithm of the proposed PIC polar codes with coupling depth J

Input: $\{\mathbf{y}_{l,1}^{\mathrm{h}}, \mathbf{y}_{l,2}^{\mathrm{h}}, \cdots, \mathbf{y}_{l,J}^{\mathrm{h}}, \mathbf{y}_l, \mathbf{y}_{l,1}^{\mathrm{t}}, \mathbf{y}_{l,2}^{\mathrm{t}}, \cdots, \mathbf{y}_{l,J}^{\mathrm{t}}\}_{l=1}^{L}$

1: **Initialization**:
$$\begin{cases} \mathbf{y}_{l,j}^{\mathrm{h}} = \infty \cdot \mathbf{1}, \text{ if } 1 \le l \le j \\ \mathbf{y}_{l,j}^{\mathrm{t}} = \infty \cdot \mathbf{1}, \text{ if } L+1-j \le l \le L \\ \{d_l^{(0)}\}_{1 \le l \le L} = \mathbf{0}, \{d_l^{(i)}\}_{l<1} = \mathbf{1}, \text{ and } \{d_l^{(i)}\}_{l>L} = \mathbf{1} \text{ for all } i \\ i = 1. \end{cases}$$

2: **while** $\{d_l^{(i)}\}_{1 \le l \le L} \neq \mathbf{1}$ or $\{d_l^{(i)}\}_{1 \le l \le L} \neq \{d_l^{(i-1)}\}_{1 \le l \le L}$ **do**

3: **FF decoding**:

4: **for** $l = 1$ to L **do**

5: **Extrinsic information updating**: Update the extrinsic information of the l-th CB by (4.2) and (4.3).

6: **CB decoding**: Decode the l-th CB using the polar CB decoder if $d_l^{(i-1)} = 0$ and $D_l^{(i)} \neq D_l^{(i-1)}$ when $i \ge 2$.

7: **Decoding indicator updating**: Update the decoding indicator $d_l^{(i)}$.

8: **Decoding state updating**: Update the decoding states $D_{l-J}^{(i)}, \cdots, D_{l-1}^{(i)}$, $D_{l+1}^{(i)}, \cdots, D_{l+J}^{(i)}$ from Definition 2, if $d_l^{(i)} = 1$.

9: **end for**

10: **Iteration index updating**: $i \leftarrow (i+1)$

11: **FB decoding**:

12: **for** $l = L$ to 1 **do**

13: **Extrinsic information updating**: Update the extrinsic information of the l-th CB by (4.2) and (4.3).

14: **CB decoding**: Decode the l-th CB using the polar CB decoder if $d_l^{(i-1)} = 0$ and $D_l^{(i)} \neq D_l^{(i-1)}$ when $i \ge 2$.

15: **Decoding indicator updating**: Update the decoding indicator $d_l^{(i)}$.

16: **Decoding state updating**: Update the decoding states $D_{l-J}^{(i)}, \cdots, D_{l-1}^{(i)}$, $D_{l+1}^{(i)}, \cdots, D_{l+J}^{(i)}$ from Definition 2, if $d_l^{(i)} = 1$.

17: **end for**

18: **Iteration index updating**: $i \leftarrow (i+1)$

19: **end while**

20: **Message concatenation**: Concatenate all $\hat{\mathbf{u}}_l^{\mathrm{h}}$, $\hat{\mathbf{u}}_l$, and $\hat{\mathbf{u}}_l^{\mathrm{t}}$ to obtain the decoded output $\hat{\mathbf{u}}$ for all l, $1 \le l \le L$.

Algorithm 4.7 Modified look-back and go-back inter-CB decoding algorithm with of the proposed PIC polar codes coupling depth $J = 2$

Input: $\{\mathbf{y}_{l,1}^{\mathrm{h}}, \mathbf{y}_{l,2}^{\mathrm{h}}, \cdots, \mathbf{y}_{l,J}^{\mathrm{h}}, \mathbf{y}_l, \mathbf{y}_{l,1}^{\mathrm{t}}, \mathbf{y}_{l,2}^{\mathrm{t}}, \cdots, \mathbf{y}_{l,J}^{\mathrm{t}}\}_{l=1}^{L}$

1: **Initialization**:
$$\begin{cases} \mathbf{y}_{l,j}^{\mathrm{h}} = \infty \cdot \mathbf{1}, \text{ if } 1 \leq l \leq j \\ \mathbf{y}_{l,j}^{\mathrm{t}} = \infty \cdot \mathbf{1}, \text{ if } L + 1 - j \leq l \leq L \\ \{d_l\}_{1 \leq l \leq L} = \mathbf{0}, \{d_l\}_{l<1} = \mathbf{1}, \text{ and } \{d_l\}_{l>L} = \mathbf{1} \\ l = 1. \end{cases}$$

2: **while** $\{d_l\}_{1 \leq l \leq L} \neq \mathbf{1}$ **do**

3: **FF**: Decode the l-th CB using the polar CB decoder, if $d_l = 0$.

a) If $l = L$ and $d_L = 0$
   1) If $d_{L-2} = 1$ and $d_{L-1} = 1$
      exit decoding and declare a TB error.
   2) Else
      update $l \leftarrow (L - 2)$ and go to **FB**.

b) If $l = L - 1$, $d_{L-1} = 0$, and $d_L = 1$
   update $l \leftarrow (L - 2)$ and go to **FB**.

c) If $d_{l-2} = 0$, $d_{l-1} = 1$, and $d_l = 1$
   update $l \leftarrow (l - 2)$ and go to **FB**. (**early conversion**)

d) If $d_{l-2} = 0$, $d_{l-1} = 1$, and $d_l = 0$
   re-decode the $(l - 2)$-th CB and update the decoding indicator d_{l-2}.
   (i) If $d_{l-2} = 0$
      update $l \leftarrow (l + 1)$ and go to **FF**.
   (ii) If $d_{l-2} = 1$
      (1) If $d_{l-3} = 0$
         update $l \leftarrow (l - 3)$ and go to **FB**. (**early conversion**)
      (2) Else
         (a) If $d_{l-4} = 0$
            update $l \leftarrow (l - 4)$ and go to **FB**. (**early conversion**)
         (b) Else
            go to **FF**.

e) Else
   update $l \leftarrow (l + 1)$ and go to **FF**.

4: **FB**: Decode the l-th CB using the polar CB decoder, if $d_l = 0$.

a) If $d_l = 0$ and $d_{l+1} = 0$
exit decoding and declare a TB error. (**early termination**)

b) If $d_{l-1} = 1$ and $d_l = 0$
exit decoding and declare a TB error. (**early termination**)

c) If $d_l = 1$ and $d_{l+1} = 0$
re-decode the $(l+1)$-th CB and update the decoding indicator d_{l+1}.

(i) If $d_{l+1} = 0$
exit decoding and declare a TB error. (**early termination**)

(ii) Else
find the $l_{\max}$ such that $d_{l_{\max}} = 0$, $d_{l<l_{\max}} = \mathbf{1}$, and $1 \leq l_{\max} \leq L$.

(1) If $l_{\max}$ does not exist
go to **Message concatenation**.

(2) If $l_{\max}$ does exist and $l_{\max} > l$
update $l \leftarrow l_{\max}$ and go to **FF**.

(3) Else
update $l \leftarrow (l-1)$ and go to **FB**.

d) If $d_l = 1$, $d_{l-1} = 1$, and $d_{l-2} = 1$
find the $l_{\max}$ such that $d_{l_{\max}} = 0$, $d_{l<l_{\max}} = \mathbf{1}$, and $1 \leq l_{\max} \leq L$.

(i) If $l_{\max}$ does not exist
go to **Message concatenation**.

(ii) If $l_{\max}$ does exist and $l_{\max} > l$
update $l \leftarrow l_{\max}$ and go to **FF**.

(iii) Else
update $l \leftarrow (l-1)$ and go to **FB**.

e) Else
update $l \leftarrow (l-1)$ and go to **FB**.

5: **end while**

6: **Message concatenation**: Concatenate all $\hat{\mathbf{u}}_l^{\mathrm{h}}$, $\hat{\mathbf{u}}_l$, and $\hat{\mathbf{u}}_l^{\mathrm{t}}$ to obtain the decoded output $\hat{\mathbf{u}}$ for all l, $1 \leq l \leq L$.

Algorithm 4.8 Sequential and probabilistic re-decoding inter-CB decoding algorithm with of the proposed PIC polar codes coupling depth J

Input: $\{\mathbf{y}_{l,1}^{\mathrm{h}}, \mathbf{y}_{l,2}^{\mathrm{h}}, \cdots, \mathbf{y}_{l,J}^{\mathrm{h}}, \mathbf{y}_l, \mathbf{y}_{l,1}^{\mathrm{t}}, \mathbf{y}_{l,2}^{\mathrm{t}}, \cdots, \mathbf{y}_{l,J}^{\mathrm{t}}\}_{l=1}^{L}$

1: **Initialization**:
$$\begin{cases} \mathbf{y}_{l,j}^{\mathrm{h}} = \infty \cdot \mathbf{1}, \text{ if } 1 \leq l \leq j \\ \mathbf{y}_{l,j}^{\mathrm{t}} = \infty \cdot \mathbf{1}, \text{ if } L+1-j \leq l \leq L \\ \{d_l\}_{1 \leq l \leq L} = \mathbf{0}, \{d_l\}_{l<1} = \mathbf{1}, \text{ and } \{d_l\}_{l>L} = \mathbf{1}. \\ l = 1. \end{cases}$$

2: **Sequential decoding**:
3: **for** $l = 1$ to L **do**
4: **Extrinsic information updating**: Update the extrinsic information of the l-th CB by (4.2) and (4.3).
5: **CB decoding**: Decode the l-th CB using the polar CB decoder.
6: **Decoding indicator updating**: Update the decoding indicator d_l.
7: **end for**

a) If $d_l = 1$ for all l, $1 \leq l \leq L$
go to **Message concatenation**.

b) Else
find $l_{\min}$ and $l_{\max}$ such that $d_{l_{\min}} = 0$, $d_{l_{\max}} = 0$, $d_{l<l_{\min}} = \mathbf{1}$, and $d_{l>l_{\max}} = \mathbf{1}$.

8: **Probabilistic re-decoding**:
9: **while** $l_{\min} \leq l_{\max}$ **do**
10: **Re-decoding**: Decode the l-th most successfully decodable CB, measured by the sequence S_l for l, $1 \leq l \leq L$, among the $l_{\min}$-th CB and the $l_{\max}$-th CB.

a) If the l_{FB}-th most successfully decodable CB is decoded
update $l \leftarrow 1$ and

(i) **while** $d_{l_{\min}} = 1$, **do** $l_{\min} \leftarrow (l_{\min} + 1)$.

(ii) **while** $d_{l_{\max}} = 1$, **do** $l_{\max} \leftarrow (l_{\max} - 1)$.

b) If the l-th most successfully decodable CB is not decoded
$l \leftarrow (l+1)$.

(i) If $l > (l_{\max} - l_{\min} + 1)$
terminate decoding and declare a TB error.

(ii) Else
go to **Re-decoding**.

11: **end while**

12: **Message concatenation**: Concatenate all $\hat{\mathbf{u}}_l^{\mathrm{h}}$, $\hat{\mathbf{u}}_l$, and $\hat{\mathbf{u}}_l^{\mathrm{t}}$ to obtain the decoded output $\hat{\mathbf{u}}$ for all l, $1 \leq l \leq L$.

Chapter 5

Design of PIC Polar Codes with Coupling Depth J Using Error Rate Evaluation and Complexity Bounds

In this chapter, the error rate performance evaluation method of PIC polar codes with coupling depth J is proposed. Recall that there are two decoding stages, called the polar CB decoding stage and the inter-CB decoding stage, in the decoding algorithm of the PIC polar codes. From the viewpoint of the computational complexity, the CASCL decoder in the polar CB decoding stage consumes most time of the entire decoding process. If the error probabilities of polar CB decoding for 2^{2J} decoding states are known, can the error rate performance of PIC polar decoder be evaluated faster? The answer is yes in the ensemble sense. The details will be discussed in Section 5.1. Also, these 2^{2J} error probabilities of each CB depending on the 2^{2J} decoding states are unchanged if the channel states and code parameters, such as code length, message length, coupling ratio, etc., are fixed. Therefore, by using the pre-measured polar CB decoding error probability, it is possible to evaluate the TBER and CBER performances of the proposed PIC polar codes.

This chapter consists of two sections. In the first section, a new idea of the TBER and CBER performance evaluation method is described. Using this method, the error probabilities of any non-degraded inter-CB decoding algorithms for any chain length

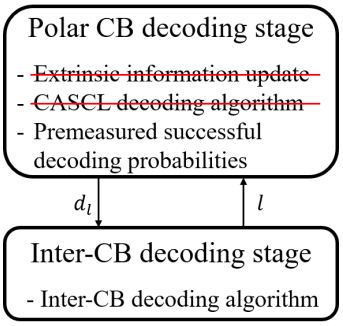

Figure 5.1: Idea of the decoding error rate evaluation.

L and coupling depth J can be quickly evaluated in the ensemble sense, if the message length of each CB, CB length, coupling ratio, channel state information, and target TBER are given. Then, it is possible to find the minimum chain length L and corresponding coupling depth J satisfying the target TBER.

In the second section, the upper bounds of the decoding complexity under parallel inter-CB decoding algorithms are derived. Using these bounds, the parallel inter-CB decoding can be terminated. Also, it is derived that the complexity upper bound of the modified parallel inter-CB decoding algorithm is lower than that of the conventional one.

5.1 Performance Evaluation and Parameter Optimization of the Proposed PIC Polar Codes

This section consists of two subsections. In the first subsection, the backgrounds and method of the TBER and CBER performance evaluation are described in the ensemble sense for the modified parallel inter-CB decoding algorithm of the proposed PIC polar codes with coupling depth J. Based on this evaluation, the optimization technique for the chain length L and coupling depth J is proposed if the message length of CB, CB length, coupling ratio, channel state information, and target TBER are given.

5.1.1 TBER and CBER Performance Evaluation

If the uncoupled message length K_{u}, coupled message length K_{c}, CB length N, coupling depth J, and the channel state information are given, each CBER depending on the 2^{2J} decoding states can be pre-measured in the ensemble sense, which is defined as

$$P_{D_l} = \Pr\{d_l^{(1)} = 0 \colon d_l^{(0)} = 0, D_l^{(0)}\}, \tag{5.1}$$

where $d_l^{(i)}$ is the decoding indicator of the l-th CB at the i-th decoding trial. Recall Algorithm 4.3, where

$$\Pr\{d_l^{(i)} = 0 \colon d_l^{(i-1)} = 0, D_l^{(i-1)} = D_l^{(i-2)}\} = 1 \tag{5.2}$$

for all $i \geq 2$. Since P_{D_l} is the CBER in the ensemble sense, it is assumed that the CBERs P_{D_l}'s are independent from the numer of decoding trials i, i.e.,

$$P_{D_l} = \Pr\{d_l^{(i)} = 0 \colon d_l^{(i-1)} = 0, D_l^{(i-1)} \neq D_l^{(i-2)}\} \tag{5.3}$$

for all $i \geq 2$.

Note that the decoding indicator $d_l^{(i)}$ is 1, if $d_l^{(i-1)} = 1$. The decoding indicator $d_l^{(i)}$ can be treated as a Bernoulli random variable with the conditional probability P_{D_l}, if $d_l^{(i-1)} = 0$ and $D_l^{(i-1)} \neq D_l^{(i-2)}$ for $i \geq 2$.

There are two decoding termination conditions, that is, successful decoding termination and failed decoding termination, in the parallel inter-CB decoding algorithm. If there exists an i such that $\{d_l^{(i)}\} = \mathbf{1}$ for all l, $1 \leq l \leq L$, the decoding is successful and there is no TB error. But if there exists an i such that $\{d_l^{(i)}\} = \{d_l^{(i-1)}\}$, for all l, $1 \leq l \leq L$, the decoding is failed and a TB error is declared. Otherwise, i is updated to $(i+1)$ and the decoding process is proceeded.

For a finite chain length L, there exists the maximum number of CB decoding trials of any inter-CB decoding algorithms satisfying the decoding termination condition. This will be proved in Section 5.2.

Let $P_l^{(i)}$ be a decoding error probability of the l-th CB at the i-th iteration defined as

$$P_l^{(i)} = \Pr\{d_l^{(i)} = 0\}. \tag{5.4}$$

Let $i_{\max}$ be the maximum number of CB decoding trials. Then, the l-th CBER in the ensemble sense is given as

$$\mathrm{CBER}_l = P_l^{(i_{\max})} \tag{5.5}$$

and the TBER can be evalutated as

$$\mathrm{TBER} = 1 - \Pr\{d_l^{(i_{\max})} = 1 \colon 1 \le l \le L\}. \tag{5.6}$$

Using a number of numerical trials, the CBER of the l-th CB and the TBER of the modified parallel inter-CB decoding algorithm in the ensemble sense can be evaluated under the assumption in (5.3). Since the inter-CB decoders in Algorithms 4.2, 4.3, and 4.5–4.8 have the same TBER performances, the evaluated TBER is comparable to the TBER of the inter-CB decoders in Algorithms 4.2 and 4.5–4.8 as well as the TBER of the modified parallel inter-CB decoder in Algorithm 4.3. The evaluated results in (5.6) will be compared to the numerical results in Section 6.8.

5.1.2 Optimized Design of Chain Length L and Coupling Depth J

In the previous subsection, the TBER of the modified parallel inter-CB decoding algorithm is evaluated in (5.6). Using this evaluation, the TBER $P_{\mathrm{e},L}$ in the ensemble sense for any chain length L and coupling depth J can be evaluated given total message block length K, coupling ratio r_{c}, code block length N, and channel state.

Suppose that the parameters of the CB, such as K_{c}, K_{u}, and N, are fixed. Let P_e^* be the target TBER. Given fixed P_e^*, for each coupling depth J, there may exist the certain chain length L^* such that $P_{e,L} < P_e^*$, for all $L \ge L^*$. Clearly, L^* can be interpreted as a function of J. Then, there may exist the optimal J^* which minimizes the chain length L^*.

Table 5.1: Evaluated TBERs of the modified parallel inter-CB decoder for $N = 1024$, $K_{\mathrm{u}} = 383$, $\frac{E_{\mathrm{b}}}{N_0} = 2$ dB, and $P_e^* = 10^{-4}$

L	$J = 1$	$J = 2$	$J = 3$
1	8.38E-05	3.60E-05	2.03E-05
2	1.00E-04	3.80E-05	2.46E-05
3	1.14E-04	1.01E-04	8.04E-05
4	1.08E-04	1.23E-04	8.04E-05
5	1.08E-04	**9.78E-05**	8.26E-05
6	1.06E-04	9.40E-05	8.41E-05
7	1.02E-04	9.40E-05	8.55E-05
8	1.02E-04	9.30E-05	8.77E-05
9	**9.85E-05**	8.90E-05	8.99E-05
10	9.85E-05	8.80E-05	9.13E-05
11	9.62E-05	8.80E-05	9.13E-05
12	9.54E-05	8.60E-05	9.13E-05
13	9.54E-05	8.40E-05	9.20E-05
14	8.69E-05	8.10E-05	1.04E-04
15	8.62E-05	7.70E-05	**9.64E-05**

From (3.8), it is known that the effective code rate R_{eff} is hardly affected by the chain length L when the CB length N and its message block length K are sufficiently large. Note that the exhaustive TBER search for various L and J is nearly impossible without the aid of the proposed TBER evaluation method.

Table 5.1 shows the evaluated TBERs of the modified parallel inter-CB decoder in the ensemble sense for $N = 1024$, $K_{\mathrm{u}} = 383$, $E_{\mathrm{b}}/N_0 = 2$ dB, and $P_e^* = 10^{-4}$. Using this evaluated TBERs, $L^*(J = 1) = 9$, $L^*(J = 2) = 5$, and $L^*(J = 3) = 15$. Therefore, the optimal J^* and corresponding chain length $L^*(J^*)$ satisfying $P_e^* = 10^{-4}$ are 2 and 5, respectively.

5.2 Complexity Bound of the Conventional and Modified Parallel Inter-CB Decoders of the Proposed PIC Polar Codes

In [36], the complexity of inter-CB decoding schemes can be measured as the average number of CB decoding trials per chain length. Each element in the decoding indicator vector $(d^{(i)})_1^L$ can be changed only from 0 to 1. In the conventional parallel inter-CB decoding algorithm, the decoding process at the i-th iteration is terminated if $(d^{(i)})_1^L = (d^{(i-1)})_1^L$, which means that at least one element in $(d^{(i)})_1^L$ is changed from 0 to 1 if $(d^{(i)})_1^L \neq (d^{(i-1)})_1^L$. Thus, the number of iterations in the conventional parallel inter-CB decoder is at most L.

Since the l-th CB with $d_l^{(i)} = 1$ is not decoded anymore with the iteration number larger than i and at least one element in $(d^{(i)})_1^L$ is changed from 0 to 1, there are at most $(L-i+1)$ decodable CBs at the i-th iteration. Therefore, the number of polar CB decoding trials under the conventional parallel inter-CB decoding algorithm is upper bounded by $\sum_{i=1}^{L}(L-i+1) = \frac{L(L+1)}{2}$.

In the modified parallel inter-CB decoding algorithm, CB decoding is performed only when the decoding state is changed. Since each element in the decoding indicator vector $(d^{(i)})_1^L$ can be changed only from 0 to 1, each CB can have at most $(2J+1)$ different decoding states under this decoding algorithm. Thus, the number of CB decoding trials is at most $L(2J+1)$ in the modified parallel inter-CB decoder. Therefore, the number of polar CB decoding trials under the modified parallel inter-CB decoding algorithm is upper bounded by $L \times \min\{(2J+1), \frac{L+1}{2}\}$.

As mentioned in Subsection 5.1.1, the number of iterations for decoding under the modified parallel inter-CB decoding algorithm is upper bounded by L. Therefore, $i_{\max} = L$.

Algorithm 5.1 Error performance evaluation

Input: P_{D_l} and $t_{\max}$

1: **Initialization**: Let $\begin{cases} \{d_l\}_{1\le l\le L} = \mathbf{0}, \{d_l\}_{l<1} = \mathbf{1}, \text{ and } \{d_l\}_{l>L} = \mathbf{1}. \\ l = 1,\ i = 1 \text{ and } t_{\text{err}} = 0. \end{cases}$

2: **for** $t = 1$ to $t_{\max}$ **do**

3: **while** $\{d_l^{(i)}\}_{1\le l\le L} \neq \mathbf{1}$ or $\{d_l^{(i)}\}_{1\le l\le L} \neq \{d_l^{(i-1)}\}_{1\le l\le L}$ **do**

4: **while** $l \le L$ **do**

5: Determine the $d_l^{(i)}$ as;

a) If $d_l^{(i-1)} = 1$

update $d_l^{(i)} \leftarrow 1$

b) If $d_l^{(i-1)} = 0$

update $d_l^{(i)} \leftarrow \begin{cases} 0, & \text{with probability } P_{D_l}^{(i-1)} \\ 1, & \text{with probability } (1 - P_{D_l}^{(i-1)}). \end{cases}$

6: **end while**

7: **Iteration index updating**: $i \leftarrow (i + 1)$

8: **end while**

9: **Error counting**

a) If $\{d_l^{(i)}\}_{1\le l\le L} = \mathbf{1}$

decoding is successful.

b) Else

decoding is failed and $t_{\text{err}} \leftarrow (t_{\text{err}} + 1)$.

10: **end for**

11: **Output:** $t_{\text{err}}/t_{\max}$.

Chapter 6

Numerical Results of PIC Polar Codes

In this chapter, various numerical results of the proposed PIC polar codes based on the Monte-Carlo simulation for various parameters are shown. The CRC code with generator polynomial $g_{\mathrm{CRC}}(x) = x^{16} + x^{15} + x^2 + 1$, called CRC-16-IBM, is the only fixed parameter through all sections in this chapter. The modified sequential inter-CB decoder is used except for Section 6.9, where the decoding complexities for various inter-CB decoding algorithms are compared. The reasons why the modified sequential inter-CB decoding algorithm is used in most sections are that it has relatively lower-complexities than the others for various $\frac{E_{\mathrm{b}}}{N_0}$ without sacrificing the TBER and CBER performances and it can be applied for arbitrary coupling depth J.

6.1 TBER Performances for Various Coupling Ratios

In this section, the TBER performances of the proposed PIC polar codes with the coupling depth $J = 1$ for various coupling ratios are compared. The simulated TBERs versus $\frac{E_{\mathrm{b}}}{N_0}$ are shown for the coupling ratios $r_{\mathrm{c}} = 0.05, 0.10, \cdots, 0.35$. The simulations are performed at

- $N = 1024$

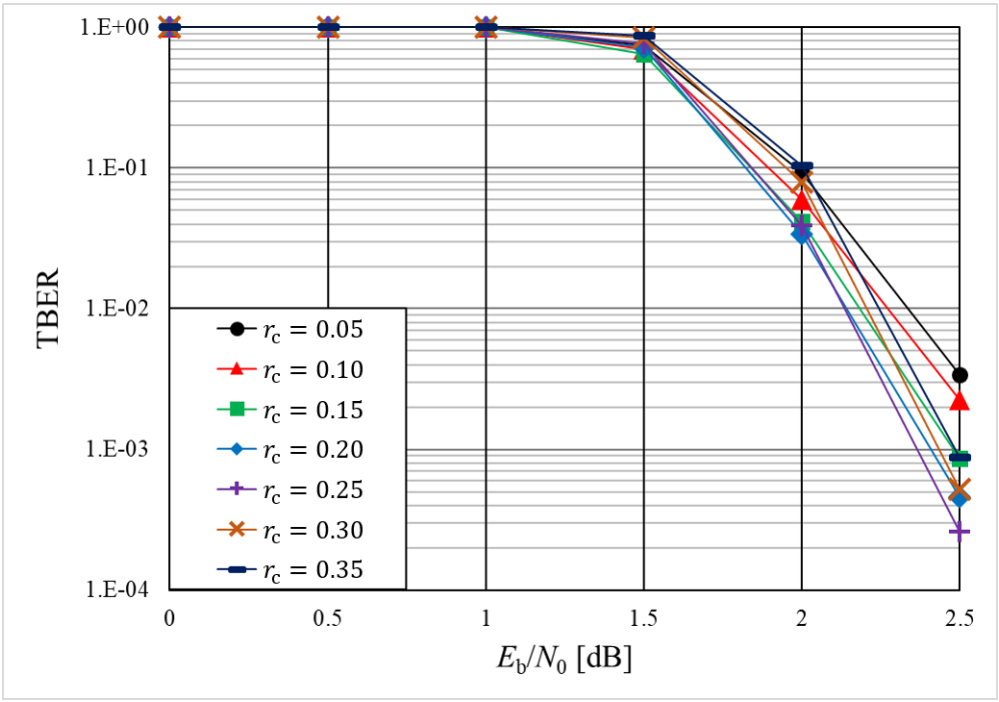

Figure 6.1: TBERs versus $\frac{E_b}{N_0}$ of the proposed PIC polar codes with coupling depth $J = 1$ for various coupling ratios.

- $(K_u, K_c) = \begin{cases} (474, 26) \\ (434, 54) \\ (390, 84) \\ (345, 115) \\ (296, 149) \\ (245, 184) \\ (190, 222) \end{cases}$
- $L = 10$,

where N is the CB length, K_u and K_c are the uncoupled and coupled message lengths, and L is the chain length. The simulations are performed under the CASCL decoder

Table 6.1: TBERs versus $\frac{E_\mathrm{b}}{N_0}$ of the proposed PIC polar codes with coupling depth $J = 1$ for various coupling ratios

$\frac{E_\mathrm{b}}{N_0}$ dB	$r_\mathrm{c} = 0.05$	$r_\mathrm{c} = 0.10$	$r_\mathrm{c} = 0.15$	$r_\mathrm{c} = 0.20$
0.0	1.00E+00	1.00E+00	1.00E+00	1.00E+00
0.5	1.00E+00	1.00E+00	1.00E+00	1.00E+00
1.0	1.00E+00	1.00E+00	1.00E+00	1.00E+00
1.5	7.44E-01	7.03E-01	6.42E-01	7.19E-01
2.0	9.28E-02	6.02E-02	4.16E-02	3.39E-02
2.5	3.38E-03	2.24E-03	8.60E-04	4.60E-04

$\frac{E_\mathrm{b}}{N_0}$ dB	$r_\mathrm{c} = 0.25$	$r_\mathrm{c} = 0.30$	$r_\mathrm{c} = 0.35$
0.0	1.00E+00	1.00E+00	1.00E+00
0.5	1.00E+00	1.00E+00	1.00E+00
1.0	1.00E+00	1.00E+00	1.00E+00
1.5	7.72E-01	8.44E-01	8.76E-01
2.0	3.93E-02	7.96E-02	1.03E-01
2.5	2.60E-04	5.20E-04	8.70E-04

with list size $\mathcal{L} = 8$. Note that this inter-CB decoding algorithm is universal for arbitrary coupling depth J and has low-complexity.

Recall (3.6)–(3.9). For a fixed CB length N, chain length L, and coupling depth J, a pair of parameters, uncoupled message block length K_u and coupled message block length K_c, are determined by a pair of parameters, effective code rate R_eff and coupling ratio r_c.

From Figure 6.1 and Table 6.1, there is the optimal coupling ratio $(r_\mathrm{c})^*$ which minimizes the TBER performance at the target $(\frac{E_\mathrm{b}}{N_0})^*$. Thus, the optimal coupling ratio $(r_\mathrm{c})^*$ and the fixed effective code rate $R_\mathrm{eff} = 0.5$ determine the optimal pair of message lengths, uncoupled message length K_u^* and coupled message length K_c^*, which minimizes the TBER performance at the target $(\frac{E_\mathrm{b}}{N_0})^*$. This optimal pair of message lengths can be obtained by using exhaustive search.

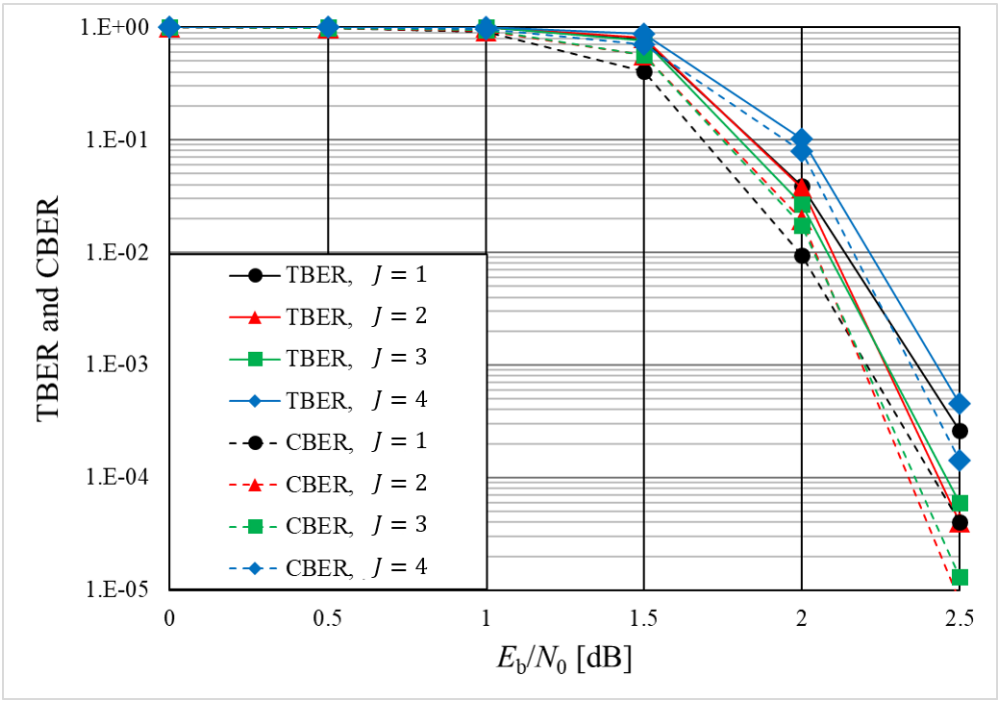

Figure 6.2: TBERs and CBERs versus $\frac{E_\mathrm{b}}{N_0}$ of the proposed PIC polar codes for various coupling depths $J = 1, 2, 3, 4$.

6.2 TBER and CBER Performances for Various Coupling Depths

In this section, the TBER and CBER performances of the proposed PIC polar codes for various coupling depths are compared when the coupling ratio is optimal to the corresponding coupling depth while other parameters, such as the CB length N, chain length L, and list size $\mathcal{L}$, are fixed. The simulated TBERs and CBERs versus $\frac{E_\mathrm{b}}{N_0}$ are shown for the coupling depths $J = 1, 2, 3, 4$.

Recall the question in the introduction of Chapter 3. There is a question that "If more than two CBs could deliver the extrinsic information, can PIC codes obtain more coding gain from the coupling diversity?". The answer is yes, up to $J = 3$ from the simulation result.

Table 6.2: TBERs and CBERs versus $\frac{E_\mathrm{b}}{N_0}$ of the proposed PIC polar codes for various coupling depths $J = 1, 2, 3, 4$

(a) TBERs versus $\frac{E_\mathrm{b}}{N_0}$

$\frac{E_\mathrm{b}}{N_0}$ dB	$J = 1$	$J = 2$	$J = 3$	$J = 4$
0.0	1.00E+00	1.00E+00	1.00E+00	1.00E+00
0.5	1.00E+00	1.00E+00	1.00E+00	1.00E+00
1.0	1.00E+00	1.00E+00	1.00E+00	1.00E+00
1.5	7.72E-01	8.14E-01	7.63E-01	8.73E-01
2.0	3.93E-02	3.74E-02	2.66E-02	1.03E-01
2.5	2.60E-04	4.00E-05	6.00E-05	4.50E-04

(b) CBERs versus $\frac{E_\mathrm{b}}{N_0}$

$\frac{E_\mathrm{b}}{N_0}$ dB	$J = 1$	$J = 2$	$J = 3$	$J = 4$
0.0	9.99E-01	1.00E+00	1.00E+00	9.99E-01
0.5	9.89E-01	9.93E-01	9.95E-01	9.96E-01
1.0	9.08E-01	9.34E-01	9.56E-01	9.62E-01
1.5	4.04E-01	5.73E-01	5.71E-01	7.05E-01
2.0	9.42E-03	1.95E-02	1.73E-02	7.94E-02
2.5	4.00E-05	8.00E-06	1.30E-05	1.43E-04

For each coupling depth $J = 1, 2, 3, 4$, there exists the optimal pair of parameters, K_u^* and K_c^*, satisfying $R_\mathrm{eff} = 0.5$ under $(\frac{E_\mathrm{b}}{N_0})^* = 2.5$ dB. The simulations are performed at

- $N = 1024$
- $(K_\mathrm{u}, K_\mathrm{c}) = \begin{cases} (296, 149), & \text{if } J\text{=1} \\ (193, 112), & \text{if } J\text{=2} \\ (193, 76), & \text{if } J\text{=3} \\ (138, 68), & \text{if } J\text{=4} \end{cases}$
- $L = 10$,

where N is the CB length, L is the chain length, and K_u and K_c are the optimal pair

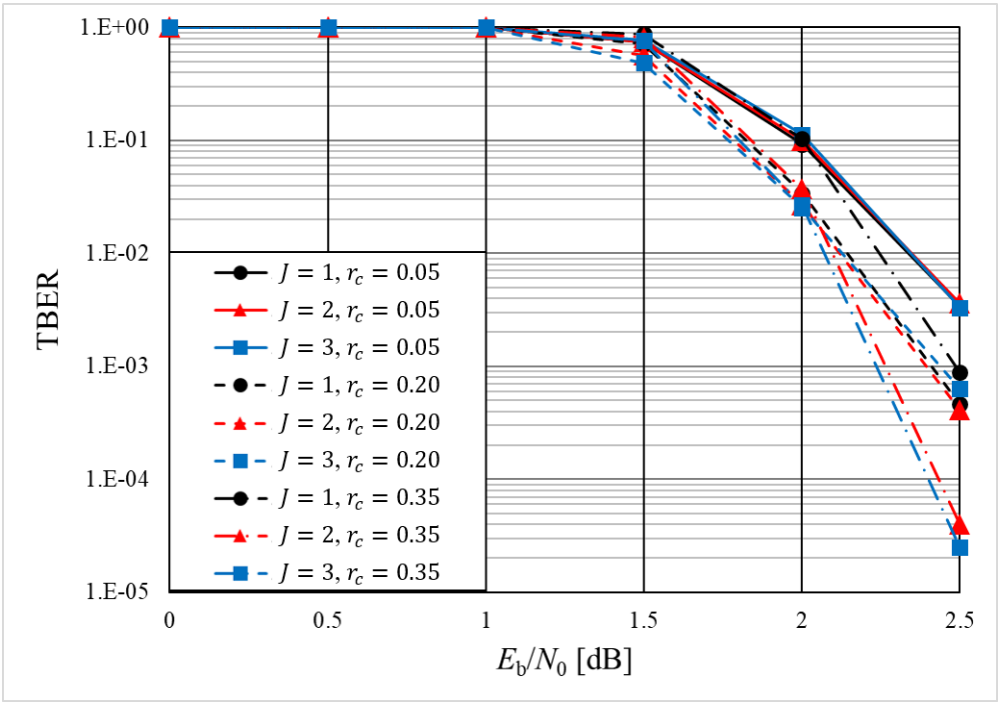

Figure 6.3: TBERs versus $\frac{E_b}{N_0}$ of the proposed PIC polar codes for various coupling depths $J = 1, 2, 3$ and coupling ratios $r_c = 0.05, 0.2, 0.35$.

of message lengths for each coupling depth J. The simulations are performed under the CASCL decoder with list size $\mathcal{L} = 8$.

As shown in Figure 6.2 and Table 6.2, it is confirmed that there are coding gains compared for the coupling depth $J = 2$ or $J = 3$, but there is no coding gain $J = 4$ for the fixed CB length $N = 1024$, the chain length $L = 10$, the CRC polynomial, and the optimized coupling ratio $(r_c)^*$ corresponding to the coupling depth J. The coding gains for the coupling depth $J = 2$ or $J = 3$ validate the proposed PIC polar codes.

Table 6.3: TBERs versus $\frac{E_b}{N_0}$ of the proposed PIC polar codes for various coupling depths $J = 1, 2, 3$ and coupling ratios $r_c = 0.05, 0.2, 0.35$

(a) $r_c = 0.05$

$\frac{E_b}{N_0}$ dB	$J = 1$	$J = 2$	$J = 3$
1.0	1.00E+00	1.00E+00	1.00E+00
1.5	7.44E-01	7.44E-01	7.66E-01
2.0	9.28E-02	1.00E-01	1.12E-01
2.5	3.38E-03	3.60E-03	3.32E-03

(b) $r_c = 0.20$

$\frac{E_b}{N_0}$ dB	$J = 1$	$J = 2$	$J = 3$
1.0	1.00E+00	1.00E+00	1.00E+00
1.5	7.19E-01	5.69E-01	4.85E-01
2.0	3.39E-02	2.68E-02	2.54E-02
2.5	4.60E-04	4.10E-04	6.30E-04

(c) $r_c = 0.35$

$\frac{E_b}{N_0}$ dB	$J = 1$	$J = 2$	$J = 3$
1.0	1.00E+00	1.00E+00	1.00E+00
1.5	8.76E-01	8.14E-01	7.63E-01
2.0	1.03E-01	3.74E-02	2.66E-02
2.5	8.70E-04	4.00E-05	2.50E-05

6.3 TBER Performances for Various Coupling Depths and Coupling Ratios

In this section, the TBER performances of the proposed PIC polar codes for various coupling depths and coupling ratios are compared. The simulated TBERs versus $\frac{E_b}{N_0}$ are shown for the coupling depths $J = 1, 2, 3$ and coupling ratios $r_c = 0.05, 0.2, 0.35$. The simulations are performed at

- $N = 1024$

- $(K_{\mathrm{u}}, K_{\mathrm{c}}) = \begin{cases} (474, 26), & \text{if } J = 1 \text{ and } r_{\mathrm{c}} = 0.05 \\ (345, 115), & \text{if } J = 1 \text{ and } r_{\mathrm{c}} = 0.20 \\ (190, 222), & \text{if } J = 1 \text{ and } r_{\mathrm{c}} = 0.35 \\ (475, 13), & \text{if } J = 2 \text{ and } r_{\mathrm{c}} = 0.05 \\ (347, 58), & \text{if } J = 2 \text{ and } r_{\mathrm{c}} = 0.20 \\ (193, 112), & \text{if } J = 2 \text{ and } r_{\mathrm{c}} = 0.35 \\ (474, 9), & \text{if } J = 3 \text{ and } r_{\mathrm{c}} = 0.05 \\ (348, 39), & \text{if } J = 3 \text{ and } r_{\mathrm{c}} = 0.20 \\ (193, 76), & \text{if } J = 3 \text{ and } r_{\mathrm{c}} = 0.35 \end{cases}$
- $L = 10$,

where N is the CB length, K_{u} and K_{c} are the uncoupled and coupled message lengths, J is the coupling depth, r_{c} is the coupling ratio, and L is the chain length. The simulations are performed under the CASCL decoder with list size $\mathcal{L} = 8$. The pair of parameters, K_{u} and K_{c}, are designed to have $R_{\mathrm{eff}} = 0.5$.

As shown in Figure 6.3 and Table 6.3, it is hard to observe the coding gains from the different coupling depths when $r_{\mathrm{c}} = 0.05$ or $r_{\mathrm{c}} = 0.20$. On the other hand, when $r_{\mathrm{c}} = 0.35$, there are 0.25 dB coding gains of the TBERs for $J = 2$ or $J = 3$. This result shows that the coding gain from the coupling depth J can be improved by the coupling ratio r_{c}.

6.4 TBER and CBER Performances for Various Chain Lengths

In this section, the TBER and CBER performances of the proposed PIC polar codes for various chain lengths are compared while other parameters are fixed and the coupling depth J is 3. The simulated TBERs and CBERs versus $\frac{E_{\mathrm{b}}}{N_0}$ are shown for the chain lengths $L = 5, 7, 9, 11, 13, 15$. The simulations are performed at

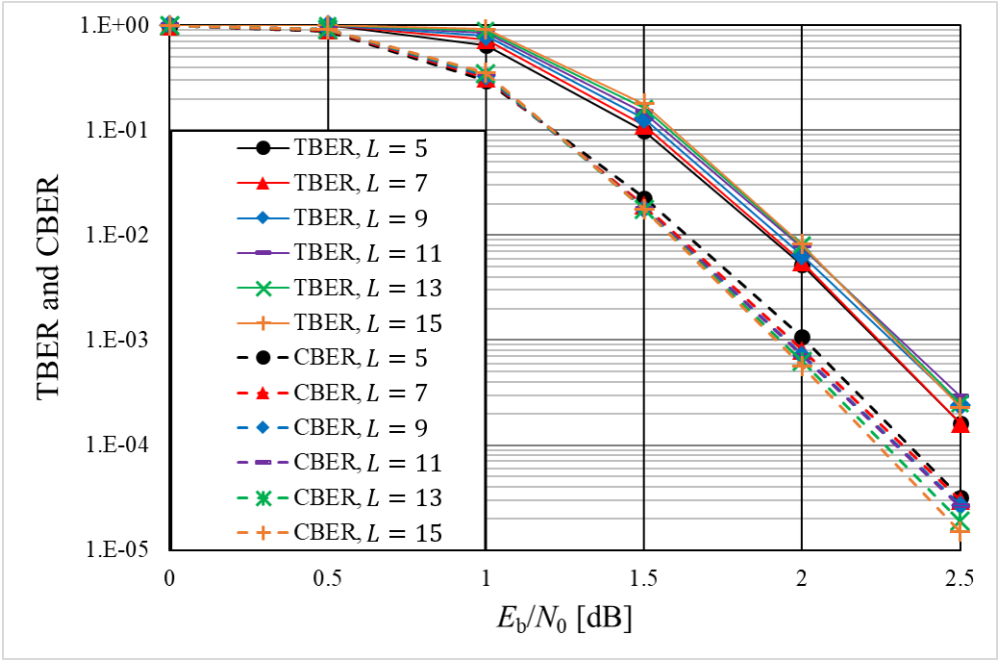

Figure 6.4: TBERs and CBERs versus $\frac{E_b}{N_0}$ of the proposed PIC polar codes for various chain lengths $L = 5, 7, 9, 11, 13, 15$.

- $N = 1024$
- $K_u = 424$
- $K_c = 21$
- $J = 3$,

under the CASCL decoder with list size $\mathcal{L} = 8$. The parameters of the message lengths K_u and K_c are designed to have $R_{eff} = 0.5$ at $L = 10$.

As shown in Figure 6.4 and Table 6.4, the CBER (dashed line) is getting better as L increases, while the TBER (solid line) is getting worse when $\frac{E_b}{N_0} \leq 2$ dB. But, when $\frac{E_b}{N_0} \geq 2.5$ dB, the TBER is getting worse as L increases until $L = 11$ and then is getting better as L increases. This observation motivates the optimal design of the pair of parameters, the coupling depth J and the chain length L, as in Subsection 5.1.2.

Table 6.4: TBERs and CBERs versus $\frac{E_\mathrm{b}}{N_0}$ of the proposed PIC polar codes for various chain lengths $L = 5, 7, 9, 11, 13, 15$

(a) TBERs versus $\frac{E_\mathrm{b}}{N_0}$

$\frac{E_\mathrm{b}}{N_0}$ dB	$L = 5$	$L = 7$	$L = 9$	$L = 11$	$L = 13$	$L = 15$
0.0	1.00E+00	1.00E+00	1.00E+00	1.00E+00	1.00E+00	1.00E+00
0.5	9.96E-01	1.00E+00	1.00E+00	1.00E+00	1.00E+00	1.00E+00
1.0	6.44E-01	7.38E-01	8.02E-01	8.55E-01	8.87E-01	9.18E-01
1.5	9.83E-02	1.12E-01	1.29E-01	1.48E-01	1.64E-01	1.80E-01
2.0	5.29E-03	5.59E-03	6.41E-03	7.71E-03	8.01E-03	8.22E-03
2.5	1.60E-04	1.60E-04	2.40E-04	2.90E-04	2.50E-04	2.30E-04

(b) CBERs versus $\frac{E_\mathrm{b}}{N_0}$

$\frac{E_\mathrm{b}}{N_0}$ dB	$L = 5$	$L = 7$	$L = 9$	$L = 11$	$L = 13$	$L = 15$
0.0	9.93E-01	9.95E-01	9.95E-01	9.96E-01	9.96E-01	9.96E-01
0.5	8.78E-01	8.96E-01	9.08E-01	9.14E-01	9.20E-01	9.24E-01
1.0	2.97E-01	3.15E-01	3.30E-01	3.44E-01	3.47E-01	3.52E-01
1.5	2.27E-02	1.92E-02	1.80E-02	1.78E-02	1.76E-02	1.75E-02
2.0	1.07E-03	8.06E-04	7.24E-04	7.11E-04	6.25E-04	5.60E-04
2.5	3.20E-05	3.00E-05	2.70E-05	2.60E-05	1.90E-05	1.50E-05

6.5 Coupled and Uncoupled CBER Performances for Various List Sizes

In this section, the CBER performances of the proposed PIC polar codes are compared to the performances of the uncoupled polar codes for various list sizes with the coupling depth $J = 2$. The simulated CBERs versus $\frac{E_\mathrm{b}}{N_0}$ are shown for the list sizes $\mathcal{L} = 1, 2, 4, 8$. The simulations are performed at

- $N = 1024$
- $K_\mathrm{u} = 424$
- $K_\mathrm{c} = 31$

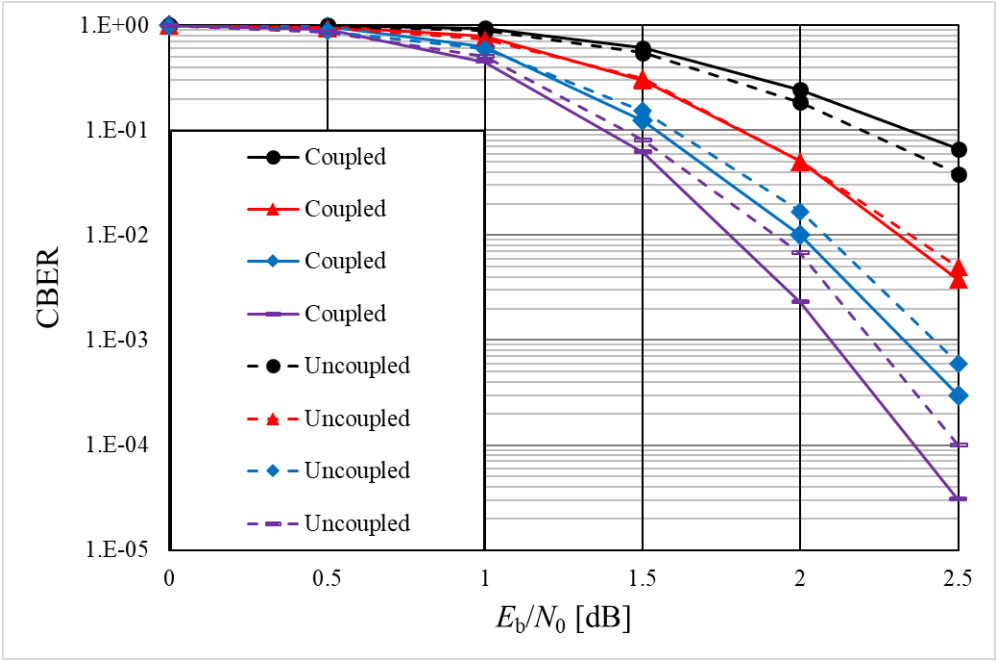

Figure 6.5: Coupled and uncoupled CBERs versus $\frac{E_b}{N_0}$ of the proposed PIC polar codes for various list sizes $\mathcal{L} = 1, 2, 4, 8$.

- $L = 10$
- $J = 2$,

under the CASCL decoder and modified sequential inter-CB decoding algorithm. The message length K of the uncoupled polar code is $K = K_u + 2JK_c = 548$.

As shown in Figure 6.5 and Table 6.5, the coupled CBER (the solid line) is getting better than the uncoupled CBER (the dashed line) for each list size more than 1. Moreover, the coding gain due to the proposed coupling scheme is improved as the list size increases. But, the coupled CBER is getting worse than the uncoupled CBER when the list size $\mathcal{L} = 1$. From the simulation result, there would be no coding gain of the proposed PIC polar codes for some small list sizes.

Table 6.5: Coupled and uncoupled CBERs versus $\frac{E_b}{N_0}$ of the proposed PIC polar codes for various list sizes $\mathcal{L} = 1, 2, 4, 8$

(a) Coupled CBERs

$\frac{E_b}{N_0}$ dB	$\mathcal{L} = 1$	$\mathcal{L} = 2$	$\mathcal{L} = 4$	$\mathcal{L} = 8$
0.0	1.00E+00	1.00E+00	9.97E-01	9.99E-01
0.5	9.95E-01	9.77E-01	9.64E-01	9.23E-01
1.0	9.37E-01	7.83E-01	6.30E-01	4.50E-01
1.5	6.11E-01	3.00E-01	1.24E-01	6.13E-02
2.0	2.43E-01	5.05E-02	1.00E-02	2.30E-03
2.5	6.63E-02	3.80E-03	3.00E-04	3.00E-05

(b) Uncoupled CBERs

$\frac{E_b}{N_0}$ dB	$\mathcal{L} = 1$	$\mathcal{L} = 2$	$\mathcal{L} = 4$	$\mathcal{L} = 8$
0.0	1.00E+00	1.00E+00	9.90E-01	9.90E-01
0.5	9.81E-01	9.44E-01	8.78E-01	8.56E-01
1.0	8.94E-01	7.37E-01	5.98E-01	5.02E-01
1.5	5.49E-01	3.12E-01	1.53E-01	8.06E-02
2.0	1.84E-01	5.05E-02	1.68E-02	6.70E-03
2.5	3.82E-02	5.00E-03	6.00E-04	1.00E-04

6.6 TBER Performances for Various CB Lengths

In this section, the TBER performances of the proposed PIC polar codes for various CB lengths and coupling depths are compared while the effective code rate, coupling ratio, and chain length are fixed. The simulated TBERs versus $\frac{E_b}{N_0}$ are shown for the CB lengths $N = 512, 1024, 2048$ and coupling depths $J = 1, 2$. The simulations are performed at

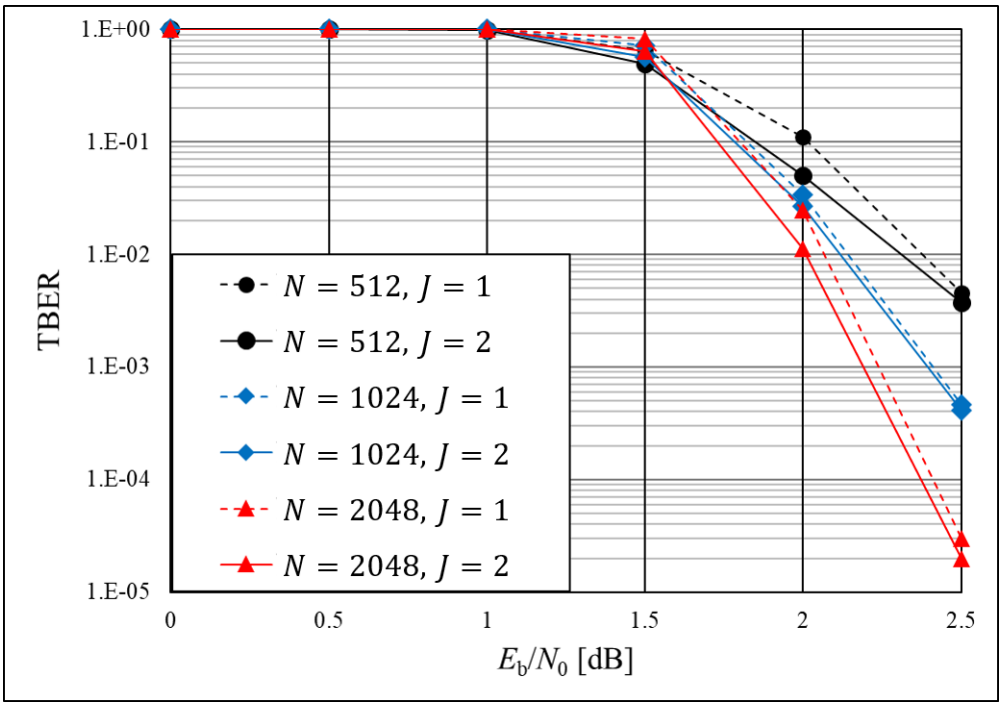

Figure 6.6: TBERs versus $\frac{E_b}{N_0}$ of the proposed PIC polar codes for various coupling depths $J = 1, 2$ and CB lengths $N = 512, 1024, 2048$.

- $(K_u, K_c) = \begin{cases} (172, 58), & \text{if } N\text{=512 and } J\text{=1} \\ (173, 29), & \text{if } N\text{=512 and } J\text{=2} \\ (345, 115), & \text{if } N\text{=1024 and } J\text{=1} \\ (347, 58), & \text{if } N\text{=1024 and } J\text{=2} \\ (690, 230), & \text{if } N\text{=2048 and } J\text{=1} \\ (693, 116), & \text{if } N\text{=2048 and } J\text{=2} \end{cases}$
- $L = 10$,

under the CASCL decoder with list size $\mathcal{L} = 8$. The uncoupled message length K_u and coupled message length K_c are designed to have $R_{\text{eff}} = 0.5$ and $r_c = 0.20$ for each CB length N.

Table 6.6: TBERs versus $\frac{E_b}{N_0}$ of the proposed PIC polar codes for various coupling depths $J = 1, 2$ and CB lengths $N = 512, 1024, 2048$

(a) $J = 1$

$\frac{E_b}{N_0}$ dB	$N = 512$	$N = 1024$	$N = 2048$
0.0	1.00E+00	1.00E+00	1.00E+00
0.5	1.00E+00	1.00E+00	1.00E+00
1.0	9.96E-01	1.00E+00	1.00E+00
1.5	6.47E-01	7.19E-01	8.33E-01
2.0	1.10E-01	3.39E-02	2.50E-02
2.5	4.56E-03	4.60E-04	3.00E-05

(b) $J = 2$

$\frac{E_b}{N_0}$ dB	$N = 512$	$N = 1024$	$N = 2048$
0.0	1.00E+00	1.00E+00	1.00E+00
0.5	1.00E+00	1.00E+00	1.00E+00
1.0	9.86E-01	1.00E+00	1.00E+00
1.5	4.95E-01	5.69E-01	6.42E-01
2.0	5.00E-02	2.68E-02	1.13E-02
2.5	3.73E-03	4.10E-04	2.00E-05

As shown in Figure 6.6 and Table 6.6, for the fixed coupling ratio and the fixed chain length, it is verified that the tendency of the TBER performance gaps between the different coupling depths are independent of the CB length.

6.7 TBER Performances for Various Effective Code Rates

In this section, the TBER performances of the proposed PIC polar codes with coupling depth $J = 2$ for various effective code rates are compared while the CB length, coupling ratio, and chain length are fixed. The simulated TBERs versus $\frac{E_b}{N_0}$ are shown for the CB lengths $R_{\text{eff}} = 0.250, 0.333, 0.500, 0.667, 0.750$. The simulations are performed at

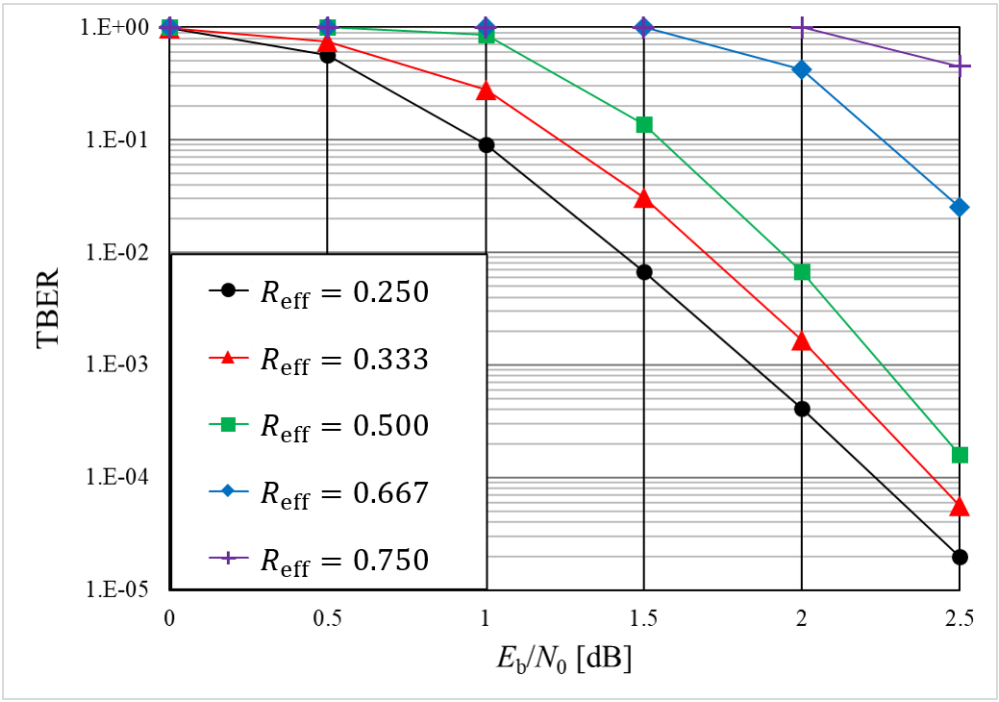

Figure 6.7: TBERs versus $\frac{E_b}{N_0}$ of the proposed PIC polar codes for various effective code rates $R_{\text{eff}} = 0.250, 0.333, 0.500, 0.667, 0.750$.

- $N = 1024$
- $(K_u, K_c) = \begin{cases} (220, 16), & \text{if } R_{\text{eff}} = 0.250 \\ (290, 21), & \text{if } R_{\text{eff}} = 0.333 \\ (424, 31), & \text{if } R_{\text{eff}} = 0.500 \\ (550, 41), & \text{if } R_{\text{eff}} = 0.667 \\ (613, 45), & \text{if } R_{\text{eff}} = 0.750 \end{cases}$
- $L = 10$
- $J = 2,$

under the CASCL decoder with list size $\mathcal{L} = 8$. The uncoupled message length K_u and coupled message length K_c are designed to have the fixed coupling ratio $r_c = 0.113$

Table 6.7: TBERs versus $\frac{E_\mathrm{b}}{N_0}$ of the proposed PIC polar codes for various effective code rates $R_\mathrm{eff} = 0.250, 0.333, 0.500, 0.667, 0.750$

$\frac{E_\mathrm{b}}{N_0}$ dB	$R_\mathrm{eff} = 0.250$	$R_\mathrm{eff} = 0.333$	$R_\mathrm{eff} = 0.500$	$R_\mathrm{eff} = 0.667$	$R_\mathrm{eff} = 0.750$
0.0	9.88E-01	9.94E-01	1.00E+00	1.00E+00	1.00E+00
0.5	5.63E-01	7.50E-01	1.00E+00	1.00E+00	1.00E+00
1.0	9.10E-02	2.80E-01	8.63E-01	1.00E+00	1.00E+00
1.5	6.75E-03	3.05E-02	1.38E-01	9.97E-01	1.00E+00
2.0	4.10E-04	1.67E-03	6.78E-03	4.26E-01	9.98E-01
2.5	2.00E-05	5.66E-05	1.60E-04	2.54E-02	4.49E-01

for each CB length N.

As shown in Figure 6.7 and Table 6.7, the relationship between the TBER performance and the effective code rate is confirmed.

6.8 Performance Comparisons Between the Simulated and Evaluated TBERs

In this section, the simulated TBERs of the proposed PIC polar codes and corresponding evaluated TBERs in the ensemble sense are compared for some coupling depths and corresponding coupled message lengths while other parameters are fixed. The simulated and evaluated TBERs versus $\frac{E_\mathrm{b}}{N_0}$ are shown for the coupling depths $J = 1, 2, 3$. The simulations are performed at

- $N = 1024$
- $K_\mathrm{u} = 424$
- $K_\mathrm{c} = \begin{cases} 63, & \text{if } J\text{=}1 \\ 32, & \text{if } J\text{=}2 \\ 21, & \text{if } J\text{=}3 \end{cases}$
- $L = 10$,

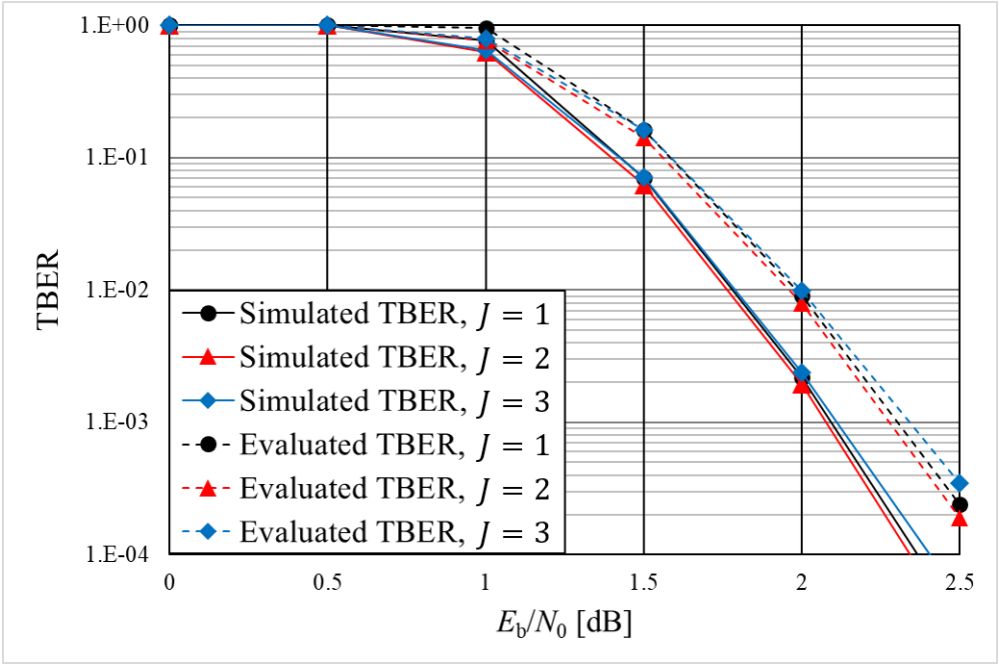

Figure 6.8: Simulated and evaluated TBERs versus $\frac{E_b}{N_0}$ of the proposed PIC polar codes for various coupling depths $J = 1, 2, 3$.

under the CASCL decoder with list size $\mathcal{L} = 8$. The uncoupled message length K_u and coupled message length K_c are designed to have the fixed effective code rate $R_{eff} = 0.500$ for each coupling depth N.

As shown in Figure 6.8 and Table 6.8, it is observed that the evaluated TBERs are very close to the simulated TBERs for each coupling depth with $\frac{E_b}{N_0}$ gap lower than 0.3 dB.

6.9 Complexity Comparisons among the Various Inter-CB Decoding Algorithms

Let $\mathcal{N}$ be the average number of the polar CB decoding trials per chain length L. In [36], the decoding complexity of the PIC polar code is evaluated by $\mathcal{N}$. In this section,

Table 6.8: Simulated and evaluated TBERs versus $\frac{E_\mathrm{b}}{N_0}$ of the proposed PIC polar codes for various coupling depths $J = 1, 2, 3$

(a) Simulated TBERs

$\frac{E_\mathrm{b}}{N_0}$ dB	$J = 1$	$J = 2$	$J = 3$
0.0	1.00E+00	1.00E+00	1.00E+00
0.5	1.00E+00	9.99E-01	9.99E-01
1.0	7.74E-01	6.24E-01	6.49E-01
1.5	7.05E-02	6.25E-02	7.08E-02
2.0	2.19E-03	1.94E-03	2.39E-03
2.5	3.30E-05	2.60E-05	4.80E-05

(b) Evaluated TBERs

$\frac{E_\mathrm{b}}{N_0}$ dB	$J = 1$	$J = 2$	$J = 3$
0.0	1.00E+00	1.00E+00	1.00E+00
0.5	9.99E-01	9.99E-01	9.98E-01
1.0	9.55E-01	7.69E-01	8.00E-01
1.5	1.61E-01	1.43E-01	1.61E-01
2.0	9.04E-03	8.00E-03	9.87E-03
2.5	2.40E-04	1.89E-04	3.49E-04

the decoding complexities of the various inter-CB decoding schemes are compared. The simulations are performed at

- $N = 1024$
- $K_\mathrm{u} = 424$
- $K_\mathrm{c} = \begin{cases} 63, & \text{if } J\text{=}1 \\ 32, & \text{if } J\text{=}2 \\ 21, & \text{if } J\text{=}3 \end{cases}$
- $L = 10$,

under the CASCL decoder with list size $\mathcal{L} = 8$. The inter-CB decoder used at these simulations are described in Algorithms 2.1, 4.2, 4.3, and 4.5–4.8.

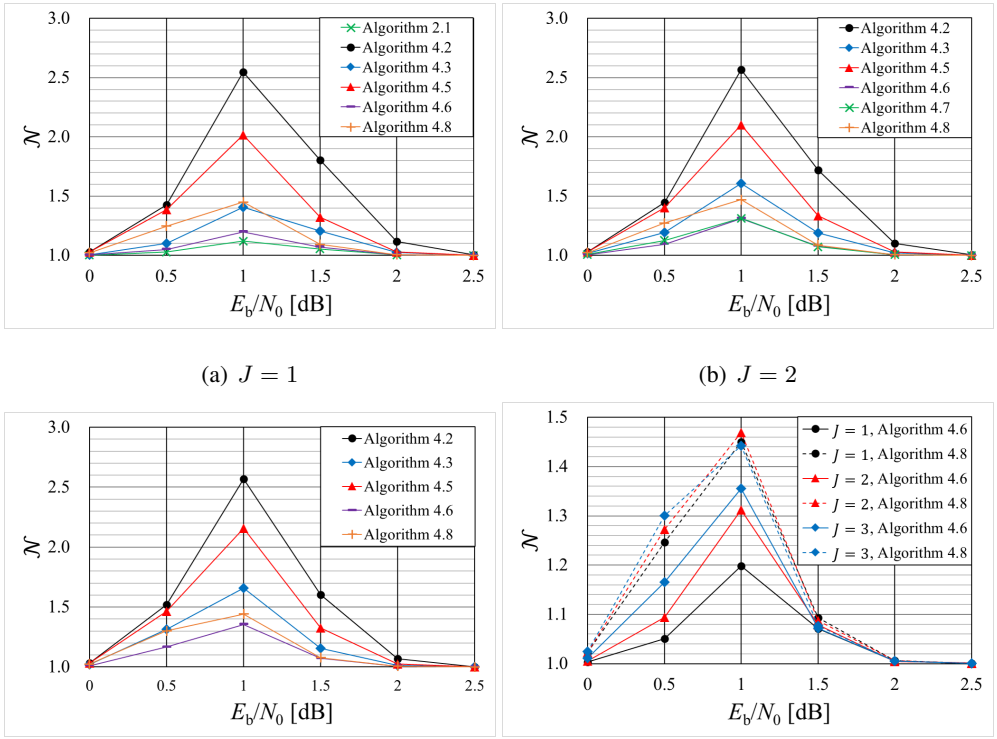

(a) $J = 1$ (b) $J = 2$

(c) $J = 3$ (d) $J = 1, 2, 3$

Figure 6.9: Complexity comparisons among the various inter-CB decoding algorithms for various coupling depths $J = 1, 2, 3$.

From Figure 6.9 and Table 6.9, the conventional parallel, conventional sequential, modified parallel, and modified sequential inter-CB decoding algorithms have low complexities in that order for any $\frac{E_b}{N_0}$ and each $J = 1, 2, 3$.

From Figure 6.9(a) and Table 6.9(a), for $J = 1$, the look-back and go-back inter-CB decoding algorithm has the lowest decoding complexity among the compared decoding algorithms. Also, the proposed sequential and probabilistic re-decoding inter-CB decoding algorithm has lower complexity than the modified parallel inter-CB decoding algorithm for $\frac{E_b}{N_0} \geq 1.5$ dB and has lower complexity than the modified sequential inter-CB decoding algorithm for $\frac{E_b}{N_0} = 2.5$ dB.

From Figure 6.9(b) and Table 6.9(b), for $J = 2$, the proposed modified look-

back and go-back inter-CB decoding algorithm has the lowest decoding complexity among the compared decoding algorithms for $\frac{E_b}{N_0} \geq 1.5$ dB and the proposed modified sequential inter-CB decoding algorithm has the lowest decoding complexity for $\frac{E_b}{N_0} \leq 1.0$ dB. Also, the proposed sequential and probabilistic re-decoding inter-CB decoding algorithm has lower complexity than the modified parallel inter-CB decoding algorithm for $\frac{E_b}{N_0} \geq 1.0$ dB and has lower complexity than the modified sequential inter-CB decoding algorithm for $\frac{E_b}{N_0} = 2.5$ dB.

From Figure 6.9(c) and Table 6.9(c), for $J = 3$, the proposed modified sequential inter-CB decoding algorithm has the lowest decoding complexity for $\frac{E_b}{N_0} \leq 1.5$ dB and the proposed sequential and probabilistic re-decoding inter-CB decoding algorithm has the lowest decoding complexity for $\frac{E_b}{N_0} \geq 2.0$ dB.

From Figure 6.9(d) and Table 6.9(d), for the proposed modified sequential inter-CB decoding algorithm, the decoding complexity of the coupling depth $J = 3$ is even lower than that of the coupling depth $J = 1$ for $\frac{E_b}{N_0} \geq 2.0$ dB. Also, for the proposed sequential and probabilistic re-decoding inter-CB decoding algorithm, the decoding complexity of the coupling depth $J = 3$ is even lower than that of the coupling depth $J = 1$ for $\frac{E_b}{N_0} \geq 1.0$ dB. Unexpectedly, although the coupling depth is larger, the decoding complexity is lowered due to the coding gain obtained from the coupling depth.

Table 6.9: Complexity comparisons among the various inter-CB decoding algorithms for various coupling depths $J = 1, 2, 3$

(a) $J = 1$

$\frac{E_b}{N_0}$ dB	Alg. 4.2	Alg. 4.5	Alg. 4.3	Alg. 4.6	Alg. 2.1	Alg. 4.8
0.0	1.0302	1.0309	1.0064	1.0032	1.0026	1.0227
0.5	1.4280	1.3855	1.1003	1.0509	1.0277	1.2467
1.0	2.5452	2.0159	1.4064	1.1980	1.1208	1.4501
1.5	1.8038	1.3228	1.2037	1.0708	1.0531	1.0930
2.0	1.1182	1.0276	1.0243	1.0055	1.0045	1.0058
2.5	1.0060	1.0011	1.0012	1.0002	1.0002	1.0002

(b) $J = 2$

$\frac{E_b}{N_0}$ dB	Alg. 4.2	Alg. 4.5	Alg. 4.3	Alg. 4.6	Alg. 4.7	Alg. 4.8
0.0	1.0289	1.0290	1.0164	1.0050	1.0088	1.0225
0.5	1.4453	1.4034	1.1942	1.0940	1.1272	1.2726
1.0	2.5686	2.1002	1.6062	1.3116	1.3125	1.4696
1.5	1.7217	1.3353	1.1880	1.0784	1.0724	1.0869
2.0	1.1007	1.0288	1.0224	1.0042	1.0053	1.0059
2.5	1.0051	1.0010	1.0012	1.0012	1.0002	1.0002

(c) $J = 3$

$\frac{E_b}{N_0}$ dB	Alg. 4.2	Alg. 4.5	Alg. 4.3	Alg. 4.6	Alg. 4.8
0.0	1.0324	1.0318	1.0210	1.0107	1.0242
0.5	1.5181	1.4640	1.3121	1.1656	1.3005
1.0	2.5691	2.1570	1.6578	1.3554	1.4425
1.5	1.6016	1.3262	1.1558	1.0723	1.0768
2.0	1.0681	1.0263	1.0140	1.0053	1.0052
2.5	1.0031	1.0011	1.0006	1.0002	1.0002

(d) $J = 1, 2, 3$

$\frac{E_b}{N_0}$ dB	$J = 1$ Alg. 4.6	$J = 1$ Alg. 4.8	$J = 2$ Alg. 4.6	$J = 2$ Alg. 4.8	$J = 3$ Alg. 4.6	$J = 3$ Alg. 4.8
0.0	1.0032	1.0227	1.0050	1.0225	1.0107	1.0242
0.5	1.0509	1.2467	1.0940	1.2726	1.1656	1.3005
1.0	1.1980	1.4501	1.3116	1.4696	1.3554	1.4425
1.5	1.0708	1.0930	1.0784	1.0869	1.0723	1.0768
2.0	1.0055	1.0058	1.0042	1.0059	1.0053	1.0052
2.5	1.0002	1.0002	1.0012	1.0002	1.0002	1.0002

Chapter 7

Conclusions

In this dissertation, there were three main contributions:

i) Proposed a new parameter, called coupling depth J which generalizes the coupling scheme of PIC polar codes [36] and a construction method of PIC polar codes with coupling depth J.

ii) Proposed a polar CB decoding algorithm and various inter-CB decoding algorithms and the modified *look-back* and *go-back* decoding algorithm introduced in [36] for the coupling depth $J = 2$.

iii) Proposed an error rate evaluation of the modified parallel inter-CB decoder and optimized a pair of parameters, the chain length and coupling depth of the proposed PIC polar codes.

The validity of those proposed methods were confirmed by the numerical results based on the Monte-Carlo simulation.

As a further work, an $L \times (L + L_{\mathrm{h}} + L_{\mathrm{t}})$ binary matrix $\mathbf{C}$ is suggested to express the PIC polar codes with generalized coupling schemes, where L_{h} and L_{t} are non-negative integers. The matrix $\mathbf{C}$ is called coupling matrix, which satisfies following rules:

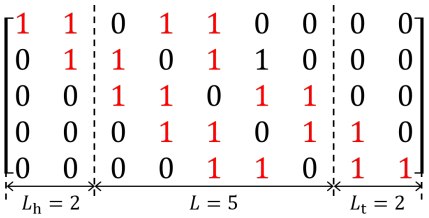

Figure 7.1: Coupling matrix $\mathbf{C}$ of the proposed polar codes with coupling depth $J = 2$ and chain length $L = 5$.

i) $(\mathbf{C})_{i,i+L_h} = 0$.

ii) $(\mathbf{C})_{i,j+L_h} = (\mathbf{C})_{j,i+L_h}$ for all i and j, $1 \leq i, j \leq L$,

where $(\mathbf{C})_{i,j}$ means the element of the matrix $\mathbf{C}$ with row index i and column index j. Using the matrix $\mathbf{C}$, it is possible to define the coupling between i-th CB and j-th CB for all $i \neq j$, $1 \leq i, j \leq L$. The i-th CB and j-th CB are coupled each other if and only if $(\mathbf{C})_{i,j+L_h} = 1$. Thus, any PIC polar codes with generalized coupling scheme can be expressed as a coupling matrix $\mathbf{C}$.

It is an open problem whether there exists a PIC polar code with coupling matrix $\mathbf{C}$ which performs better than the proposed PIC polar codes, when $L_h + L_t = 2J$. In addition, research on the coupling matrix C, which enables efficient decoding, is also an open problem.

Even for $J = 2$, it is complicated to modify the FF and FB decoding processes to generalize the look-back and go-back inter-CB decoding algorithm. As another further work, the modified look-back and go-back inter-CB decoding algorithm for $J \geq 3$ is an open problem suggested by this dissertation.

Bibliography

[1] C. E. Shannon, "A mathematical theory of communications," *Bell Syst. Tech. J.*, vol. 27, pp. 379–423, Jul. 1948.

[2] S. Haykin, *Communication Systems*. 4th Ed. NY, NY, USA: John Wiley & Sons, Inc., 2001.

[3] J. G. Proakis and M. Salehi, *Digital Communications*, 5th Ed. NY, NY, USA: MacGraw-Hill, 2008.

[4] F. J. MacWilliams and N. J. A. Sloane, *The Theory of Error-Correcting Codes.* Amsterdam, The Netherlands: North-Holland, 1977.

[5] R. E. Blahut, *Algebraic Codes for Data Transmission.* NY, NY, USA: Cambridge University Press, 2003.

[6] S. Lin and D. J. Costello, Jr., *Error Control Coding*. 2nd Ed, Upper Saddle River, NJ, USA: Prentice Hall, 2004.

[7] T. J. Richardson and R. L. Urbanke, *Modern Coding Theory*. NY, NY, USA: Cambridge University Press, 2008.

[8] R. W. Hamming, "Error detecting and error correcting codes," *Bell Syst. Tech. J.,* vol. 26, no. 2, pp. 147–160, 1950.

[9] M. J. E. Golay, "Notes on digital coding," *Proc. IRE*, vol. 37, pp. 657–657, Jun. 1949.

[10] I. S. Reed, “A class of multiple-error-correcting codes and the decoding scheme,” *IRE Trans. Inf. Theory*, vol. PGIT-4, pp. 38–49, 1954.

[11] R. E. Muller, “Application of Boolean algebra to switching circuit design and to error detection,” *IRE Trans. Electron. Comput.,* vol. EC-3, pp. 6–12, 1954.

[12] A. Hocquenghem, “Codes correcteurs d’erreurs,” *Chiffres*, vol. 2, pp. 147–156, 1959.

[13] R. C. Bose and D. K. Ray-Chaudhuri, “On a class of error-correcting binary group codes,” *Inf. Control*, vol. 3, pp. 68–79, Mar. 1960.

[14] I. S. Reed and G. Solomon, “Polynomial codes over certain finite fields,” *SIAM J.,* vol. 8, no. 2, pp. 300–304, Jun. 1960.

[15] R. G. Gallager, *Low-Density Parity-Check Codes*. Cambridge, MA, USA: MIT Press, 1963.

[16] D. J. C. MacKay and R. M. Neal, “Near Shannon limit performance of low density parity check codes,” *Electron. Lett.,* vol. 32, no. 18, pp. 1645–1646, Aug. 1996.

[17] D. J. C. MacKay, “Good error correcting codes based on very sparse matrices,” *IEEE Trans. Inf. Theory*, vol. 45, no. 2, pp. 399–431, Mar. 1999.

[18] E. Arikan, “Channel polarization: a method for constructing capacity-achieving codes for symmetric binary-input memoryless channels,” *IEEE Trans. Inf. Theory,* vol. 55, no. 7, pp. 3051–3073, Jul. 2009.

[19] P. Elias, “Coding for noisy channels,” *IRE Int. Convent. Record*, Mar. 1955, pp. 37–46.

[20] C. Berrou, A. Glavieux, and P. Thitimajshima, “Near Shannon limit error-correcting coding and decoding,” in *Proc. IEEE Int. Conf. Commun.*, Geneva, Switzerland, May 1993, pp. 1064–1070.

[21] Y. Li, R. Liu, and R. Wang, "A low-complexity SNR estimation algorithm based on frozen bits of polar codes," *IEEE Commun. Lett.*, vol. 20, no. 12, pp. 2354–2357, Dec. 2016.

[22] J. Dai, K. Niu, Z. Si, C. Dong, and J. Lin, "Does Gaussian approximation work well for the long-length polar code construction?," *IEEE Access,* vol. 5, pp. 7950–7963, Apr. 2017.

[23] A. B.-Stimming, M. B. Parizi, and A. Burg, "LLR-based successive cancellation list decoding of polar codes," *IEEE Trans. Signal Process.*, vol. 63, no. 19, pp. 5165–5179, Oct. 2015.

[24] S.-N. Hong and M.-O. Jeong, "An efficient construction of rate-compatible punctured polar (RCPP) codes using hierarchical puncturing," *IEEE Trans. Commun*., vol. 66, no. 11, pp. 5041–5052, Nov. 2018.

[25] M. E.-Khamy, H. Mahdavifar, G. Feygin, J. Lee, and I. Kang, "Relaxed polar codes," *IEEE Trans. Inf. Theory,* vol. 63, no. 4, pp. 1986–2000, Apr. 2017.

[26] E. Sasoglu and L. Wang, "Universal polarization," *IEEE Trans. Inf. Theory,* vol. 62, no. 6, pp. 2937–2946, Oct. 2016.

[27] E. Arikan and E. Telatar, "On the rate of channel polarization," in *Proc. IEEE Int. Symp. Inf. Theory (ISIT)*, Seoul, South Korea, Jun. 2009, pp. 1493–1495.

[28] S. B. Korada, E. Sasoglu, and R. Urbanke, "Polar codes: Characterization of exponent, bounds, and constructions," *IEEE Trans. Inf. Theory,* vol. 56, no. 12, pp. 6253–6264, Dec. 2010.

[29] M. Mondelli, S. H. Hassani, and R. L. Urbanke, "Unified scaling of polar codes: Error exponent, scaling exponent, moderate deviations, and error floors," *IEEE Trans. Inf. Theory,* vol. 62, no. 12, pp. 6698–6712, Dec. 2016.

[30] I. Tal and A. Vardy, "List decoding of polar codes," *IEEE Trans. Inf. Theory,* vol. 61, no. 5, pp. 2213–2226, May 2015.

[31] I. Tal and A. Vardy, "How to construct polar codes," *IEEE Trans. Inf. Theory,* vol. 59, no. 10, pp. 6562–6582, Oct. 2013.

[32] P. Trifonov and V. Miloslavskaya, "Polar subcodes," *IEEE J. Sel. Areas Commun.*, vol. 34, no. 2, pp. 254–266, Feb. 2016.

[33] A. A.-Yazdi and F. R. Kschischang, "A simplified successive-cancellation decoder for polar codes," *IEEE Commun. Lett.*, vol. 15, no. 12, pp. 1378–1380, Dec. 2011.

[34] P. Trifonov, "Efficient design and decoding of polar codes," *IEEE Trans. Commun.*, vol. 60, no. 11, pp. 3221–3227, Nov. 2012.

[35] L. Yang, Y. Xie, X. Wu, and J. Yuan, "Partially information-coupled turbo codes for LTE systems," *IEEE Trans. Commun.*, vol. 66, no. 10, pp. 4381–4392, Oct. 2018.

[36] X. Wu, L. Yang, Y. Xie, and J. Yuan, "Partially information coupled polar codes," *IEEE Access,* vol. 6, pp. 63689–63702, Sep. 2018.

[37] E. Arikan, "Systematic polar coding," *IEEE Commun. Lett.*, vol. 15, no. 8, pp. 860–862, Aug. 2011.

[38] K. Niu and K. Chen, "Stack decoding of polar codes," *IEEE Elec. Lett.*, vol. 48, no. 12, pp. 695–697, Jun. 2012.

[39] U. U. Fayyaz and J. R. Barry, "Low-complexity soft-output decoding of polar codes," *IEEE J. Sel. Areas Commun.*, vol. 32, no. 5, pp. 958–966, May 2014.

[40] E. Arikan, "A performance comparison of polar codes and Reed-Muller codes," *IEEE Commun. Lett.*, vol. 12, no. 6, pp. 447–449, Jun. 2008.

[41] Y. Polyanskiy, H. V. Poor, amd S. Verdu, "Channel coding rate in the finite block-length regime," *IEEE Trans. Inf. Theory,* vol. 56, no. 5, pp. 2307–2359, May 2010.

[42] R. Mori and T. Tanaka, "Channel polarization on q-ary discrete memoryless channels by arbitrary kernels," in *Proc. IEEE Int. Symp. Inf. Theory (ISIT)*, Austin, Texas, USA, Jun. 2010, pp. 894–898.

[43] H. Mahdavifar and A. Vardy, "Achieving the secrecy capacity of wiretap channels using polar codes," *IEEE Trans. Inf. Theory,* vol. 57, no. 10, pp. 6428–6443, Oct. 2011.

[44] E. Sasoglu, E. Telatar, and E. M. Yeh, "Polar codes for the two-user multiple-access channel," *IEEE Trans. Inf. Theory,* vol. 59, no. 10, pp. 6583–6592, Oct. 2013.

[45] A. B.-Santos, "Polar codes for the Rayleigh fading channel," *IEEE Commun. Lett.*, vol. 17, no. 12, pp. 2352–2355, Dec. 2013.

[46] H. Si, O. O. Koyluoglu, and S. Vishwanath, "Polar coding for fading channels: binary and exponential channel cases," *IEEE Trans. Commun.*, vol. 62, no. 8, pp. 2638–2650, Aug. 2014.

[47] S. H. Hassani, K. Alishahi, and R. L. Urbanke, "Finite-length scaling for polar codes," *IEEE Trans. Inf. Theory,* vol. 60, no. 10, pp. 5875–5898, Oct. 2014.

[48] A. Fazeli and A. Vardy, "On the scaling exponent of binary polarization kernels," *in Proc. Allerton Conf. Commun. Control Comput.*, Monticello, IL, Oct. 2014, pp. 797–804.

[49] V. Miloslavskaya, "Shortened polar codes," *IEEE Trans. Inf. Theory,* vol. 61, no. 9, pp. 4852-4865, Sep. 2015.

[50] Y. Wang, K. R. Narayanan, and Y.-C. Huang, "Interleaved concatenations of polar codes with BCH and convolutional codes," *IEEE J. Sel. Areas Commun.*, vol.34, no.2, pp. 267–277, Feb. 2016.

[51] H. Vangala, Y. Hong, and E. Viterbo, "Efficient algorithms for systematic polar encoding," *IEEE Commun. Lett.*, vol. 20, no. 1, pp. 17–20, Jan. 2016.

[52] N. Presman, O. Shapira, S. Litsyn, T. Etzion, and A. Vardy, "Binary polarization kernels from code decompositions," *IEEE Trans. Inf. Theory,* vol. 61, no. 5, pp. 2227–2239, May 2015.

[53] G. Sarkis, I. Tal, P. Giard, A. Vardy, C. Thibeault, and W. J. Gross, "Flexible and low-complexity encoding and decoding of systematic polar codes," *IEEE Trans. Commun.*, vol. 64, no. 7, pp. 2732–2745, Jul. 2016.

[54] H. Yoo and I.-C. Park, "Efficient pruning for successive-cancellation decoding of polar codes," *IEEE Commun. Lett.*, vol. 20, no. 12, pp. 2362–2365, Dec. 2016.

[55] T. Wang, D. Qu, and T. Jiang, "Parity-check-concatenated polar codes," *IEEE Commun. Lett.*, vol. 20, no. 12, pp. 2342–2345, Dec. 2016.

[56] K. Tian, A. Fazeli, A. Vardy, and R. Liu, "Polar codes for channels with deletions," *in Proc. Allerton Conf. Commun. Control Comput.*, Monticello, IL, Oct. 2017, pp. 572–579.

[57] J. Choi and I.-C. Park, "Improved successive-cancellation decoding of polar codes based on recursive syndrome decomposition," *IEEE Commun. Lett.*, vol. 21, no. 11, pp. 2344–2347, Nov. 2017.

[58] C. Condo, S. A. Hashemi, and W. J. Gross, "Blind detection with polar codes," *IEEE Commun. Lett.*, vol. 21, no. 12, pp. 2550–2553, Dec. 2017.

초 록

본 학위 논문에는 크게 3가지 기여가 있다:

i) 결합 길이라 불리는 새로운 파라미터를 제안하였고 이를 이용하여 기존의 부분 정보 결합 극 부호[36]의 결합 방식을 일반화하였으며, 결합 길이가 J인 부분 정보 결합 극 부호의 구성 방법을 제안하였다.

ii) 제안한 부분 정보 결합 극 부호의 극 부호 블록 복호 알고리즘 및 다양한 부호 블록 간 복호 알고리즘을 제안하였고 *look-back* and *go-back* 부호 블록 간 복호 알고리즘[36]을 제안한 부호에 맞게 일반화하였다.

iii) 제안한 수정된 병렬 부호 블록 간 복호기의 오류 성능 평가 방법을 제시하였고 이를 바탕으로 제안한 부분 정보 결합 극 부호의 파라미터인 블록 개수와 결합 길이를 동시에 최적화하였다.

기존의 부분 정보 결합 극 부호[36]는 체계적 극 부호로 부호화된 부호 블록들이 일렬로 결합되어 구성된다. 이때, 각 부호 블록은 바로 인접한 양 옆의 블록들하고만 부호화된 정보를 부분적으로 공유한다. 반면에 제안하는 부호에서는, 각 부호 블록이 양옆으로 각각 인접한 여러 개의 부호 블록들과 부호화된 정보를 부분적으로 공유한다. 하나의 부호 블록이 특정 방향으로 정보를 공유하는 부호 블록의 갯수를 J로 표기하고 이를 결합 길이라고 정의한다. 또한, 제안하는 부호를 결합 길이가 J인 부분 정보 결합 극 부호라고 명명한다.

부분 결합 극 부호의 부호화 과정은 3가지 단계로 순차적으로 이루어져 있다: i) 메시지 분할 및 더미 비트 삽입 단계, ii) 부호 블록의 체계적 극 부호화 단계, 그리

고 iii) 부호 블록의 연결 단계로 이루어져 있다. 부분 결합 극 부호에 제안하는 결합 길이의 개념을 도입하기 위해서, 일반화된 메시지 분할 및 더미 비트 삽입 기법을 제안하였다. 또한, 이러한 기법 하에서 결합 길이를 고려한 유효 부호 길이 및 부호율을 유도하였다.

부분 결합 극 부호의 복호화 과정은 크게 2가지 단계의 반복으로 이루어져 있다: i) 극 부호 블록의 복호화 단계와 ii) 부호 블록 간 복호화 단계로 이루어져 있다. 본 논문에서는, 새롭게 도입한 파라미터인 결합 길이를 고려한 극 부호 블록의 복호 방법을 제안하였다. 또한, 몇 가지의 부호 블록 간 복호 알고리즘들을 제안하였다: i) 개선된 부호 블록 간 복호 알고리즘들 ii) 결합 길이가 2일 때 일반화된 look-back and go-back 블록 간 복호 알고리즘 iii) 순차적 복호 및 확률기반 재복호 알고리즘이라 불리는 새로운 부호 블록 간 복호 알고리즘을 제안하였다.

계산 복잡조 측면에서, 부분 결합 극 부호의 복호화 과정 중 가장 시간이 오래 걸리는 단계는 바로 극 부호 블록의 복호화 단계이다. 이러한 이유로, 해당 단계를 건너뛰고 계산을 하는 수정된 병렬 부호 블록 간 복호기의 오류 평가 방법을 새롭게 제안하였다. 이러한 평가 방법을 이용하여 제안하는 부분 정보 결합 극 부호의 두 파라미터인 블록 개수 L과 결합 길이 J를 최적화하였다. 또한, 복잡도 분석의 일환으로, 병렬 부호 블록 간 복호 알고리즘의 복잡도의 상한을 제안하고 증명하였다. 시뮬레이션 결과를 통하여 본 논문에서 제안하는 부분 정보 결합 극 부호의 성능 및 제안하는 성능 평가 방법의 신뢰성을 확인할 수 있다.

주요어: 오류 정정 부호, 극 부호, 공간 결합 부호, 부분 정보 결합 부호, 리스트 연속 소거 복호, 결합 길이

학번: 2014-21672